Oil & Natural Gas Technology

DOE Award No.: DE-FE0024297

Quarterly Research Performance

Progress Report (Period Ending 6/30/2021)

Marcellus Shale Energy and Environment Laboratory (MSEEL)

Project Period (October 1, 2014 – September 30, 2021)

Submitted by:
Samuel Taylor

Signature

West Virginia University Research Corporation
DUN's Number: 191510239
886 Chestnut Ridge Road,
PO Box 6845, Morgantown WV, 26505
Tim.Carr@mail.wvu.edu
304-293-9660

Prepared for:
United States Department of Energy
National Energy Technology Laboratory

6/30/2021

U.S. DEPARTMENT OF ENERGY | NATIONAL ENERGY TECHNOLOGY LABORATORY

Office of Fossil Energy

Executive Summary
Quarterly Progress Report

April 1 – June 30, 2021

The objective of the Marcellus Shale Energy and Environment Laboratory (MSEEL) is to provide a long-term field site to develop and validate new knowledge and technology to improve recovery efficiency and minimize environmental implications of unconventional resource development.

Impacts from COVID-19 have diminished and work has progressed relatively on-schedule, and analysis from the samples and data collected from the Boggess Pad has continued as planned.

This quarter's work focused on extending to 50 years decline curve analyses (DCA) and reservoir simulations. The history matches and results for individual wells at the Boggess and MIP pads provided good results. The simulations were extrapolated for 10, 30 and 50-years to estimate ultimate recovery (EUR) and compare the productivity of individual wells. 50-year EUR ranged from 1.35 to 3.76 billion cubic feet per 1,000 feet. The MIP 3H well had the best recovery while the Boggess 1H was the best exterior well and the Boggess 3H was the best interior well. These two wells were designed using the WVU completion procedures. Work will continue to refine the simulations to understand the role of fractures, water saturations, and completion interactions.

Improved understanding of the locations for high-intensity natural fractures is critical for efficient development of Marcellus shale gas assets by placing perforation clusters at optimized locations to improve the efficiency of hydraulic fracture completion. We used the image tools to design improved completions for the Boggess 1H and 3H wells. However, data acquisition and interpretation is expensive, time consuming and subject to the humane interpretation biases. The acoustic borehole image logging tool acquired vibration signals in addition to borehole images along the Boggess horizontal laterals. We used the low-cost high-resolution drill-string vibration signals as an input dataset to machine-learning (ML) model to predict in near-real time fracture intensity along the laterals. Initial results are very promising and we will work with LANL and others to optimize this rapid and low-cost ML approach for fracture stimulation design. If successful, the ML approach could have broad applicability to unconventional reservoir development, geothermal wells, and geologic carbon storage.

We continue to sample and monitor produced fluids, and monitor air quality and performance at both MSEEL sites (MIP and Boggess). All methane and energy audit data have been collected and processed. with various models to assess temporal variability of methane emissions, methods to indirectly quantify methane emissions, and energy recovery through combined heat and power (CHP) operation during unconventional well drilling.

Work on the interaction of fracture stimulation fluids with the Marcellus shale under high temperature and pressure conditions and the type of produced fluid demonstrate that, although oxidative breakers generally added to fracturing fluids for increasing well productivity by improving the viscosity of gel-based fluids, these oxidizers can significantly degrade shale organic matter (OM) and improve shale permeability.

The structural parameters of the kerogen from Boggess 17H sample compared with the kerogen from MIP-3H show the majority of the aliphatic and aromatic structural parameters for both samples are similar. Such resemblance in molecular structural parameters indicates that the deposition environment, sources of organic matter, and thermal history were similar and the type and amount of hydrocarbons generated in both formations would be similar

We have developed a 3D visualization model using the open source programming language. The model was constructed in order to visualize the Boggess wells, fracture data and microseismic events. Interactive controls include a slider bar control to interactively scroll through the completion stages, and zoom and pan along the wellbore. Additional user controls will allow for turning layers on and off or viewing the microseismic events through time.

MSEEL data appears in numerous presentations, posts, and papers. We continue to develop software to process the 108 terabytes of DAS and completion data from the Boggess pad and are working to develop an improved workflow for continuing to deliver the data to the public.

Project Performance

This report summarizes the activities of Cooperative Agreement DE-FE0024297 (Marcellus Shale Energy and Environment Laboratory – MSEEL) with the West Virginia University Research Corporation (WVURC) during the 3rd quarter of FY2021 (April 1 through June 30, 2021).

This report outlines the approach taken, including specific actions by subtopic. If there was no identified activity during the reporting period, the appropriate section is included but without additional information.

A summary of major lessons learned to this point of the project are provided as bullet points and will be added to as research progresses. New lessons listed below are:

- The engineered wells at the Boggess Pad (1H and 3H) demonstrate the importance of understanding the intensity of naturally occurring fractures in order to better design stages and cluster placement to improved well performance.

Phase 3 Plans

In phase 3 of MSEEL, we continue to monitor production and DTS data from the Boggess Pad. Six 10,000+ foot horizontal Marcellus Shale wells off a single pad (Boggess) are near the initial MIP pad (Figure 0.1). The pad has one permanent fiber optic (FO) cable installed in the Boggess 5H lateral provided digital acoustic sensing (DAS) during stimulation, and was monitored during initial production. Distributed temperature sensing (DTS) was monitored during stimulation and continues during production. We acquired DAS data for the entire 5H well, but the FO failed around stage 30 and we do not have long-term DTS data below that stage to the toe. We have data from the upper stages through the heel and continue to download the data. Deployable FO systems were proposed (Boggess 1H and 17H), but due to the fiber failure in the 5H the fiber was not placed in the 17H. However, we acquired significant DAS and DTS and microseismic data from the 5H and 1H that provided insight of stimulation effectiveness in near real-time and the 100's of terabytes of data to evaluate and model the reservoir across each individual stage, and at individual clusters within stages for the 5H, which will be used for all Boggess wells.

Based on production, rate transient analysis (RTA), and fracture analysis (FRACPRO) the new methodology appears to improve completion efficiency. As the wells have come on production, the 1H and 3H wells still have a higher gross production efficiency that either the geometrically

completed wells (9H and 17H with identical 200 feet stages with identical number of clusters in each stage) or the commercial design provided which only used the geomechanical logs and ignored the imaged fractures (5H and 13H) (Figure 0.2). On a net production efficiency controlling for variable lateral length (Mcf/1000') outside wells (1H and 17H) are better than interior wells, but engineered wells had a slower ramp-up but are gaining on their counterparts (Figure 0.3).

We are working with Premier to develop a high-resolution geomechanical model (stratigraphy) to type each 6 inches of the Marcellus. Logging while drilling (LWD) logs in each of the six laterals provided similar geomechanical logs and image logs to geomechanically type each foot of the laterals as the horizontal laterals move stratigraphically up and down through the Marcellus. This approach will permit direct coupling and evaluation of cost-effective LWD technologies to the relatively high-cost permanent FO data and the basis for engineering stages in all wells. It was applied to two of the Boggess wells.

We continue to gather fiber optic and production data from the Boggess wells to compare across each of the six wells, and with the two wells at the MIP pad (MSEEL 1) and use these data to form the basis for robust big data modeling.

We are working on a new workflow for simplified access to MSEEL data especially the large multi-terabyte data from the Boggess pad. We are working with NETL, LANL, and other labs on various projects of the Marcellus at the MIP and Boggess site.

A presentation is scheduled for the NETL Virtual Oil and Gas Review Meeting in August.

Figure 0.1: Boggess Pad with new generation permanent fiber in the central well (Boggess 5H, red star)) and deployable fiber in adjoining wells skipping one (orange stars). We were able to monitor in near-real time fracture stimulation in the central 3 wells (3H, 5H and 9H). A vertical pilot was drilled, cored and logged. We continue to collect DTS data from the 5H.

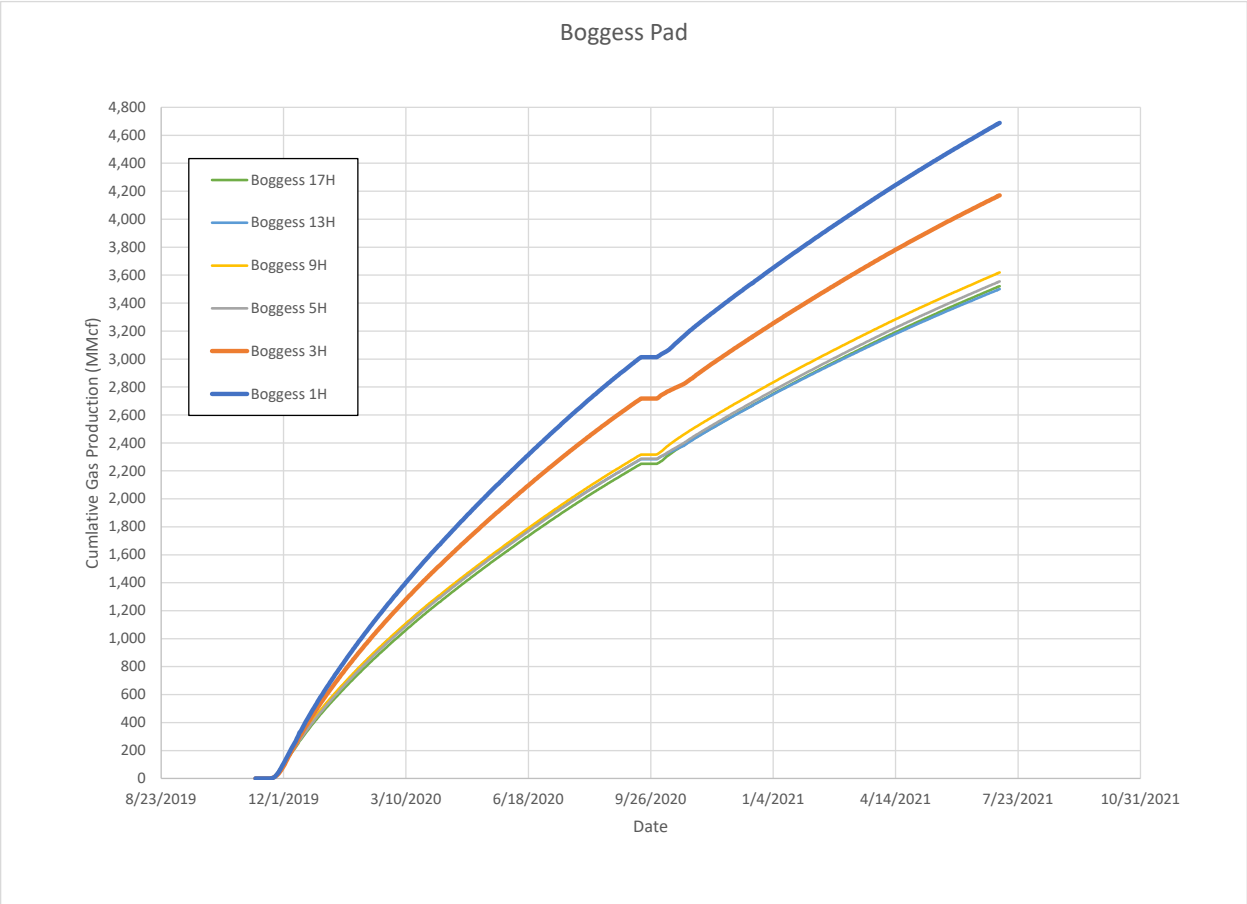

Figure 0.2: Initial daily gross production from the Boggess Pad. The wells engineered using the MSEEL software are highlighted with thicker lines (1H and 3H). Wells have different lateral lengths that need to be evaluated to derive a better evaluation of production efficiency. Also outside wells typically perform better than interior wells due to reduced competition. The production is very early and the picture could very easily change. The wells were shut-in for a period because of low gas prices.

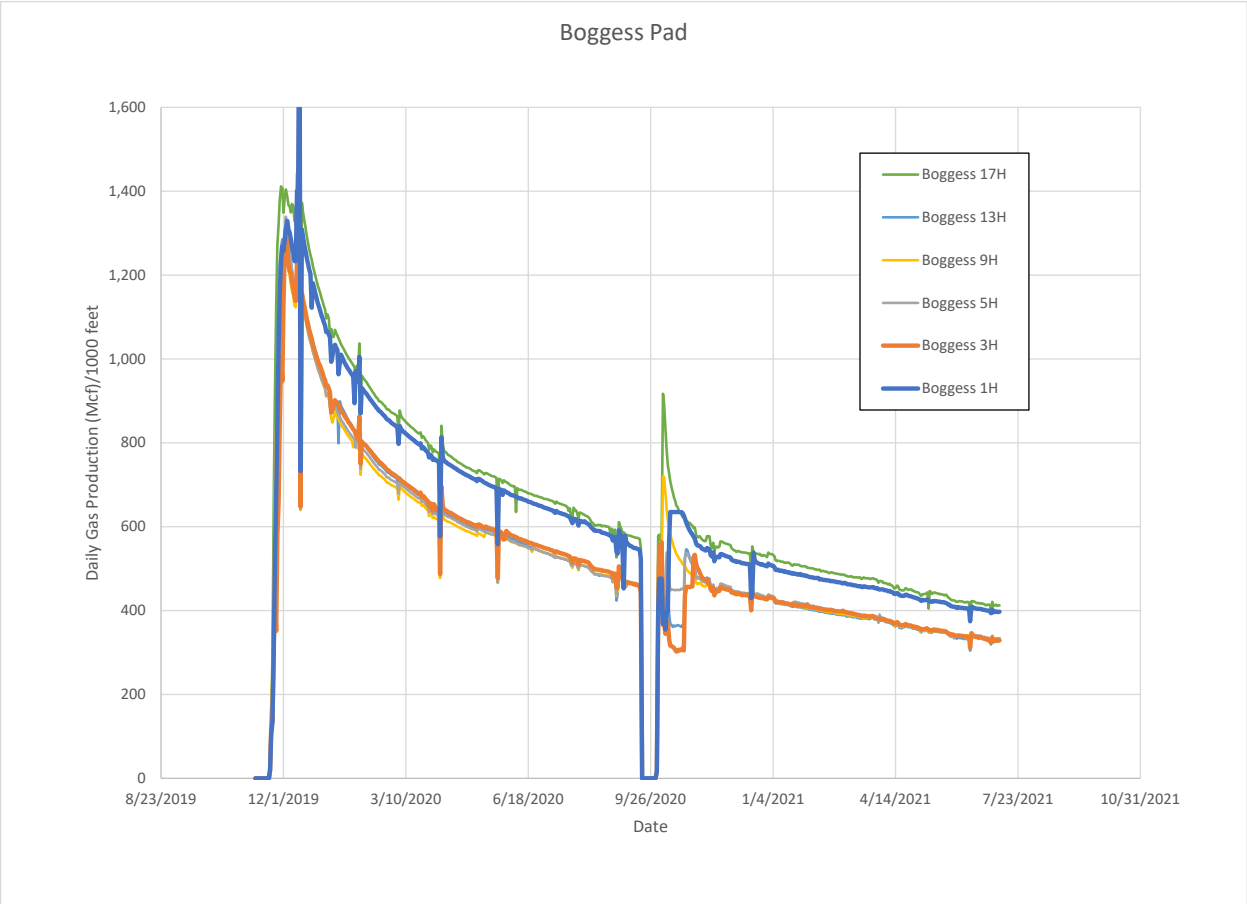

Figure 0.3: Initial daily net production from the Boggess Pad adjusted for Mcf per 1000' of completed lateral. The wells engineered using the MSEEL software are highlighted with thicker lines (1H and 3H). As you can see outside wells (1H and 17H) perform better than interior wells due to reduced competition. Also wells engineered using the MSEEL approach (1Hand 3H) got off to a slower start but have narrowed the gap in daily production and in the case of the 3H, it is producing more than any other interior well. In the case of the 17H more sand was used per stage and we need to adjust for sand per foot. The production is early and is in transient flow. The picture could easily change. The wells were shut-in for a period because of low gas prices.

Project Management Update

Approach

The project management team will work to generate timely and accurate reporting, and to maintain project operations, including contracting, reporting, meeting organization, and general oversight.

Results and Discussion

The project team is tracking ten (10) milestones in this budget period.

	Task	Milestone	Status	Due Date
1.	3.2.1	Sample collection and analysis of flowback/produced water; data analysis	Complete	20-Mar

2.	3.2.1	Comparison of OTM33A vs. Methane Audits vs. Eddy Covariance System Measurements Complete	This task is ongoing, with initial results expected next quarter (June 2020). There was a short delay in tower deployment at MSEEL 1.0. During this delay, the team focused on the baseline analysis of controlled data from the NSF project. This will lead to two collaborative publications to highlight refinement of approach prior to application to MSEEL data. Early analysis of MSEEL 1.0 have been completed to detect periods for further analysis.	20-Mar
3.	3.1.2	Characterization of organic matter - kerogen extraction and characterization complete	Completed the extraction and 13C NMR analysis of kerogen. Preliminary interpretation included in this report.	21-Mar
4.	3.1.2	Isotopic characterization of produced water and gases - comparison between MIP and Boggess wells and other wells in Marcellus and interpretation.	Complete.	20-Jun
5.	3.1.2	High-pressure and temperature fracture fluid/shale interaction experiments complete.	Complete and ready for publication	21-March
6.	3.1.4	Complete final reservoir characterization using Boggess 17H pilot well. Compare 17H to MIP 3H	Completed but will continue to refine with new production data any additional well data, and also well monitoring (DTS)	21-March
7.	3.2.1	Methane Audit 14 Completed	Complete	20-Jun

8.	3.4.2	Synthetic data developed for model use	Complete	21-March
9.	3.2.1	Energy Audit Model Completed	Complete and moving to publication	20-Sep
10.	3.1.4	Extend reservoir characterization using logs, completion data and production data to identify good producing stages in Boggess wells.	Complete through 50 years of production but will continue to enhance.	21-June

Topic 1 – Geologic Engineering

Approach

Forecasting the production rates and expected ultimate recovery (EUR) of the well is of special interest in the oil and gas industry. For this purpose, both decline curve analysis (DCA) and reservoir simulation forecasting using history matched models developed for each well (stand-alone) is used. Three different techniques including multi-segment decline curve analysis (MDCA), Duong decline and stretched exponential are used for DCA analysis. MDCA consists of three segments 1) Hyperbolic decline with a higher b value 2) Hyperbolic decline with a lower b value 3) Transition from the second hyperbolic to an exponential decline. Duong rate decline analysis is also developed for fractured shale reservoir, where long term linear flow is considered, and stretched exponential, which is modified version of Arps model that provides the cumulative time relation is also implemented using IHS Harmony. The 10, 30 and 50 years of EUR forecasts are obtained from each DCA and the average of EUR obtained from all three techniques is compared with history matched reservoir simulation forecasts.

The quality of reservoir simulation history matched model will essentially determine the quality of the EUR predictions. To improve the quality of history-matched model the following steps were performed:

1) The fiber optics DAS data available for Boggess 5H is used to quantify the cluster efficiency of the Boggess 5H.
2) Flow backwater is studied to quantify the hydraulic fracture, and near wellbore water saturation after hydraulic fracturing.
3) The natural fracture characteristics obtained using image logs are used

Results and Discussion

Figure 1.1 shows the cumulative production forecast of Boggess wells compared with MIP3H obtained using the CMG reservoir simulation history matched models presented in our previous quarterly report. We have divided the analysis into three-time intervals after 10, 30, and 50 years. In all time spans, Boggess 1H shows the highest cumulative gas production. In first 10 years after Boggess 1H, Boggess 3H has the highest cumulative gas production and the MIP3H shows the lowest cumulative gas production. However, after 30 and 50 years the MIP3H shows the highest cumulative gas production after Boggess 1H and Boggess 5H shows the lowest cumulative gas production.

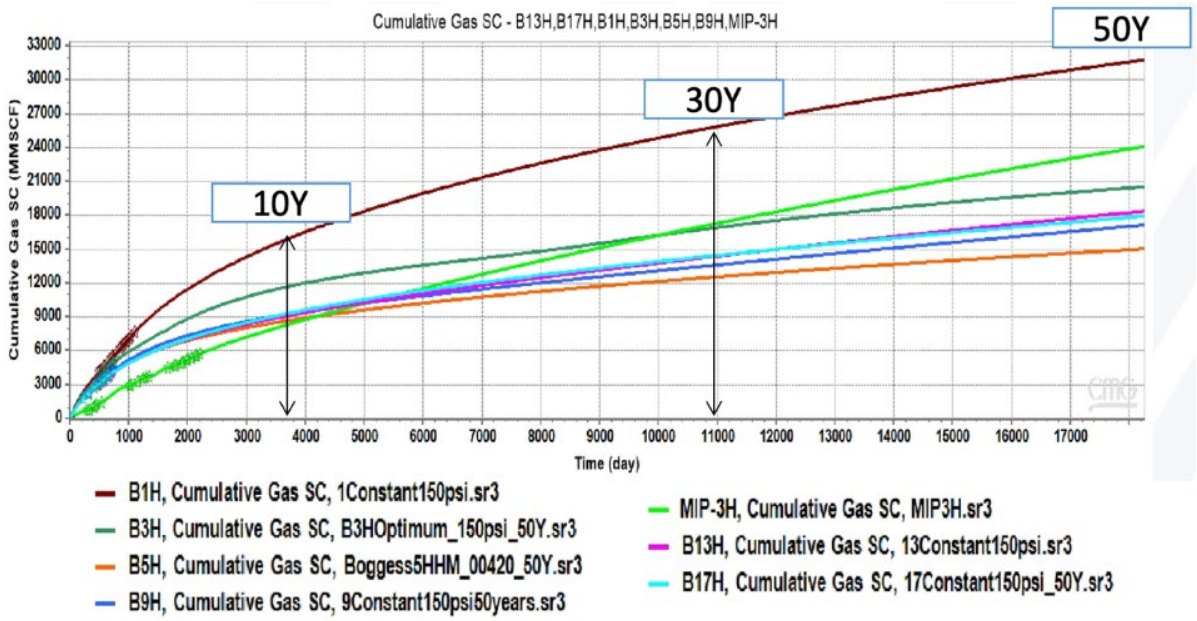

Figure 1.1: Cumulative gas production forecasts of Boggess wells and MIP3H

To be able to make a better comparison the 10, 30 and 50 years forecast obtained using history matched models are normalized per 1000 ft of lateral for all the wells and presented in Figure 1.2. In 10 years forecast MIP3H and Boggess 1H show the highest cumulative gas production per 1000 ft of lateral. However, MIP3H shows the highest cumulative gas production for 30 and 50 years forecast. In Boggess pad the Boggess 1H shows the highest cumulative gas production per 1000 ft of lateral followed by Boggess 17H and Boggess 5H shows the lowest cumulative gas production.

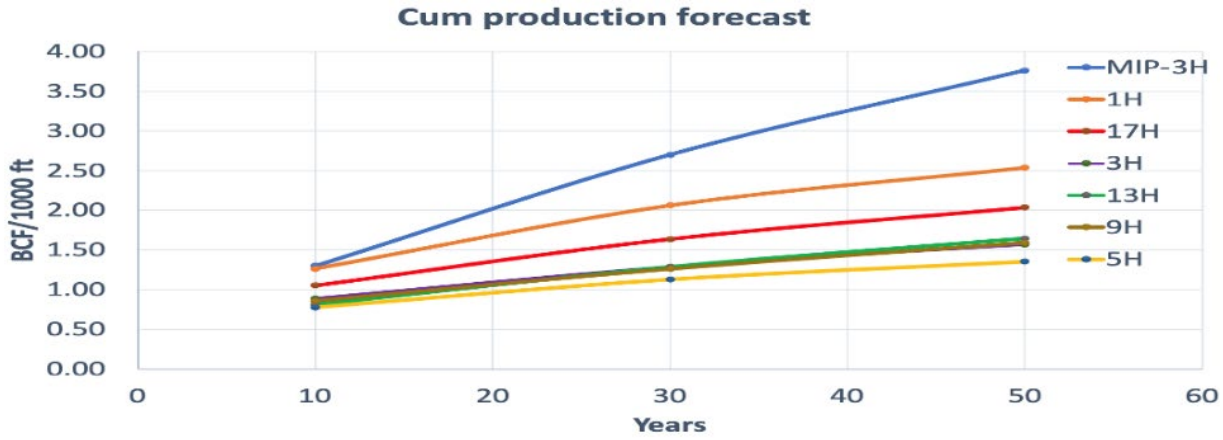

Figure 1.2: Cumulative gas production forecasts of Boggess Pad and MIP3H in BCF/1000 ft of lateral

The fiber optics DAS data collected from Boggess 5H is used for qualitative analysis of Boggess 5H completions design specially the cluster efficiency. Figure 1.3 shows DAS data collected from stage 18 of the Boggess 5H. It clearly shows, clusters 3 and 4 accepted slurry throughout the entire frac stage. Therefore, they can be inferred to have remained open and are therefore contributing to production. Clusters 1 and 2 on the other hand stopped accepting slurry prior to the completion of the stage and therefore assumed to not be contributing to the production. DAS data collected from the fiber optic cable for all 56 stages, used to obtain the cluster efficiencies for Boggess 5H. Figure 1.4 shows the final interpretation of the DAS data. Red blocks represent clusters that were closed after reviewing the DAS data, while white blocks represent clusters that were left open. Cluster efficiency was calculated by comparing the total number of clusters to the number of clusters remaining opened. Using this methodology, the Boggess 5H

Lateral is estimated to have at least 52.5% cluster efficiency. Even though the cluster efficiencies obtained for Boggess 5H was more qualitative, however, it provides us with good insights regarding Boggess 5H production. In our next report we will quantify the cluster efficiencies in a more quantitative manner.

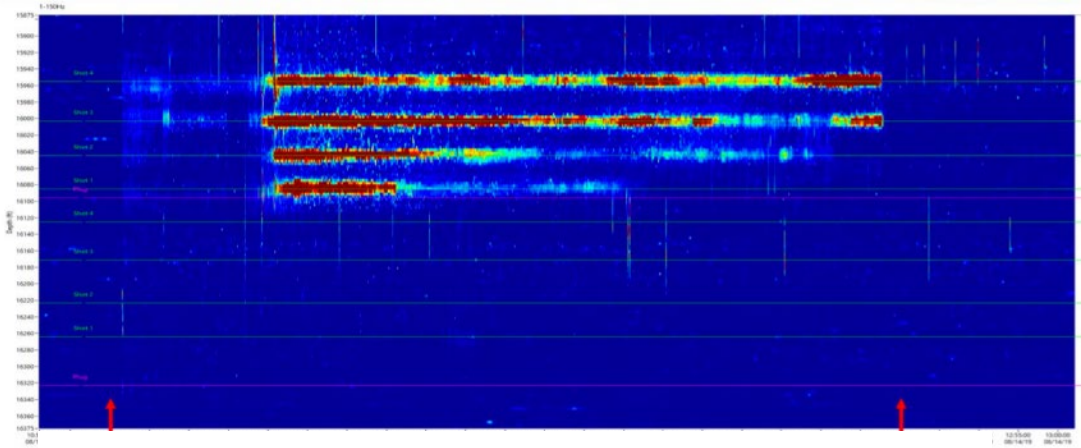

Figure 1.3: Boggess 5H-Stage 18 DAS data

Boggess 5H CMG Clusters					
	Legend:	OPEN	SHUT		
Stage	Frac Templat	Cluster #4	Cluster #3	Cluster #2	Cluster #1
Stg 1	3		275	276	277
Stg 2	3	274	273	272	271
Stg 3	4	270	269	268	267
Stg 4	3	266	265	264	263
Stg 5	3	262	261	260	259
Stg 6	3	258	257	256	255
Stg 7	3	254	253	252	251
Stg 8	4	250	249	248	247
Stg 9	3	246	245	244	243
Stg 10	3	242	241	240	239
Stg 11	3	238	237	236	235
Stg 12	3	234	233	232	231
Stg 13	3	230	229	228	227
Stg 14	3	226	225	224	223
Stg 15	2	222	221	220	219
Stg 16	2	218	217	216	215
Stg 17	3	214	213	212	211
Stg 18	3	210	209	208	207
Stg 19	2	206	205	204	203
Stg 20	4	202	201	200	199
Stg 21	3	198	197	196	195
Stg 22	2	194	193	192	191
Stg 23	2	190	189	188	187
Stg 24	2	186	185	184	183
Stg 25	2	182	181	180	179
Stg 26	3	178	177	176	175
Stg 27	2	174	173	172	171
Stg 28	3	170	169	168	167
Stg 29	1	166	165	164	163
Stg 30	2	162	161	160	159
Stg 31	2	158	157	156	155
Stg 32	2	154	153	152	151
Stg 33	2	150	149	148	147
Stg 34	2	146	145	144	143
Stg 35	1	142	141	140	139
Stg 36	1	138	137	136	135
Stg 37	1	134	133	132	131
Stg 38	2	130	129	128	127
Stg 39	1	126	125	124	123
Stg 40	4	122	121	120	119
Stg 41	2	118	117	116	115
Stg 42	2	114	113	112	111
Stg 43	1	110	109	108	107
Stg 44	1	106	105	104	103
Stg 45	4	102	101	100	99
Stg 46	3	98	97	96	95
Stg 47	3	94	93	92	91
Stg 48	3	90	89	88	87
Stg 49	3	86	85	84	83
Stg 50	3	82	81	80	79
Stg 51	1	78	77	76	75
Stg 52	1	74	73	72	71
Stg 53	4	70	69	68	67
Stg 54	4	66	65	64	63
Stg 55	4	62	61	60	59
Stg 56	4	58	57	56	55

Figure 1.4: Boggess 5H cluster efficiency

The water production from Boggess wells is compared and total water recovered after hydraulic fracturing is obtained as shown in figure 1.5 and table 1.1. Boggess 9 H and 5H shows the maximum water production per foot of lateral. Boggess 5 H also shows the maximum water recovered in compared to other Boggess wells as shown in Table 1.

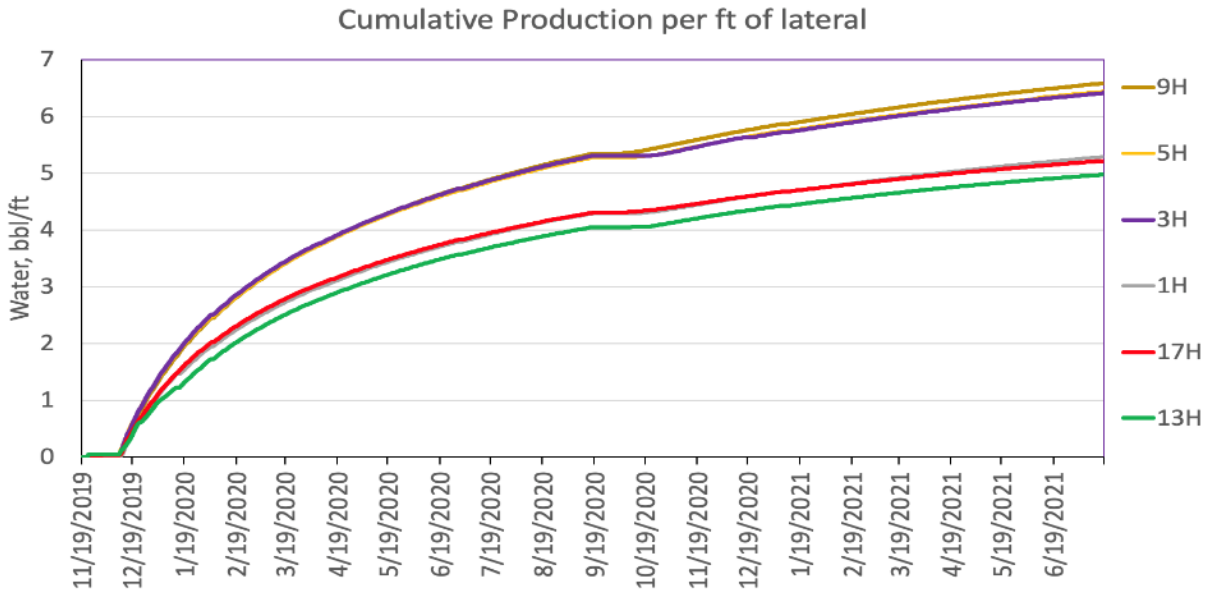

Figure 1.5: Water production from Boggess wells recovered after hydraulic fracturing.

Table 1.1: comparison of water production, hydraulic fracturing water injected and the water recovery of Boggess wells

Pad	Boggess						MIP
Well	B1H	B3H	B5H	B13H	B9H	B17H	MIP3H
LL	12544	13117	11128	10801	11201	8823	6420
EUR BCf/1000ft CMG. (10 years forecast)	1.26	0.89	0.78	0.85	0.81	1.05	1.3
EUR BCf/1000ft CMG. (30 years forecast)	2.06	1.29	1.13	1.26	1.28	1.64	2.7
EUR BCf/1000ft CMG. (50 years forecast)	2.54	1.57	1.35	1.59	1.64	2.04	3.76
EUR BCf/1000ft DCA. (50 years forecast)	1.79	1.64	1.63	1.49	1.50	2.24	NA

Well	B1H	B3H	B5H	B13H	B9H	B17H
Total Water injected bbl/ft	47	42	40	41	42	50
cum produced (bbl)	66331	84060	71647	55691	71096	46003
injected (bbl)	586247	546537	448576	441769	465854	444031
water recovered (%)	11	15	16	13	15	10

Table 1.2 summarizes the EUR comparison of Boggess wells and MIPH3 well.

Products

History matched reservoir models built for all the Boggess wells and MIP3H. DCA performed for all the wells and 10-, 30-, and 50-years EUR forecasts are provided.

Plan for Next Quarter

Fine tuning the simulation by incorporating improved estimates of fracture stimulation efficiency.

Topic 2 – Geophysical & Geomechanical

Approach

Fractures were identified in the Boggess 5H lateral from image logs derived from LWD logs acquired by Petromar. Fractures were identified by two different interpreters and plotted on stereonet diagrams and show the differences in orientations (figure 2.1). The plots of facture intensity along the lateral show similar distributions, but the second interpretation identified many more fractures over the same length.

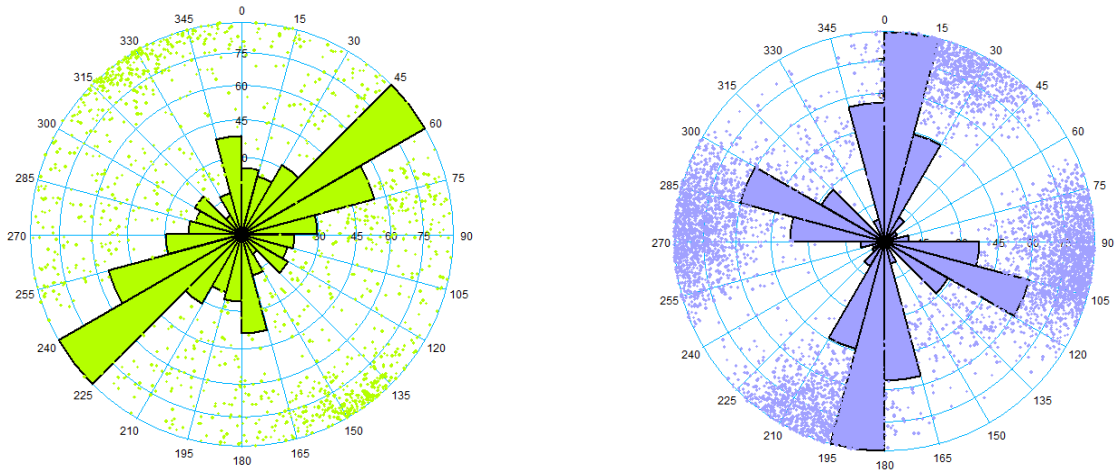

Figure 2.1: Stereonet plots of the fractures identified by two different interpreters in the Boggess 5H.

The same two interpreters are currently identifying fractures in the Boggess 1H and 3H for further analysis.

Fractures were loaded into the Geographix database and plotted as tadpoles on a well log plot (figure 2.2). A fracture intensity curve was generated from the fractures using a 5-foot window for the calculation. These values were plotted alongside cluster efficiency values. Using the DAS data, obtained from the fiber optic cable in the Boggess 5H wellbore, each perforation cluster was identified as either open and flowing or closed.

The cluster efficiencies were then averaged for each stage and were plotted against number of fractures identified in each stage (figure 2.3). Stage efficiencies range from an average of 1, in which all clusters in the stage are open, to a value of 0, where all clusters in a stage are closed.

Identified fractures were then compared to the microseismic data acquired during the completion of the Boggess 5H. Stage efficiencies were plotted against the number of microseismic events recorded during each stage (figure 2.4) and against the maximum distance from the center of each stage a microseismic event was recorded (figure 2.5).

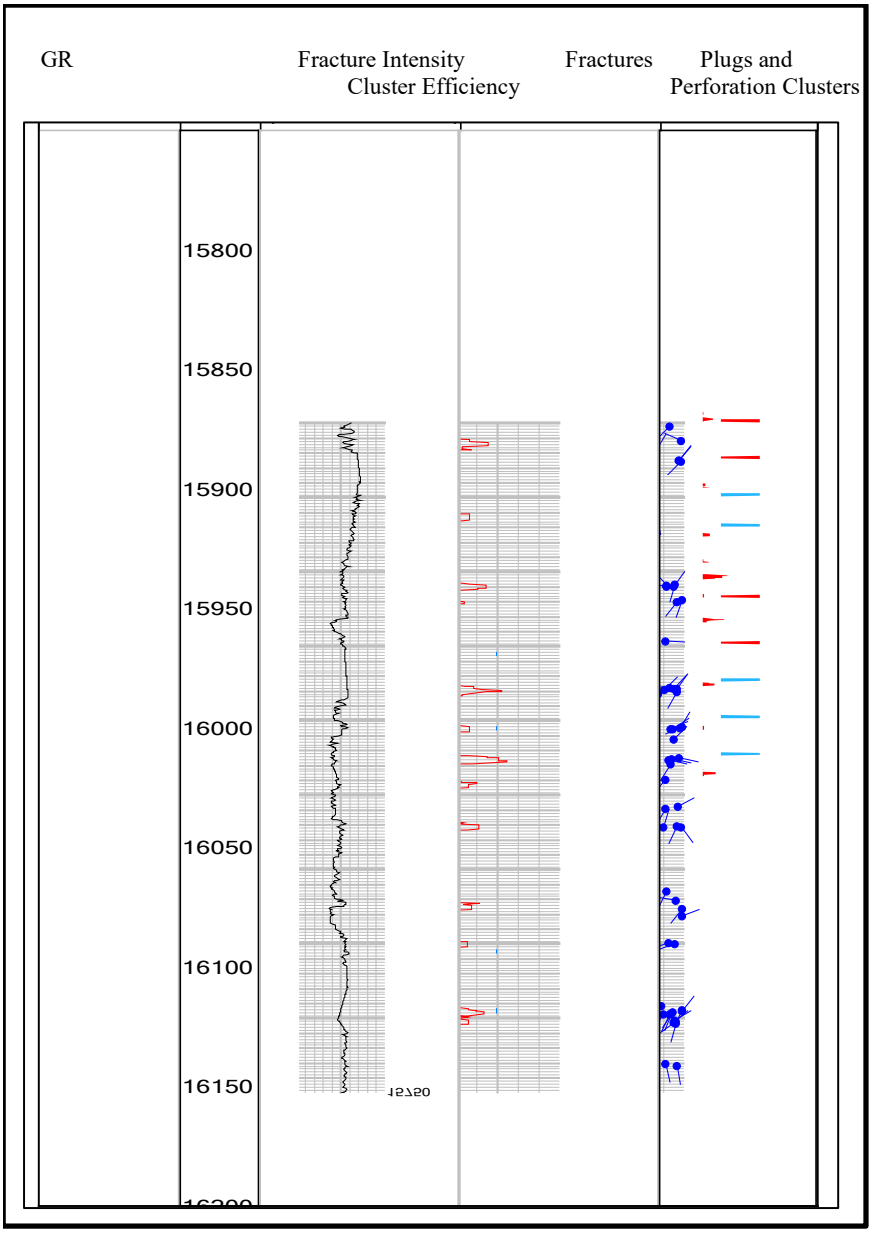

Figure 2.2: Boggess 5H well log. Cluster efficiencies are shown as either open (blue) or closed (red) on the middle track.

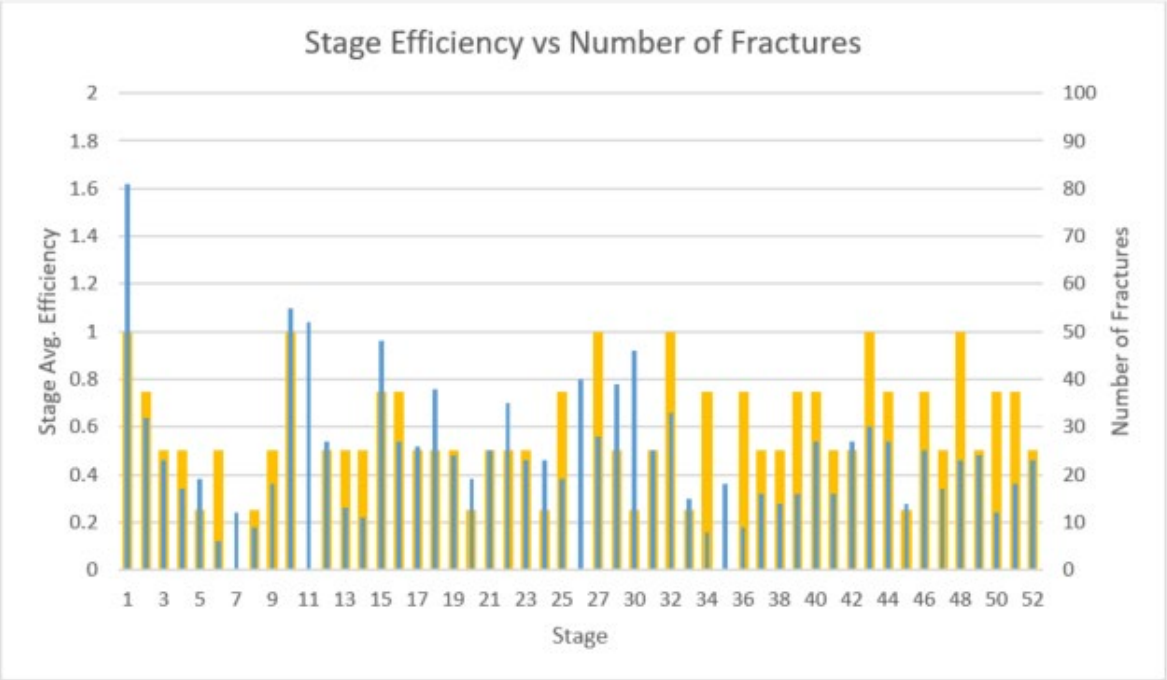

Figure 2.3: Average stage efficiency plotted against number of fractures in each stage. Stage efficiency is shown in yellow and number of fractures in blue.

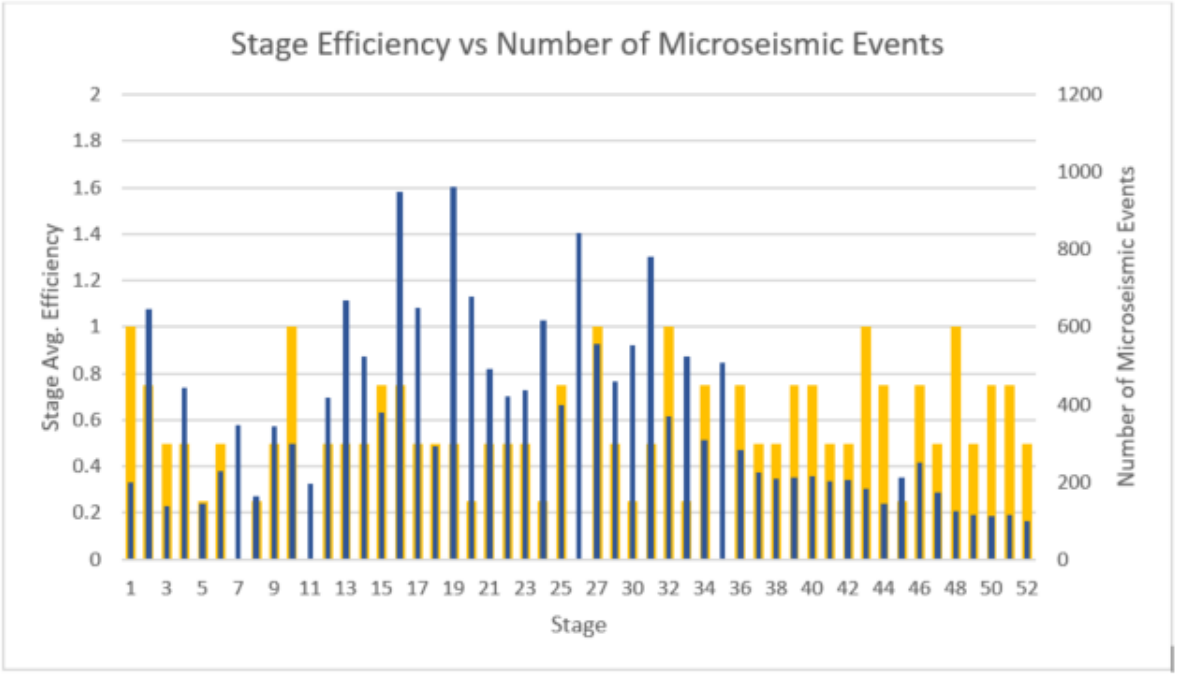

Figure 2.4: Average stage efficiency plotted against number of microseismic events recorded for each stage. Stage efficiency is shown in yellow and number of events in blue.

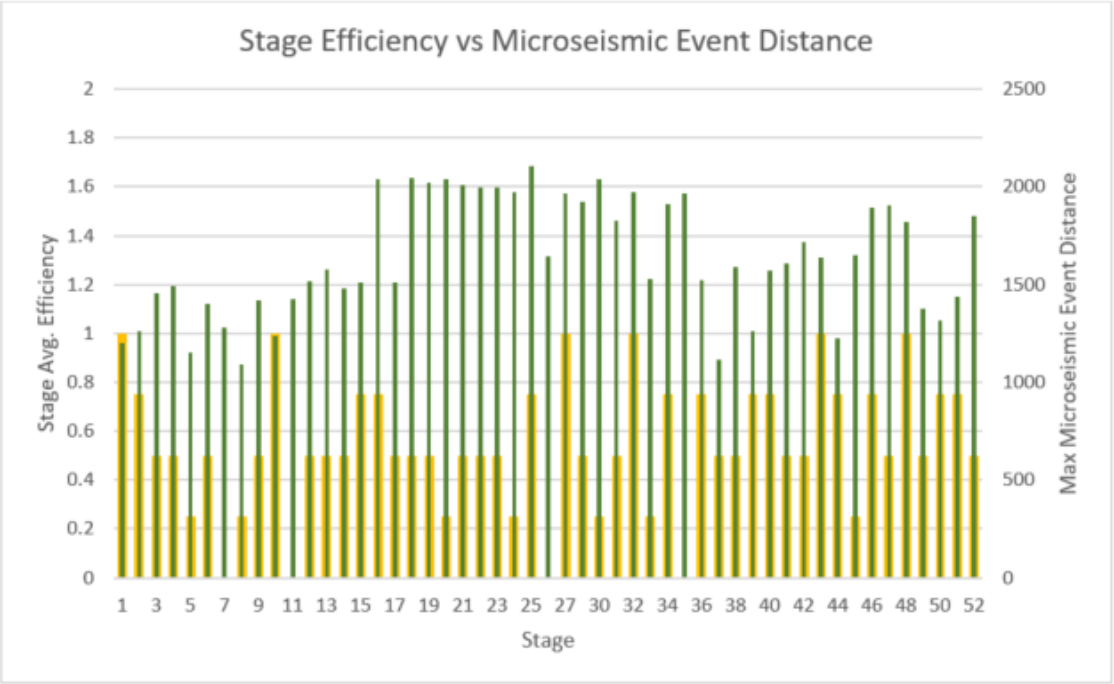

Figure 2.5: Average stage efficiency plotted against maximum distance away from center of each stage a microseismic event was recorded. Stage efficiency is shown in yellow and maximum distance in green.

Improved understanding of the locations for high-intensity natural fractures is critical for efficient development of Marcellus shale gas assets by placing perforation clusters at optimized locations to improve the efficiency of hydraulic fracture completion. We used the image tools to design improved completions for the Boggess 1H and 3H wells. However, data acquisition and interpretation is expensive, time consuming and subject to the humane interpretation biases. The acoustic borehole image logging tool acquired vibration signals in addition to borehole images along the Boggess horizontal laterals. We used the low-cost high-resolution drill-string vibration signals as an input dataset to machine-learning (ML) model to predict in near-real time fracture intensity along the laterals. The results as predicted using a initial supervised machine-learning model (random forest) achieves a 70% accuracy and subsequent ML approaches appear to significantly improve accuracy (90%).

Results and Discussion

The borehole images for natural fractures in the Marcellus shale along the horizontal laterals for Boggess 5H have been acquired during logging-while-drilling using an acoustic logging tool. The interpretations of the natural fracture intensities and orientations have been conducted by independent consultant (Petromar Andy Duncan). Based on the interpretation, two classes can be created, i.e., high natural-fracture (NF) intensity class and low NF intensity class. A threshold value of 0.4 helps creating balanced binary classification dataset. Figure 2.6 shows the histogram of the interpreted natural fracture intensity.

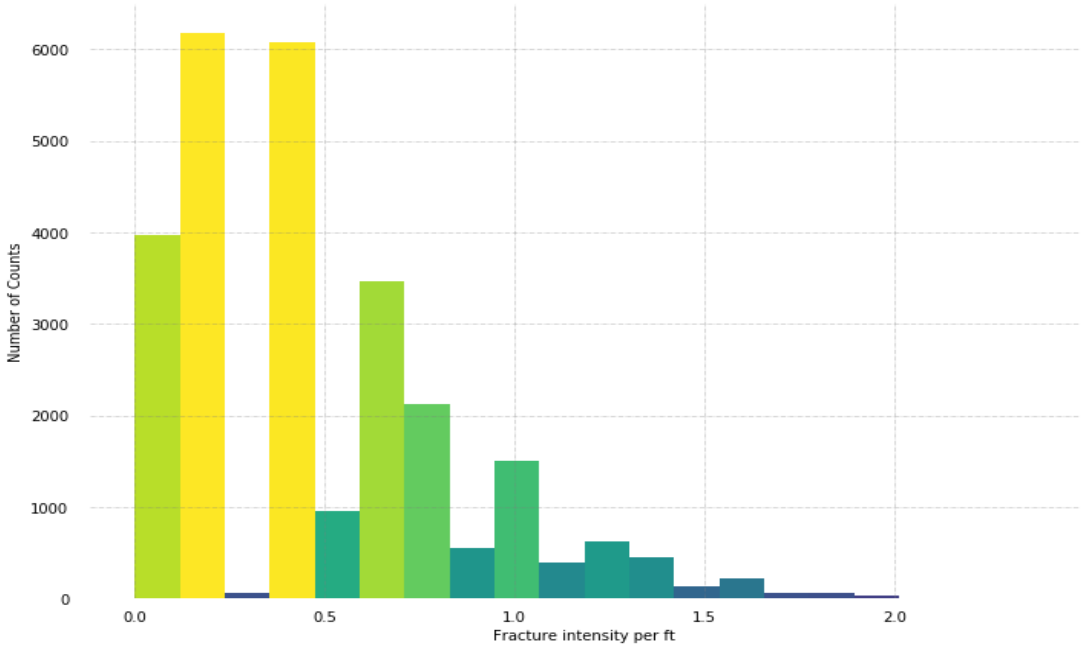

Figure 2.6: Histogram of the natural fracture intensity interpretation.

Meanwhile, the same borehole imager measured high frequency vibration signals close to the drill bit. We used Schlumberger software [1] to convert DLIS file to LAS file. The following signal channels have been converted per 0.5 ft, including Gamma ray (GR), rotations per minute (RPM), rate of penetration (ROP), tri-axial vibrations and shocks.

The above signals are considered as the input dataset in the machine learning approach and the interpretation of natural fracture intensities are used as the labeled dataset. Exploratory data analysis has been implemented in the input dataset. Figure 2.7 shows the comparisons between GR converted from DLIS file in the aforementioned step (Top) and GR measurement during drilling versus measured depth (Bottom).

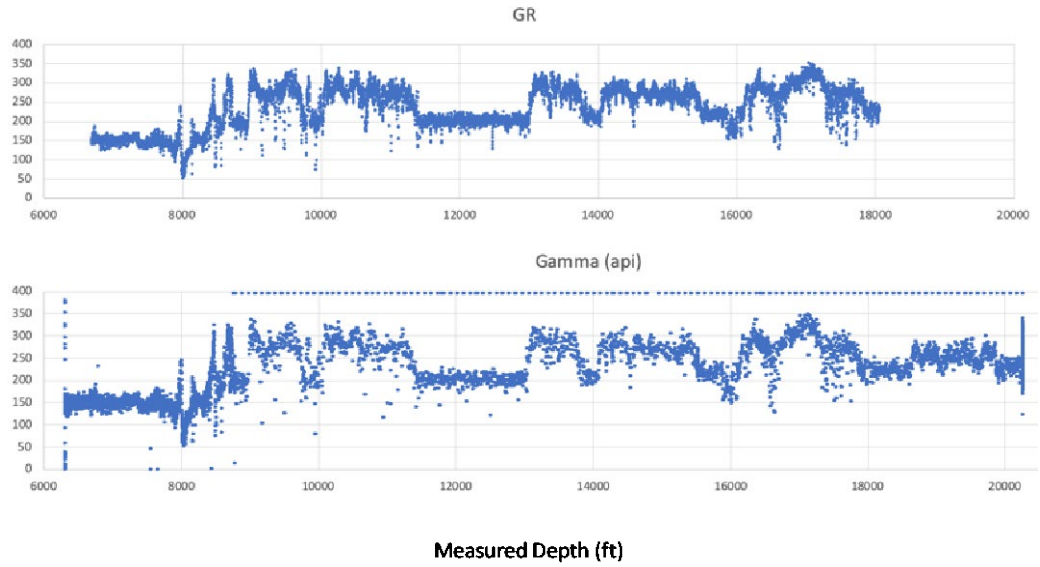

Figure 2.7: Gamma ray comparisons.

The pairwise plot, as shown in Figure 2.8, explores every channel against every channel from the data. The diagonal plots represent a univariate distribution of the data in each column.

The Python script "vibration_rf.py" is generated to perform the task. CSV files "vibration.csv" and "fracture_eval_2" are the raw input and output dataset, respectively. The code includes the data workflow including data preprocessing, exploratory data analysis, feature engineering, and random forest classification.

Different features have been selected to build a machine learning classifier. We selected XAcc, ZAcc, ROP, GR, SHOCKX, SHOCKY, and SHOCKZ as input signals. The dataset is split into 75% training and 25% testing. The improvement on dataset balance could be further implemented.

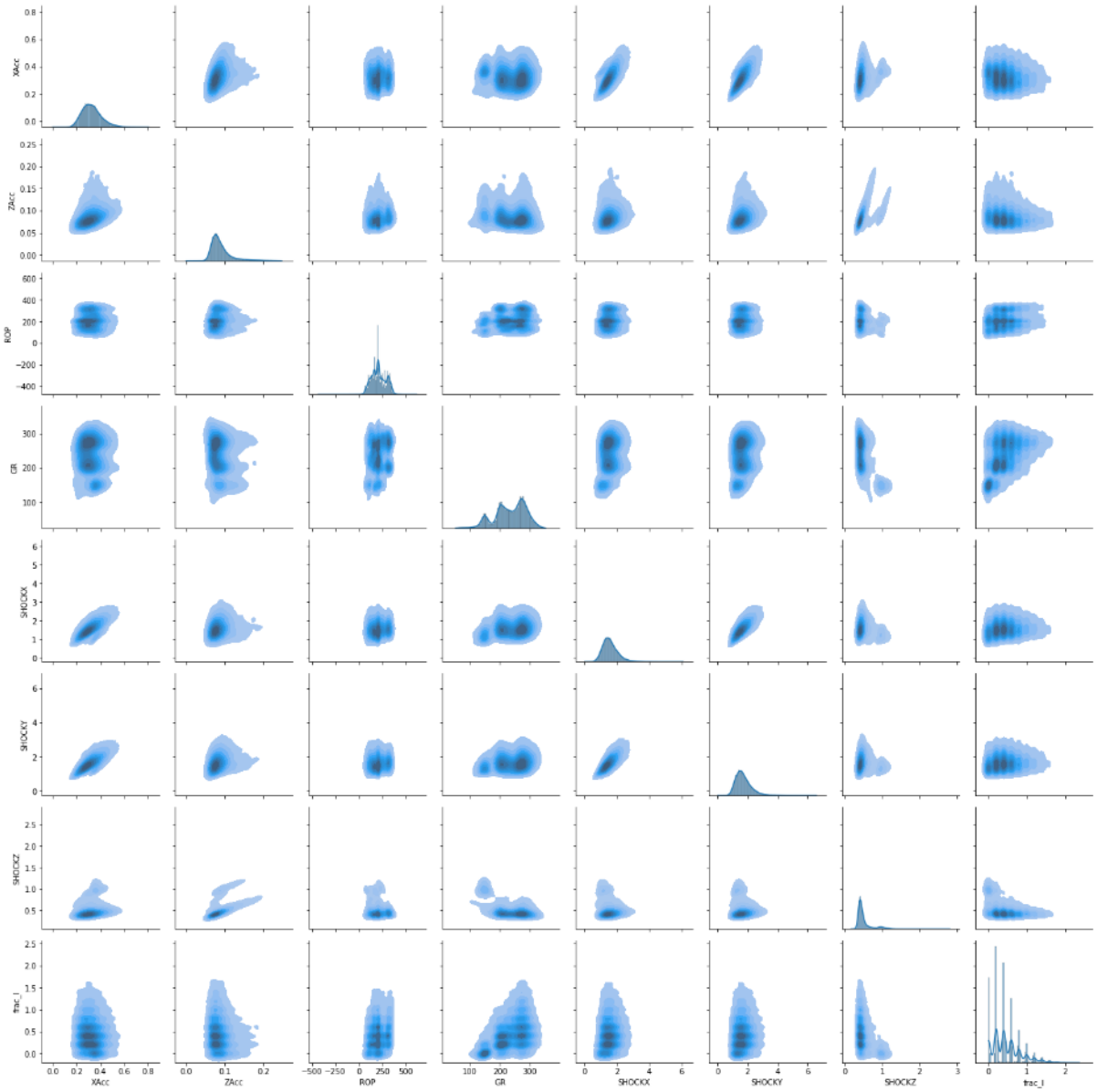

Figure 2.8: Pair-wise histogram

Products

A 3D model was created using the open-source programming language. The model was constructed in order to visualize the Boggess wells, fracture data and microseismic events. Initially, a 2D map view display was created to visualize the microseismic events for each stage (figure 2.9). A slider bar control was added, to interactively scroll through the completion stages. The display also has the ability to zoom and pan. Then a full 3D model was created to show as much well data as possible. Figures 2.10 and 2.11, show all 6 wellbores for the Boggess pad. Microseismic events for the Boggess 5H are color coded by stage. Frack plugs, separating each stage are shown in green and perforation clusters are shown in red. The structural contour surface of the Onondaga Limestone is shown below the wellbores. The display is interactive permitting the user to zoom, rotate, and pan the display.

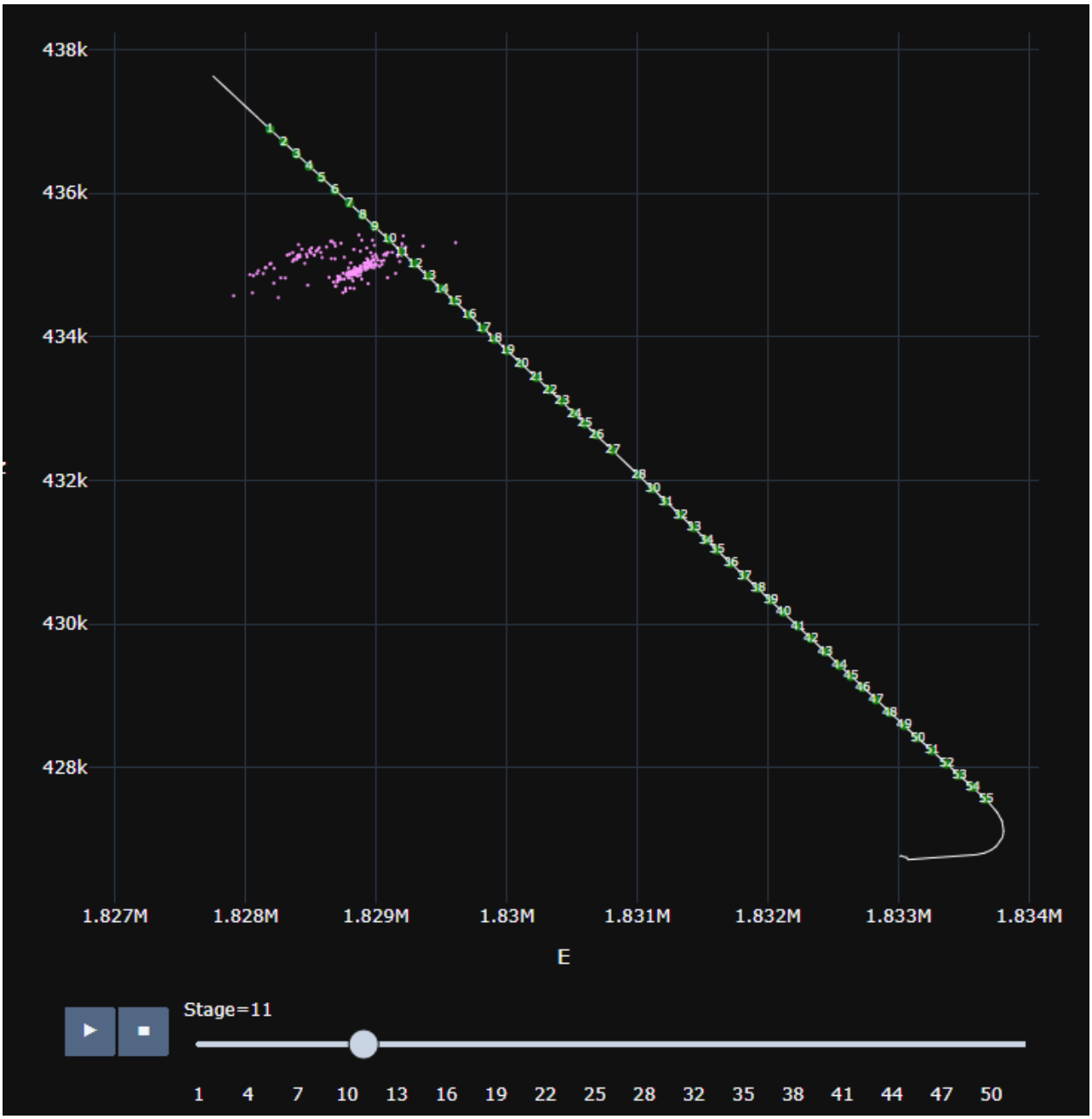

Figure 2.9: 2D map view display of the Boggess 5H and microseismic events for each stage. Display was created using python. Plugs are shown in green.

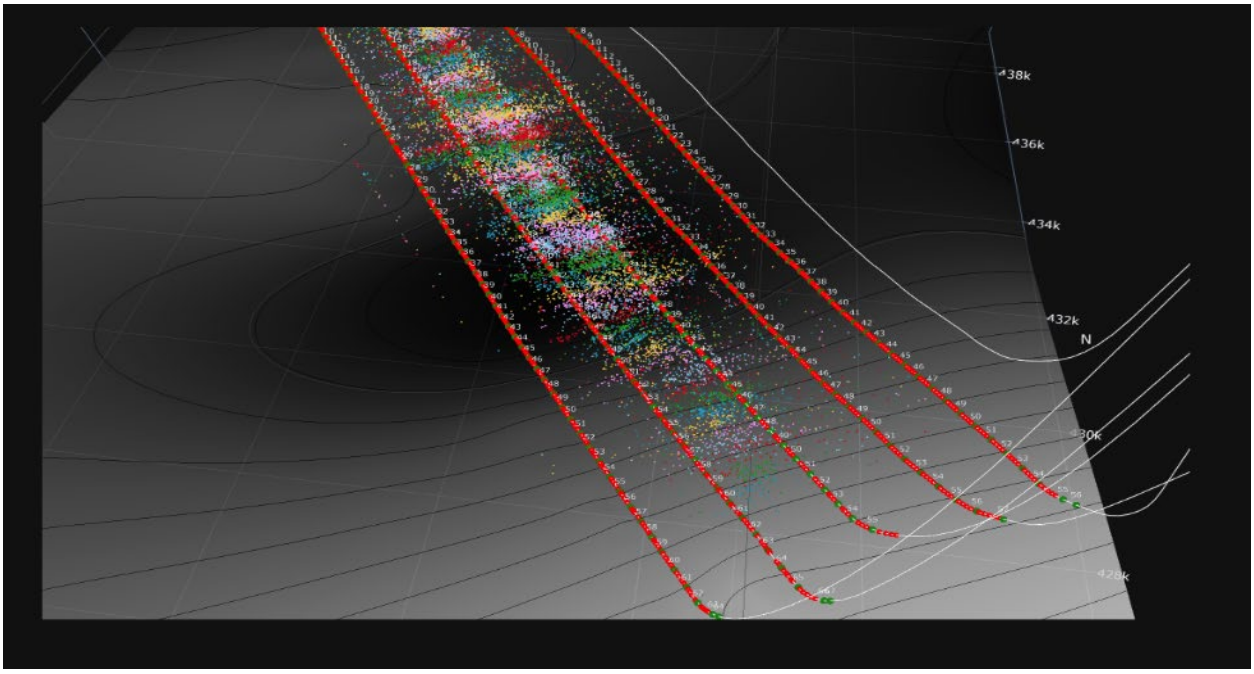

Figure 2.10: 3D model of the Boggess well pad showing Boggess 5H microseismic events color coded by stage, plugs shown in green, and perforation clusters shown in red. The Onondaga formation structural surface is shown below.

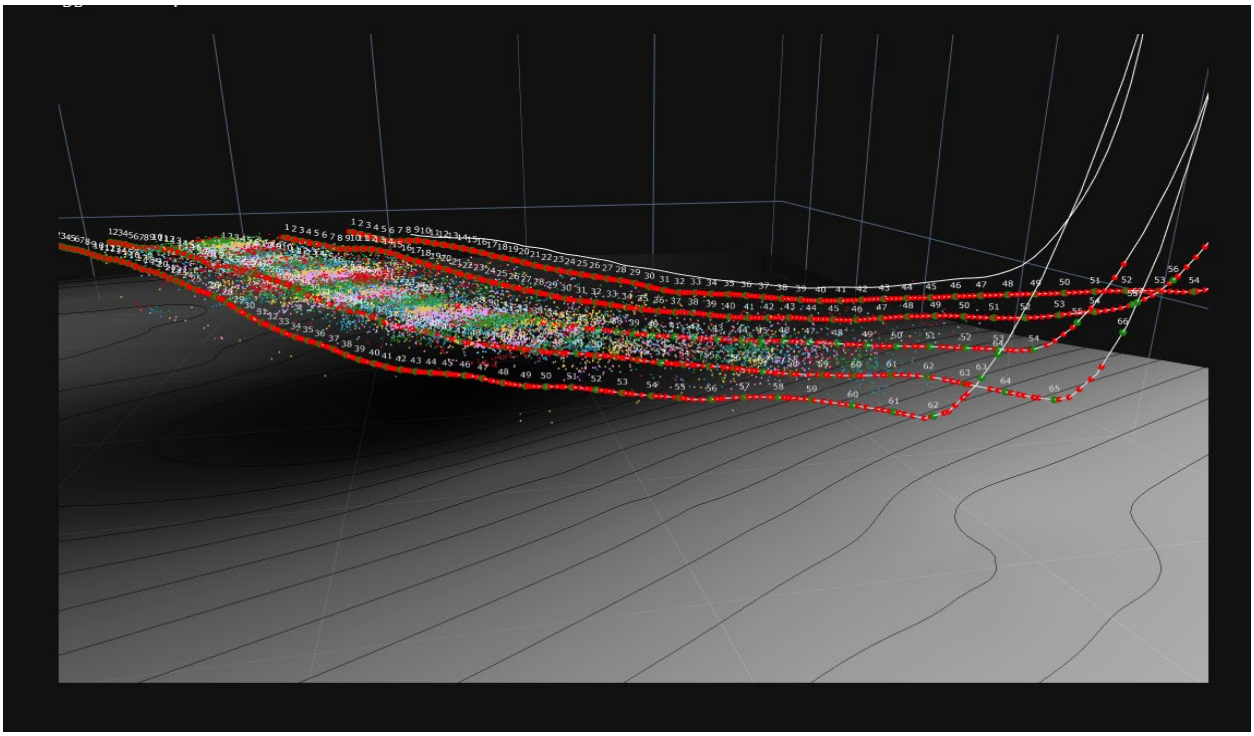

Figure 2.11: 3D model of the Boggess well pad showing Boggess 5H microseismic events color coded by stage, plugs shown in green, and perforation clusters shown in red. The Onondaga formation structural surface is shown below.

Plan for Next Quarter

Add additional user controls to the python 3D model that allow layers to be turned on and off or viewing the microseismic events by time.

Analyze additional fracture interpretations for the Boggess 1H and 3H.

Topic 3 – Deep Subsurface Rock, Fluids, & Gas

Sharma Group MSEEL Report

1. **Characterization of organic matter - kerogen extraction and characterization.** The interpretation of the ^{13}C solid-state analysis of the kerogen sample extracted from Boggess 17H is complete. Different aliphatic and aromatic structural parameters were determined as shown in Table. 3.1 and Figures 3.1 and 3.2. The structural parameters indicate that aromatic carbon atoms dominate the kerogen. In the aromatic fraction, 77% of carbon atoms are contributed by protonated and aromatic bridgehead carbon atoms, followed by alkyl-substituted aromatics (15.4 %), then by oxygen substituted aromatics (0.9%). In the aliphatic fractions, the majority of the carbon atoms are contributed by alkyl carbon atoms (6.8), with minor amounts of methoxyl and amine (0.2 %), then by O and O_2 substituted alkyl (0.1%). Mobile and immobile fractions of alkyl carbon atoms were also determined by dipolar dephasing technique, which indicated that the alkyl fraction is mainly dominated by immobile alkyl (4.4%), followed by mobile and quaternary alkyl (1 %), immobile methyl (0.7%), and mobile methyl (0.6%).

Structural parameters	**Chemical Shift (ppm)**	**Boggess 17H**	**MIP-3H**
Total aliphatic	(0-90)	7.2	6.7
Total alkyl	(0-45)	6.8	6.3
Mobile methyl	(0-20)*	0.6	0.6
Mobile and quaternary alkyl	(20-45)*	1.0	1.7
Immobile methyl	(0-20)**	0.7	1.7
Immobile alkyl	(20-45)**	4.4	2.3
Methoxyl and amine	(45-60)	0.2	0.0
Methoxyl	(45-60)*	0.0	0.2
O and O_2 substituted alkyl	(60-90)	0.1	0.4
Total aromatic	(90-165)	93.3	91.5
Protonated and bridgehead aromatic	(90-135)	77.0	72.0
Alkyl substituted aromatic	(135-150)	15.4	16.7
Oxygen substituted aromatic	(150-165)	0.9	2.2
Carboxyl and amide	(165-190)	0.0	1.6
Aldehyde and ketone	190-240	0.4	0.1
*Calculated using dipolar dephasing **Calculated by subtracting multiCP spectra with dipolar dephasing spectra			

Table. 3.1: Different structural parameters (with their chemical shifts) of Boggess 17H and MIP-3H kerogen samples determined using ^{13}C solid-state NMR analysis.

The structural parameters of the Kerogen from Boggess 17H sample were compared with the kerogen from MIP-3H. Both the kerogen samples belonged to the lower Marcellus formation and have the same thermal maturity (VR_o = 3). The majority of the aliphatic and aromatic structural parameters for both samples were similar (Table. 3.1 and figures 3.1 and 3.2). Such resemblance in molecular structural parameters indicates that the deposition environment, sources of organic matter, and thermal history for both regions were similar. Such similarity also indicated that the type and amount of hydrocarbons generated in both formations would be similar.

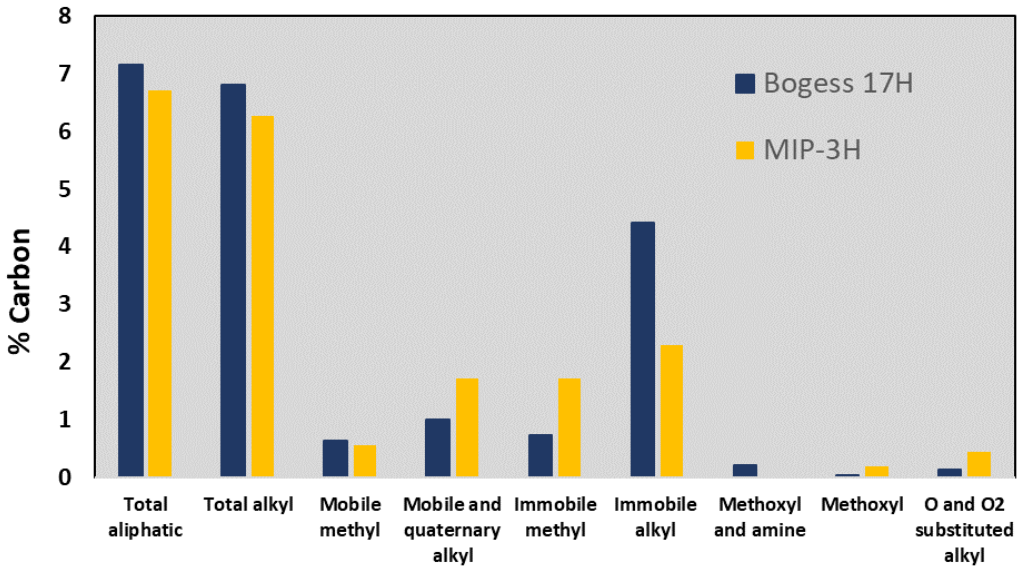

Figure 3.1: Aliphatic Structural Parameters of Boggess 17H and MIP-3H kerogen

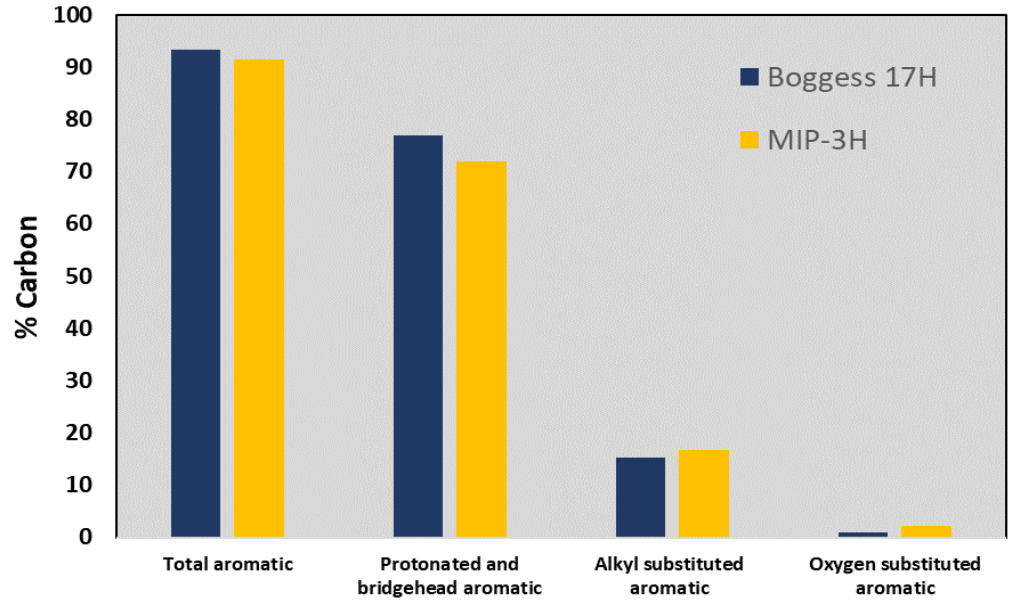

Figure 3.2: Aromatic Structural Parameters of Boggess 17H kerogen

Deliverables: 1) Present key findings in a conference in Fall 2021.

2. **High-pressure and temperature fracture fluid/shale interaction experiments.** Shale-hydraulic fracturing fluid experiments (HFF) of results using core Boggess 17H and synthetic fracturing fluid was completed (reported in the last report). The results and interpretations of these experiments and other shale-HFF experiments have been compiled in a manuscript that is expected to be submitted to a journal in Fall 2021.

To determine the heterogeneities in organic matter-HFF interactions and OM degradation mechanism at the molecular level, we performed another batch of experiments using synthetic fracturing fluids with three different oxidative breakers and kerogen concentrates from lower Marcellus (derived from a wet-gas well LM-1). The hypothesis for these experiments was that strong oxidizers could potentially degrade shale organic matter (OM) and improve shale permeability. Three synthetic HFF solutions containing oxidative breakers, namely ammonium persulfate, sodium hypochlorite, sodium bromate, were reacted with kerogen concentrate for a 14-day period (to mimic the shut-in period). Using ^{13}C solid-state NMR analysis, the molecular structural parameters of shale kerogen were characterized before and after the reaction. We also determined the net change in organic carbon percentage of original and reacted kerogen samples using Elemental Analyzer (EA) at the IsoBioGeM lab. Our preliminary results indicate sodium hypochlorite, sodium bromate-based HFF can significantly degrade kerogen by 46% and 60%, respectively (Table. 2). Ammonium persulfate, on the other hand, does not degrade organic matter (Table. 2).

^{13}C NMR analysis indicated that the total aromatic carbon percentage decreased. In contrast, the aliphatic carbon chains and carboxyl and amide groups significantly increased on reaction with oxidative breakers sodium hypochlorite, sodium bromate (Table. 3, Figures 3 and 4). The increase in aliphatic carbons and decreased aromatic carbons are mainly controlled by the degradation of the protonated aromatic fraction (Table. 3, fig. 4). The fractions of alkyl-substituted aromatics, O-substituted aromatics, aldehydes, and ketone generally remained similar before and after the reaction. Our findings suggest that hydrogenated aromatic carbons are most susceptible to oxidative degradation, whereas aliphatic, carboxyl and amide groups have low susceptibility to oxidative degradation.

Our results demonstrate that, although oxidative breakers are generally added to fracturing fluids for increasing well productivity by improving the viscosity of gel-based fluids, these oxidizers can significantly degrade shale organic matter (OM) and improve shale permeability. Our results also indicate that several organic contaminants (such as BTEX and PAHs) could also be released due to these degradation reactions, which should be tested in future studies.

Table. 3.2 Organic carbon percentage of original kerogen concentrate and reacted kerogen concentrate with three synthetic HFF solutions containing oxidative breakers sodium hypochlorite and sodium bromate

Sample ID	Sample Description	C%
LM-1	LM-1 kerogen concentrate	24.42
LM-1 SB	Kerogen reacted with HFF containing Sodium Bromate	13.3
LM-1 SH	Kerogen reacted with HFF containing Sodium Hypochlorite	9.78
LM-1 AMP	Kerogen reacted with HFF containing Ammonium Persulfate	25.62

Table. 3.3: Different structural parameters of LM-1 kerogen and kerogen samples reacted with HFF containing Sodium Bromate (LM1-SB) and Sodium Hypochlorite (LM1- SH) determined using ^{13}C solid-state NMR analysis.

Structural parameters	LM-1	LM1- SB	LM1-SH
Total aliphatic	13	25.61	30.29
Total alkyl	8	15.43	17.79
Methoxyl and amine	0	3.66	3.3
O and O2 substituted alkyl	0	6.52	9.2
Total aromatic	89	64.82	53.78
Aromatic Bridgehead	32	24.56	24.03
Protonated aromatic	39	16	8
Alkyl substituted aromatic	16	19.9	15.76
Oxygen substituted aromatic	3	4.37	5.51
Carboxyl and amide	2	7.75	12.27
Aldehyde and ketone	3	1.81	3.66

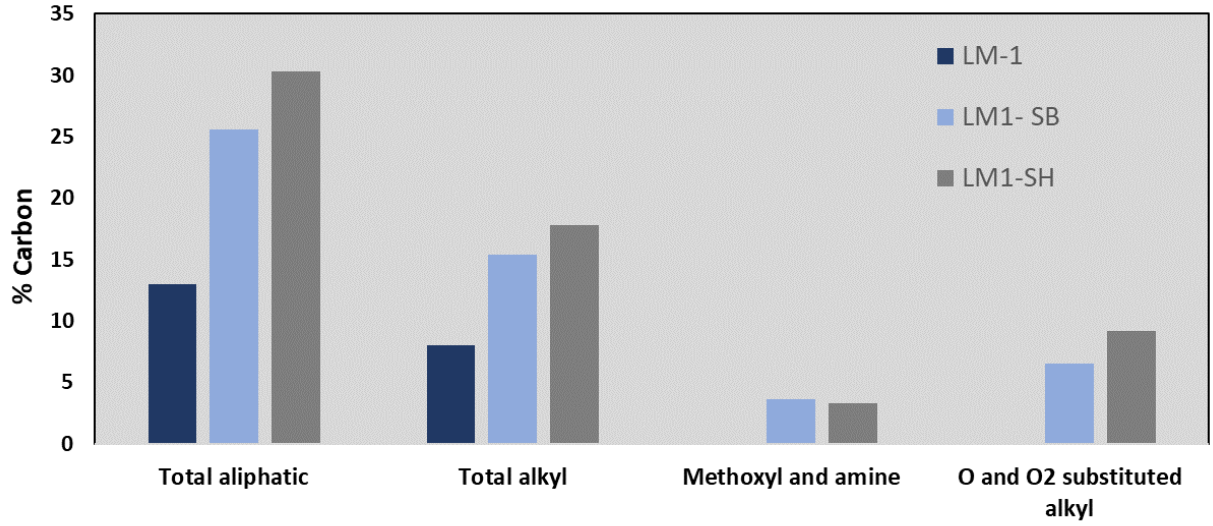

Figure 3.3: Aliphatic carbon % of LM-1 kerogen and kerogen samples reacted with HFF containing Sodium Bromate (LM1-SB) and Sodium Hypochlorite (LM1- SH)

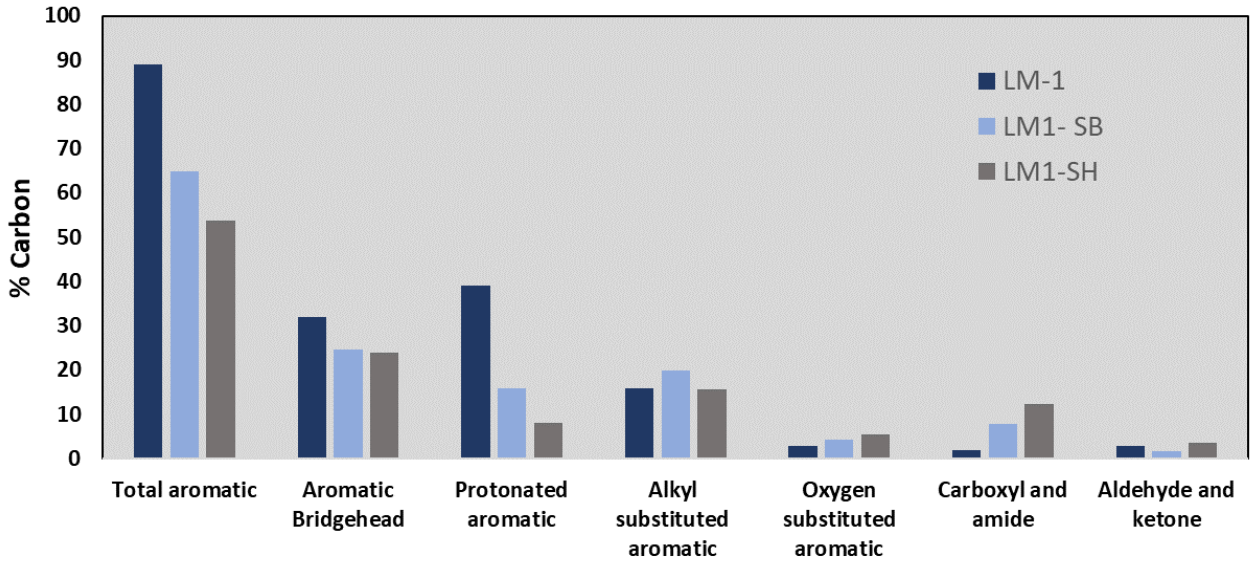

Figure 3.4: Aromatic, carboxyl, and carbonyl % of LM-1 kerogen and kerogen samples reacted with HFF containing Sodium Bromate (LM1-SB) and Sodium Hypochlorite (LM1- SH)

Deliverables: 1) Submit two manuscripts with the results of high P-T fracture fluid interaction experiments in Fall 2021. 2) Present key findings at a conference in Fall 2021.

OSU MSEEL Input April-May 2021

Mouser Group

The team collected new samples at the MSEEL II field site this quarter, and sent a large number of samples to EMSL (under their FICUS proposal) for analysis of proteins, lipids, metabolites.

Cole Group

Manuscript in preparation:

High resolution mineralogy of organic matter-rich horizons from the Marcellus Shale Energy and Environment Laboratory

Authors: Julia M. Sheets, Susan A. Welch, Rebecca A. Daly, Andrea J. Hanson, Alexander M. Swift, Tingting Liu, Tim Kneafsey, Stefano Cabrini, Paula Mouser, Shikha Sharma, Tim Carr and David R. Cole

Journal submission to: AAPG bulletin

Topic 4 – Produced Water and Solid Waste Monitoring

Approach

MIP Site

Over five years into the post-completion part of the program, the produced water and solid waste component of MSEEL has continued to monitor changes in produced water quality and quantity systematically. During year one of the study, hydraulic fracturing fluid, flowback, produced water, drilling muds and drill cuttings were characterized according to their inorganic, organic and radiochemistries. In addition, surface water in the nearby Monongahela River was monitored upstream and downstream of the MSEEL drill pad. Toxicity testing per EPA method 1311 (TCLP) was conducted on drill cuttings in both the vertical and horizontal (Marcellus) sections to evaluate their toxicity potential. Sampling frequency has been slowly scaled back following well development. Table 1 shows an "X" for sample collection dates. Wells 4H and 6H were brought back online in late 2016. Other blank sample dates in Table 1 indicate that samples were not collected, due to lack of availability of produced water from the well(s).

Table 4.2. MIP sampling events are indicated with an "X".

Year	2015		
Day/Month	10-Dec	17-Dec	22-Dec
3H	X		X
4H			
5H	X	X	X
6H			

Year	2016												
Day/Month	6-Jan	20-Jan	3-Feb	2-Mar	23-Mar	20-Apr	18-May	2-Jul	17-Aug	21-Jun	19-Oct	16-Nov	14-Dec
3H	X	X	X		X	X	X	X	X	X	X		X
4H												X	X
5H	X	X	X	X	X	X	X	X	X	X	X	X	
6H												X	X

Year	2017							
Day/Month	13-Jan	14-Feb	13-Mar	7-Apr	5-May	12-Jul	3-Nov	20-Dec
3H	X	X	X	X	X	X	X	X
4H	X	X	X	X	X			
5H		X			X			X
6H	X	X	X	X	X			

Year	2018					
Day/Month	22-Jan	23-Feb	16-May	2-Aug	16-Oct	15-Dec
3H	X	X	X	X		X
4H	X	X	X	X	X	X
5H	X		X		X	X
6H			X	X		

Year	2019							
Day/Month	24-Jan	5-Mar	6-May	13-Jun	18-Sep	21-Oct	21-Nov	30-Dec
3H	X	X	X	X	X	X	X	X
4H	X	X					X	X
5H	X	X	X	X	X	X	X	X
6H		X					X	X

Year	2020									
Day/Month	30-Jan	27-Feb	25-Mar	28-Apr	27-May	30-Jul	5-Oct	26-Oct	24-Nov	30-Dec
3H	X	X	X	X	X	X	X	X	X	X
4H	X	X	X	X	X				X	X
5H		X	X	X	X	X	X	X	X	X
6H	X	X	X	X						X

Year	2021				
Day/Month	27-Jan	26-Feb	25-Mar	28-Apr	27-May
3H	X	X	X	X	X
4H	X	X	X	X	X
5H	X	X	X	X	X
6H	X	X	X		

Boggess Site

Two control wells; 9H and 17H were selected for solids and aqueous studies at the newly developed Boggess well site.

Tophole was completed in Feb 2019 for 9H and Jan 2019 for 17H. Samples of vertical drilling were not obtained due to completion prior to the start of the Boggess project.

Horizontals were initiated on 19 June 2019 for 17H and 20 May 2019 for 9H (Table 4.2). A drilling mud sample along with depth samples at 8,500ft; 10,000ft; 11,000ft; 13,000ft; and 15,000ft were collected and analyzed for parameters shown in Table 3.

Table 4.3. Sample depth and dates for collection of horizontal drilling mud and cutting samples.

Depth/Well	Mud 9H	8500 9H	10000 9H	11000 9H	13000 9H	15000 9H
Date	5/27/2019	5/27/2019	5/28/2019	5/29/2019	5/29/2019	5/30/2019

Depth/Well	Mud 17H	8500 17H	10000 17H	11000 17H	13000 17H	15000H
Date	7/1/2019	7/1/2019	7/1/2019	7/1/2019	7/1/2019	7/1/2019

Table 4.4. Solids analysis list.

Analysis	Method	Units	Parameter
Diesel Range Organics by GC-FID	SW8015M	mg/kg-dry	DRO (C10-C28)
			ORO (C28-C40)
		% Rec	Surr: 4-terphenyl-d14
Gasoline Range Organics by GC-FID	SW8015D	ug/Kg	GRO C6-C10)
		% Rec	Surr: Toluene-d8
Volatile Organic Compounds	SW8260B	ug/kg-dry	Ethylbenzene
			m,p- Xylene
			o- Xylene
			Styrene
			Toluene
			Xylenes total
		% Rec	Surr: 1,2- Dichloroethane-d4
			Surr: 4-Bromofluorobenzene
			Surr: Dibromofluoromethane
			Surr: Tolouene-d8
Radionuclides	EPA 901.1	pCi/g	Potassium-40
			Radium-226
			Radium-228
	9310		Gross Alpha
			Gross Beta
Inorganics	SW9056A	mg/kg-dry	Br
			Cl
			SO4
	SW9034		sulfide
	E353.2		nitrate
	E354.1		nitrite
	A2510M	µS/cm	EC
	SW9045D	units	pH
	A4500-CO2 D	mg/kg-dry	alk bicarb
			alk carb
			alk t
	E365.1 R2.0		TP
	SW6020A		Ag
			Al
			As
			Ba
			Ca
			Cr
			Fe
			K
			Li
			Mg
			Mn
			Na
			Ni
			Pb
			Se
			Sr
			Zn
Moisture	E160.3M	%	Moisture
Chemical Oxygen Demand	E4104 R2.0	mg/kg-dry	COD
Organic Carbon - Walkley-Black	TITRAMETRIC	% by wt-dry	OC-WB
Oil & Grease	SW9071B - OG	mg/kg-dry	O&G

Flowback sampling was initiated on 18 Nov 2019 with weekly collection at 9H and 17H for the first four weeks (Table 4.4). Monthly sampling began following the initial weekly sampling effort.

Table 4.5. Boggess sampling events are indicated with an "X".

Year	2019			
Day/Month	18-Nov	25-Nov	2-Dec	10-Dec
9H	X	X	X	X
17H	X	X	X	X

Year	2020									
Day/Month	30-Jan	27-Feb	25-Mar	28-Apr	27-May	30-Jul	5-Oct	26-Oct	24-Nov	16-Dec
9H	X	X	X	X	X	X	X	X	X	X
17H	X	X	X	X	X	X	X	X	X	X

Year	2021				
Day/Month	27-Jan	26-Feb	25-Mar	28-Apr	27-May
9H	X	X	X	X	X
17H	X	X	X	X	X

Results & Discussion

MIP Site

Major ions – trends in produced water chemistry

While makeup water was characterized by low TDS (total dissolved solids) and dominance of calcium and sulfate ions, produced water from initial flowback is essentially a sodium/calcium chloride water (**Figure 4.1**).

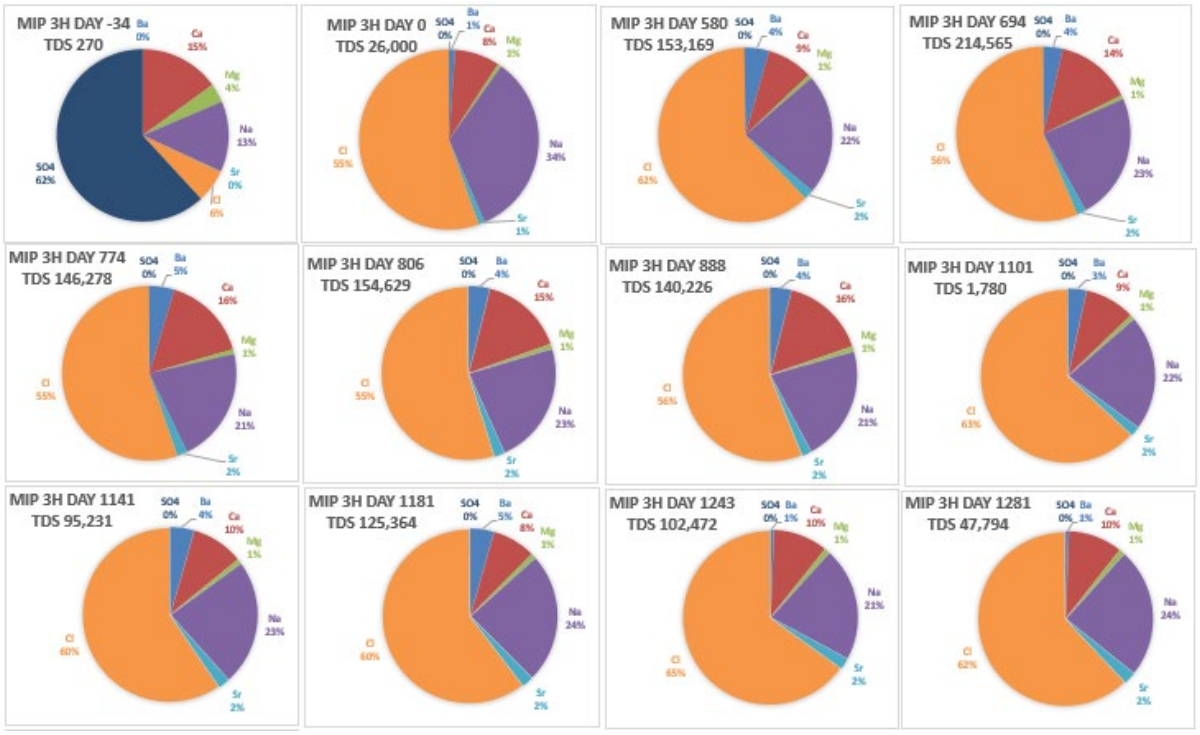

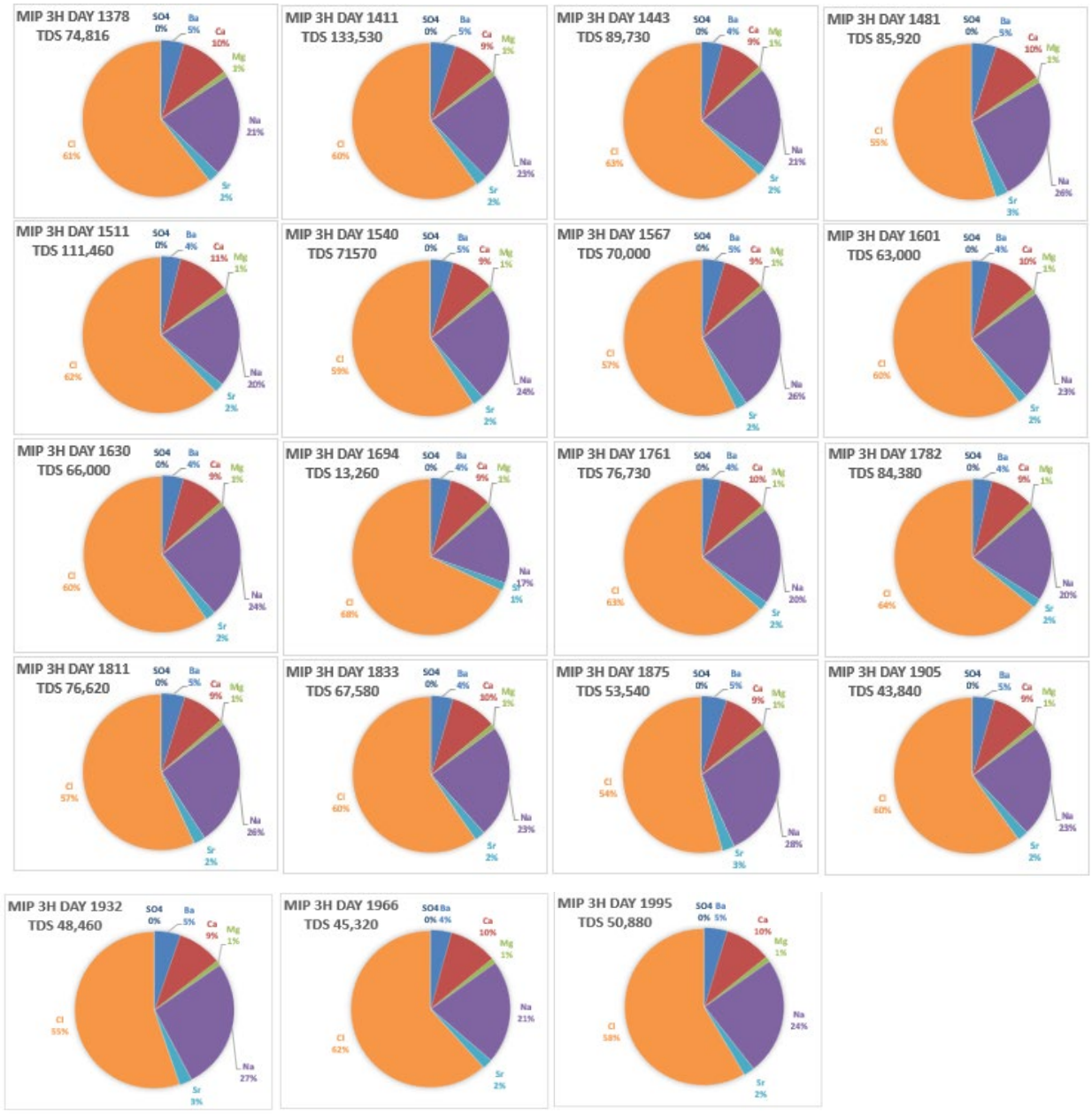

Figure 4.5. Changes in major ion concentrations in produced water from well MIP 3H. Top left Day -34 represents makeup water from the Monongahela River, produced water on the first day (Day 0) and the remainder of pie charts show flowback and produced water on sampling dates through the 1995th day post-completion.

TDS in wells 3H and 5H increased rapidly over the initial 90 days post-completion, while TDS stabilized between 100,000 and 215,000 mg/L through day 1181(3H). Note that 3H and 5H were both shut-in near day 966 and brought back online before sampling day 1101. Values varied between sampling dates 1101 through day 1411 and again on day 1694, which may reflect additional well closures. Beginning on day 1443, 5H stabilizes between 120,000 and 186,000 mg/L (Figure 4.2), with the exception of day 1694. 3H shows a decreasing trend in recent sampling events (post day 1811).

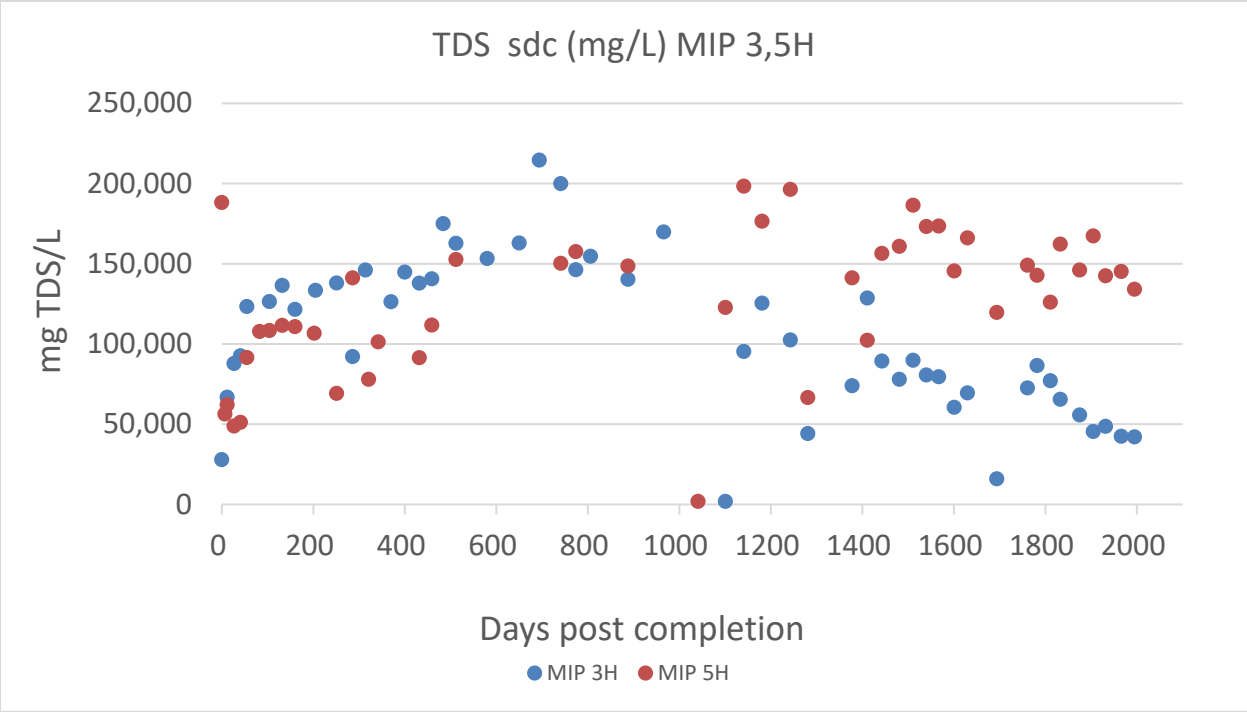

Figure 4.6. Changes in produced water TDS sdc (sum of dissolved constituents) through the first 1995 days post-completion (3,5H).

The older 4H and 6H wells were shut down numerous times during the study period. When wells return online, TDS values increase during subsequent sampling events. TDS ranges at 4H from 50,000 to 150,000 mg/L during times when wells are online and from 30,000 to 150,000 mg/L at 6H (Figure 4.3).

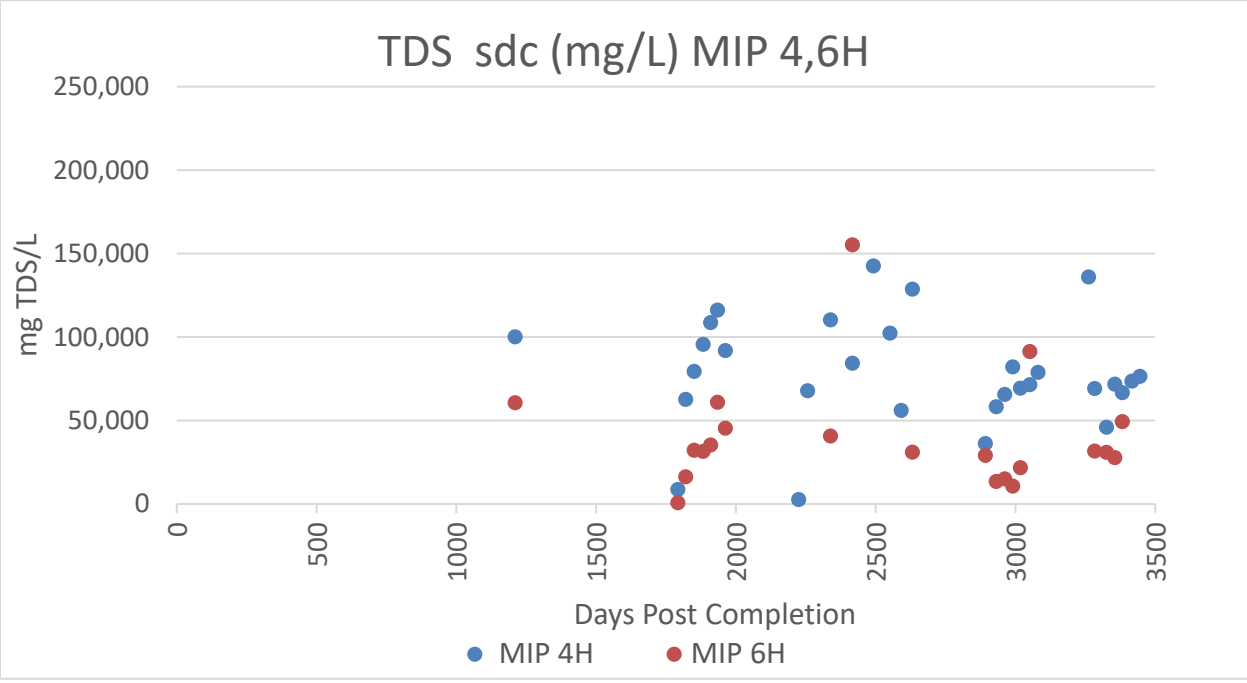

Figure 4.7. Changes in produced water TDS sdc (sum of dissolved constituents) from day 1793 through 3446 days post completion (4,6H).

Water soluble organics

The water-soluble aromatic compounds in produced water: benzene, toluene, ethylbenzene and xylene were never high. With two exceptions at post completion day 314 and 694, benzene remained below 30 µg/L during the first 600 days. This seems to be a characteristic of dry gas geologic units. After five years, benzene has mostly declined below the drinking water standard of 5 µg/L. Toluene ranged between 12 and 31 µg/L, with the exception of day 41. Values have remained below 5 µg/L since day 580 (Figure 4.4).

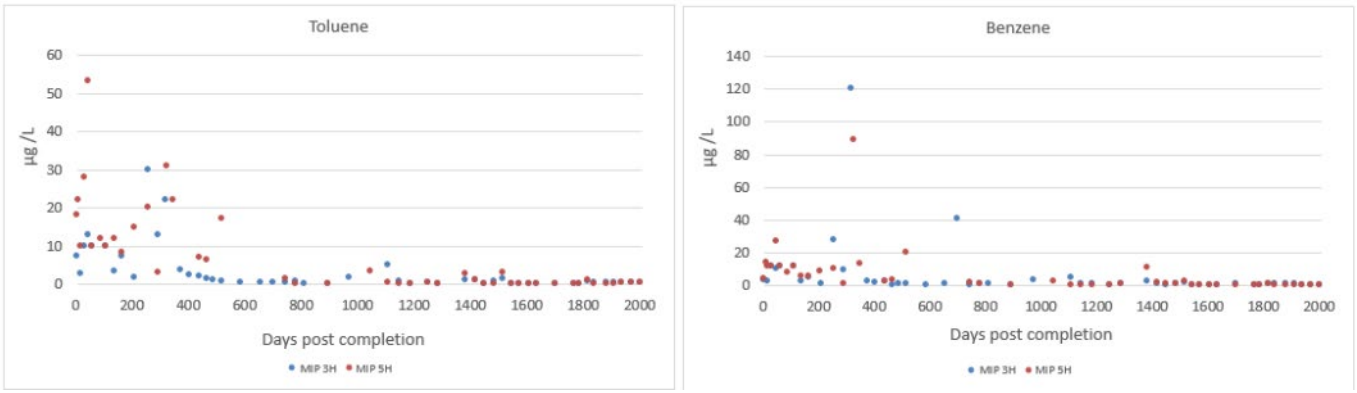

Figure 4.8. Changes in benzene and toluene concentrations. The figure shows data from well both 3H and 5H through day 1995.

Wells 4H and 6H have remained below 5 µg/L for both Toluene and Benzene for the duration of sampling events (Figure 4.5), with the exception of 6H on day 1793 with a toluene value of 5.4 µg/L.

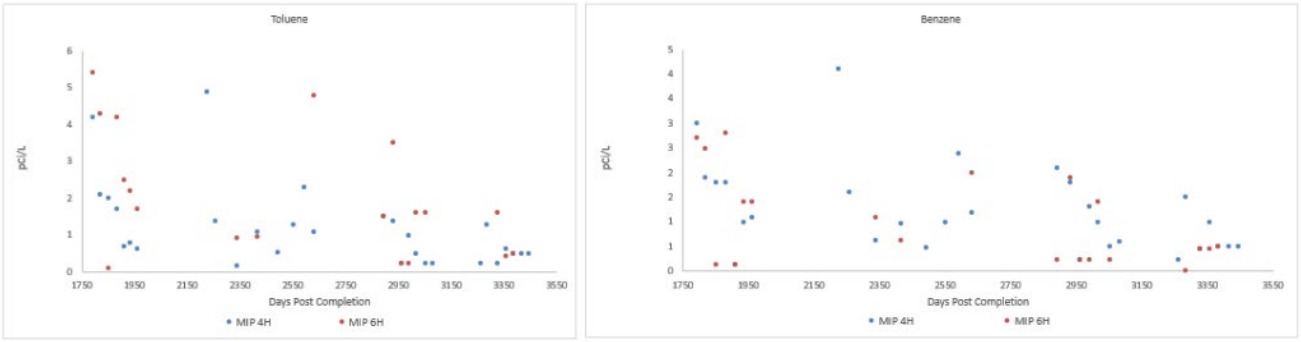

Figure 4.9. Changes in benzene and toluene concentrations. The figure shows data from well both 4H and 6H through day 3446.

Radium isotopes

The radiochemical concentrations were determined by Pace Analytical in Greensburg PA, a state certified analytical lab. Radium concentrations generally increased through 880 days post completion at wells MIP 3H and 5H. Maximum levels of the radium isotopes reached about 22,942 pCi/L at the unchoked 3H well and around 18,809 pCi/L 5H. After returning online prior to day 966, both wells have remained below 16,000 pCi/L through day 1995 (Figure 4.6).

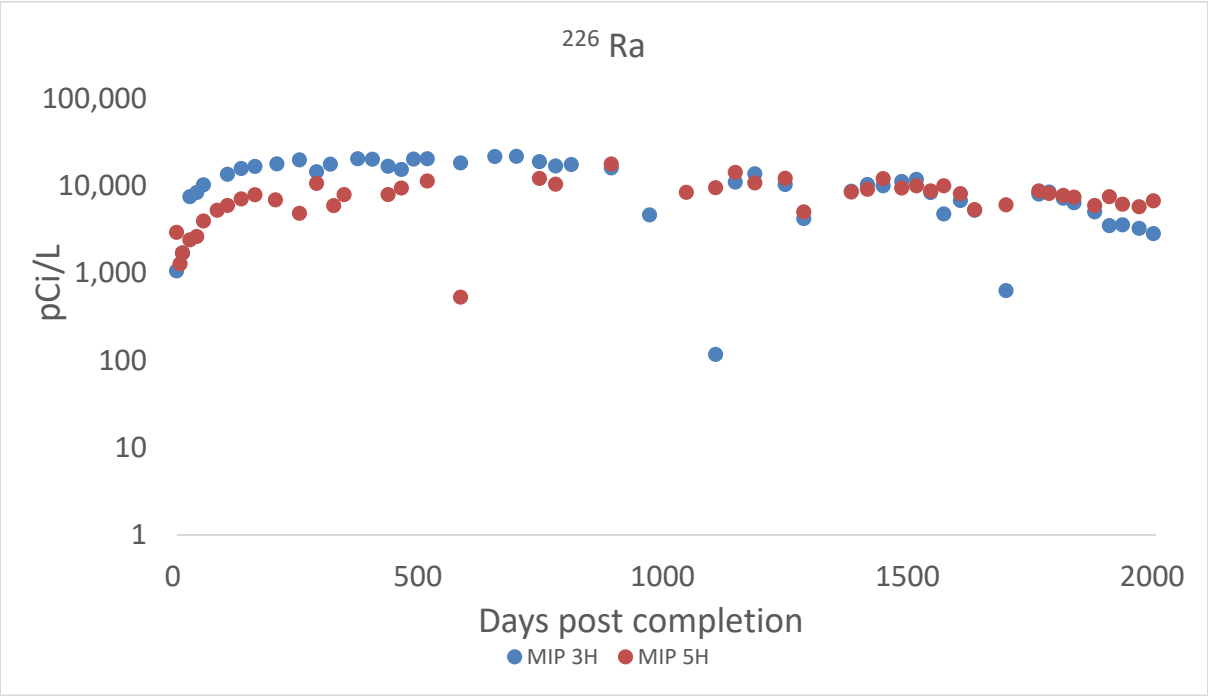

Figure 4.10. The radium isotopes are plotted against days post well completion through day 1995.

Radium concentrations at wells 4H and 6H were below 9,000 pCi/L during all sampling periods. Both wells were choked after day 1963. Well 4H was reopened at day 2225, radium was 58 pCi/L on the first sampling after the reopening and 3719 pCi/L at day 2257, a month later (Figure 4.7) peaked at 5,127 pCi/L then returned to 3,892 pCi/L. The same trend is noted at day 2492 when 4H returned online with 57 pCi/L then peaked at day 2632 with 8,197 pCi/L.

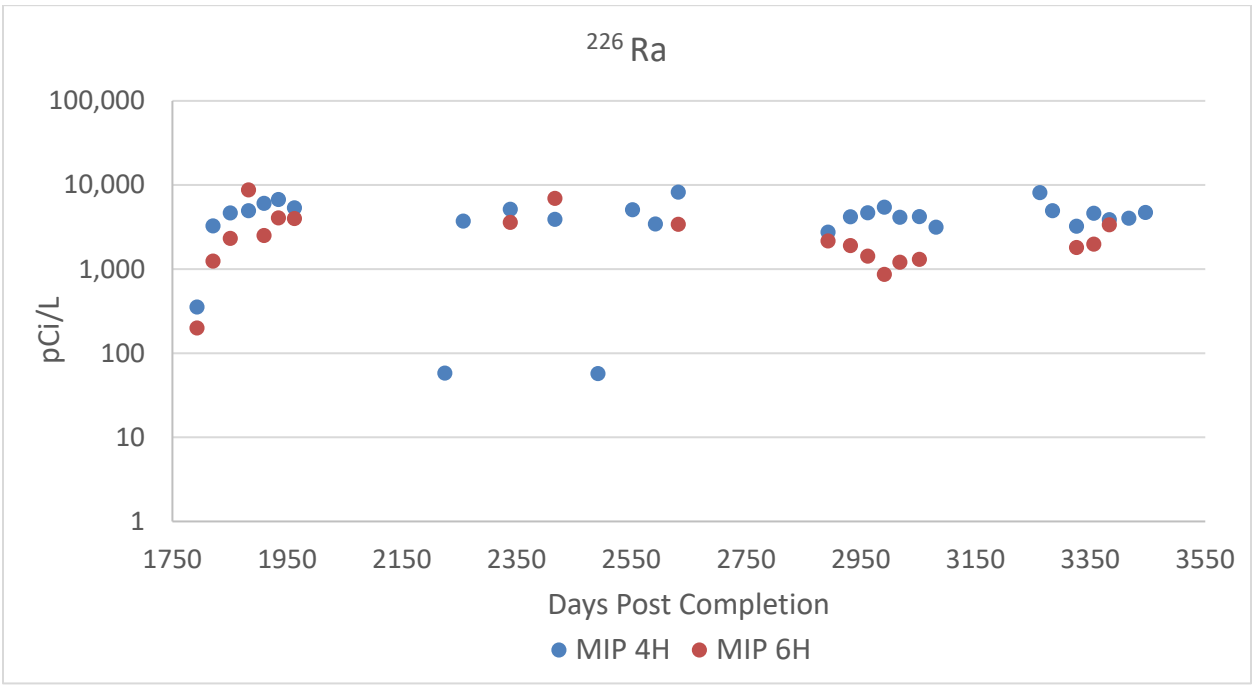

Figure 4.11. The radium isotopes are plotted against days post well completion through day 3446.

Figure 8 and Figure 9 show the relationship between gross alpha and ^{226}Ra at 3H and 5H through day 1995. Analysis for alpha was not conducted after day 1181.

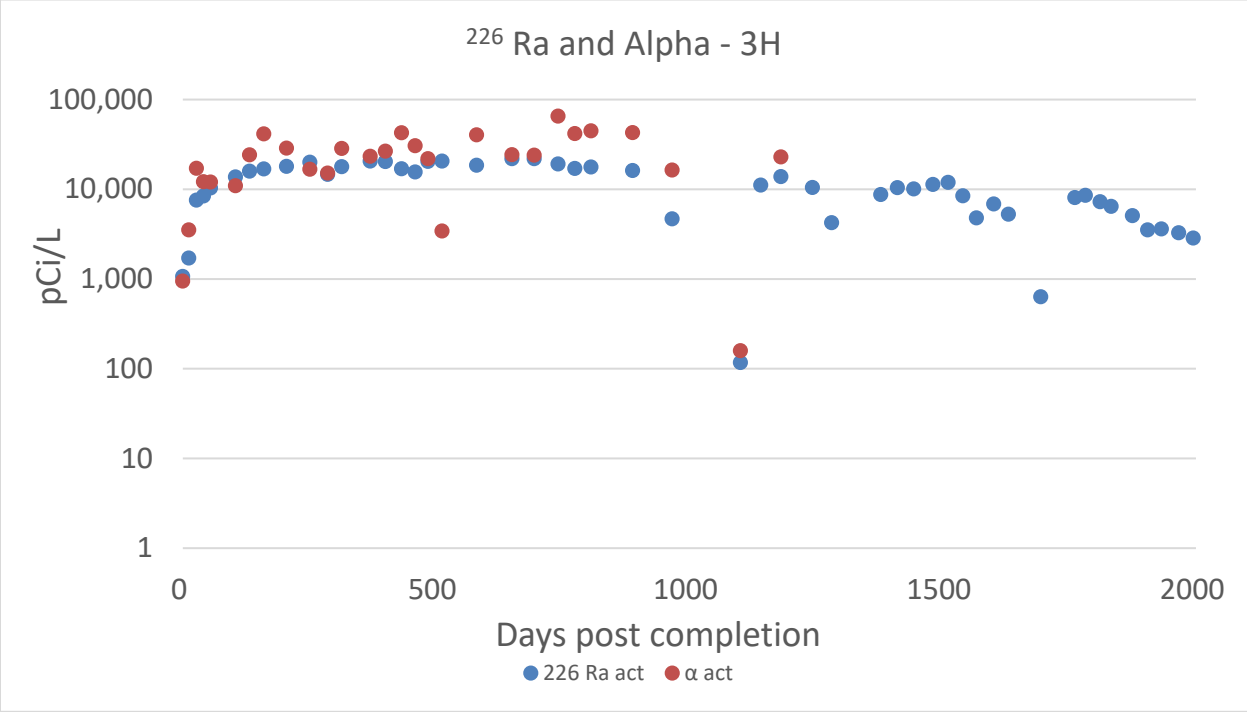

Figure 4.12. The relationship between gross alpha and ^{226}Ra as a function of time post completion at 3H. Note: analysis for alpha was not conducted after day 1181.

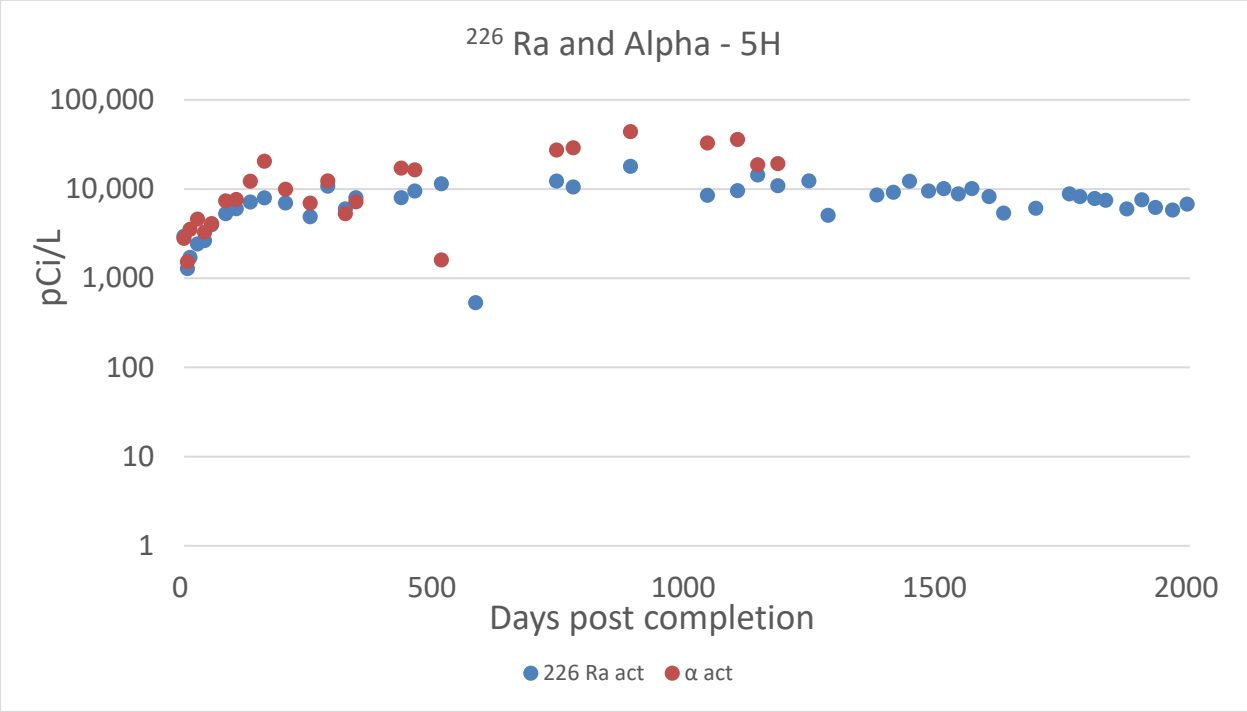

Figure 4.13. The relationship between gross alpha and ^{226}Ra as a function of time post completion at 5H. Note: analysis for alpha was not conducted after day 1181.

The highest values reported in the older wells at 4H and 6H were 17,550 pCi/L gross alpha and 8,197 pCi/L ^{226}Ra. The relationship between gross alpha and ^{226}Ra for wells 4H and 6H are shown in Figure 10 and Figure 11. Alpha was not determined after day 2632. Sample volume was not sufficient to perform analysis for radiologicals at 6H on day 3284. Values for Ra^{226} ranged from 1,821 to 3,262 pCi/L with the exception of days 228, 2225, and 2492 when 4H presumably came back online.

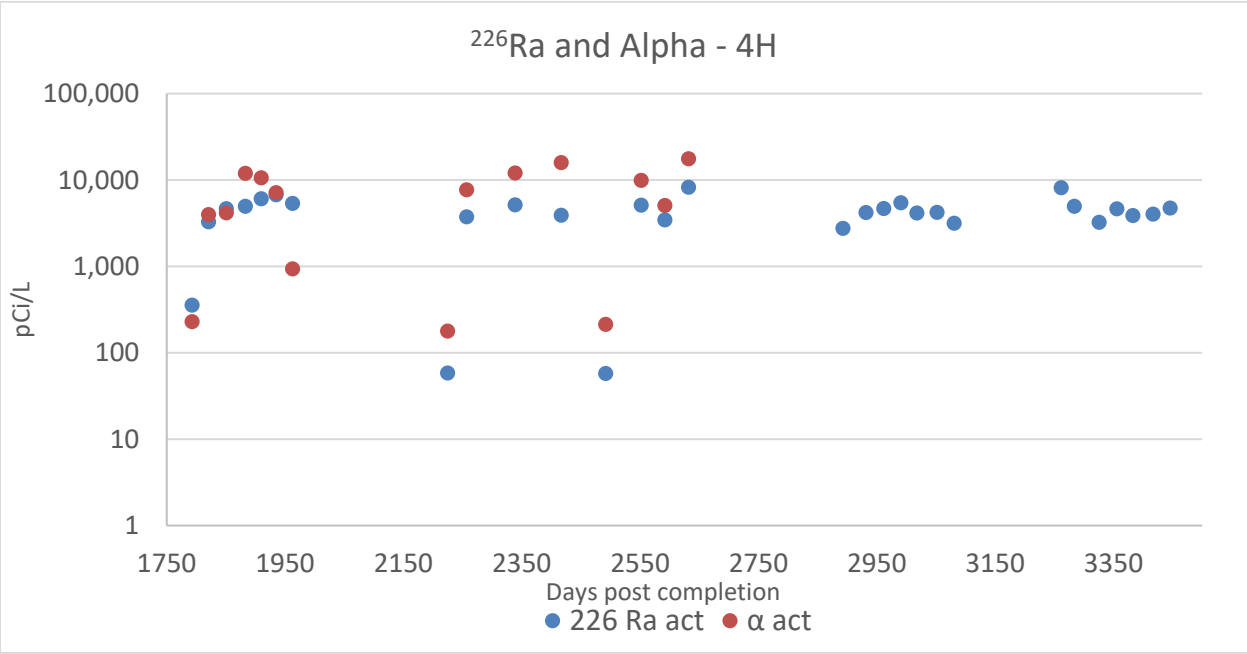

Figure 4.14. The relationship between gross alpha and ^{226}Ra as a function of time post completion at 4H. Note: analysis for alpha was not conducted after day 2632.

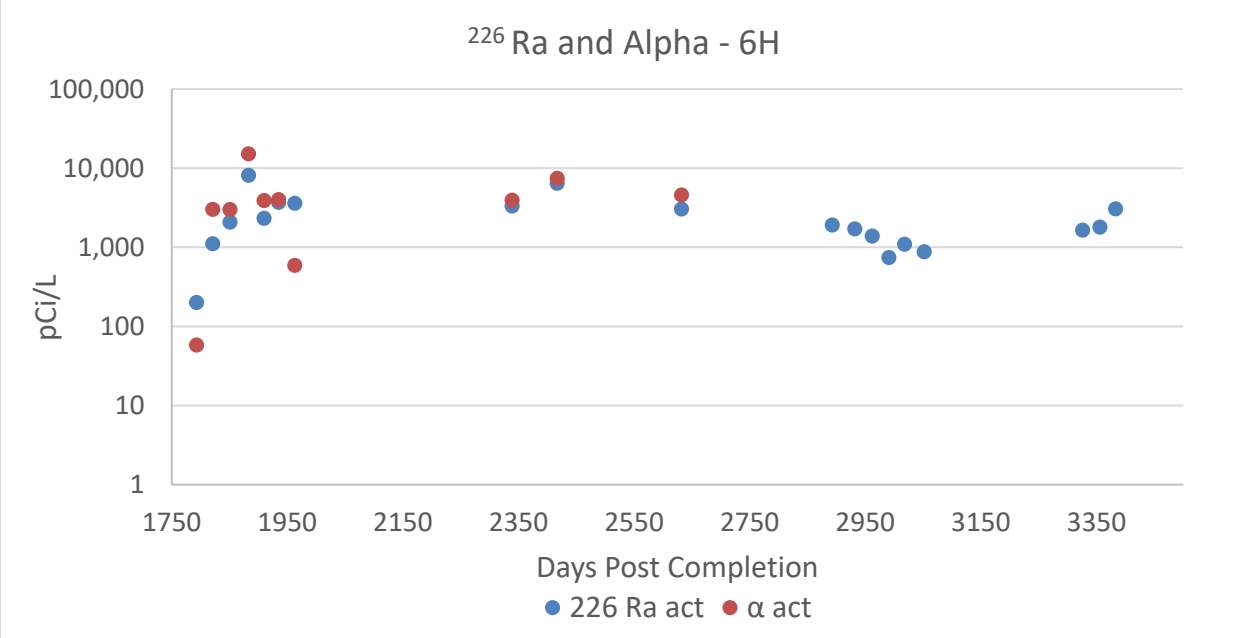

Figure 4.15. The relationship between gross alpha and ^{226}Ra as a function of time post completion at 6H. Note: analysis for alpha was not conducted after day 2632.

Boggess Well

The drilling mud and drill cutting samples were prepared using USEPA method SW3050. The resulting extracts were then analyzed using ICPMS. Method SW3050B uses both hydrochloric acid, nitric acid and hydrogen peroxide. It is used to identify components of the solid matrix that are may become mobile. It does not normally break down a rock's alumino-silicate structure. The acids would dissolve any carbonates and the peroxide would oxidize pyrites which are abundant in the Marcellus formation. This accounts for the high concentrations of Ca, Mg and Fe. Presumably, most sulfates generated during pyrite oxidation would precipitate as gypsum, barite and strontianite given the abundance of Ca, Ba and Sr in Marcellus formation fluids.

Solids

Drilling muds and cuttings were collected from 9H at depth intervals of 8,500ft; 10,000ft; 11,000ft; 13,000ft; and 15,000ft. Parameters (e.g. alk, Al, Ba, Ca, Cl, Fe, K, Mg, Mn, Na, and Sr) are shown in Figure 4.12. Drill cuttings from 9H are predominately calcium (Ca) and iron (Fe). The full list of solids parameters and methods are shown in Figure 4.3.

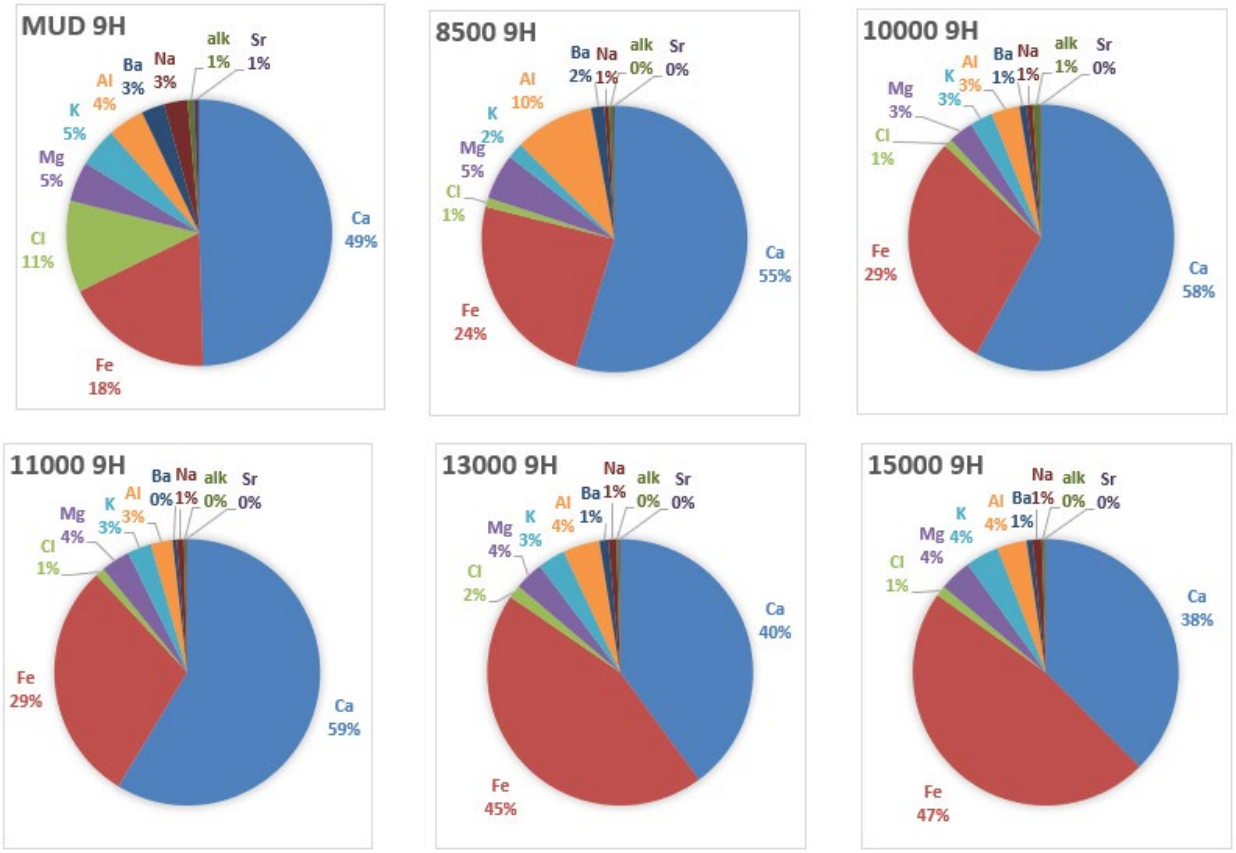

Figure 4.16. Anions/cations of drilling mud and cutting solids from 9H.

Figure 4.13 depicts parameters for drilling mud and cuttings from 17H. Shallower depths showed more variability in chemical composition in 17H in comparison to 9H. Deeper depths were predominately iron and calcium.

Figure 4.17. Anions/cations of drilling mud and cuttings solids from 17H.

Figure 4.14 and Figure 4.15 depict combined radium 226 and 228 of solids in drilling mud and cuttings solids from 9H and 17H.

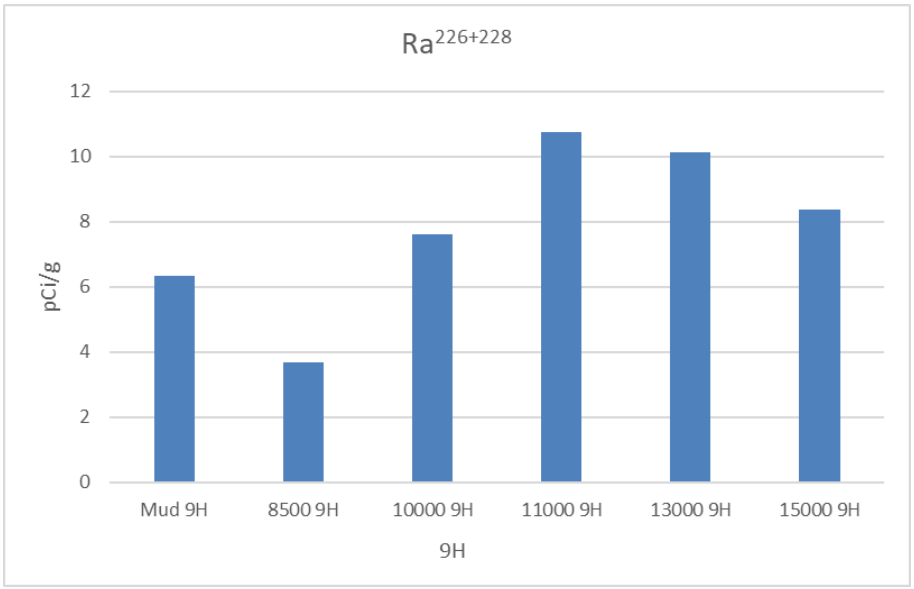

Figure 4.18. 9H Combined radium 226 and 228 for drilling mud and cuttings solids.

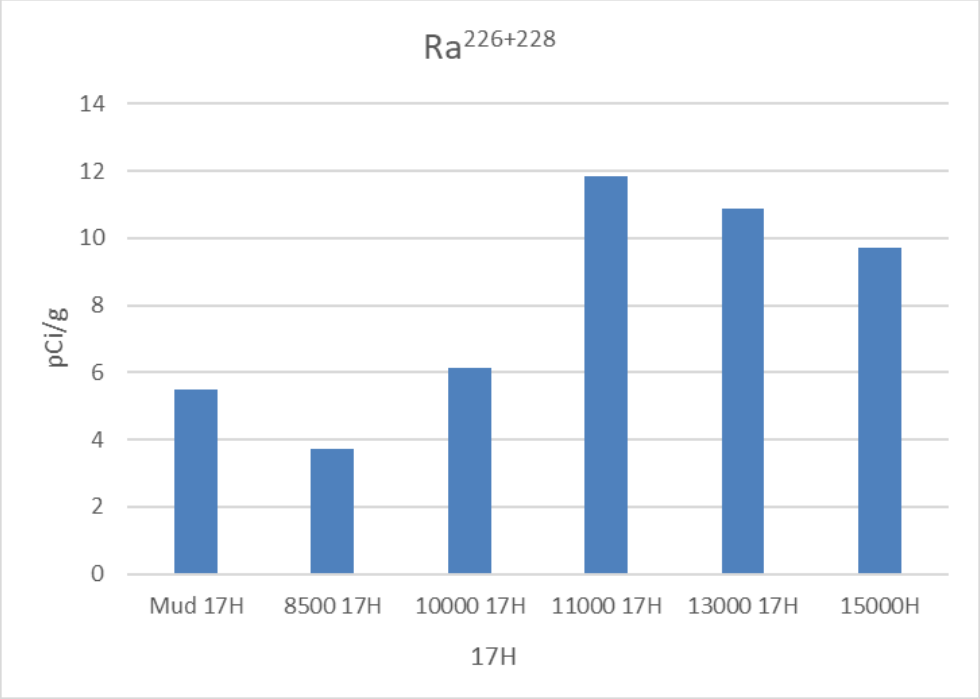

Figure 4.19. 17H Combined radium 226 and 228 for drilling mud and cuttings solids.

For comparison purposes, solids radium analysis from MIP 5H and 3H are shown in Figure 4.16 and Figure 4.17. In all wells analyzed, 3H and 5H from MIP along with 9H and 17H at Boggess, combined radium 226 and 228 remained below 12 pCi/g.

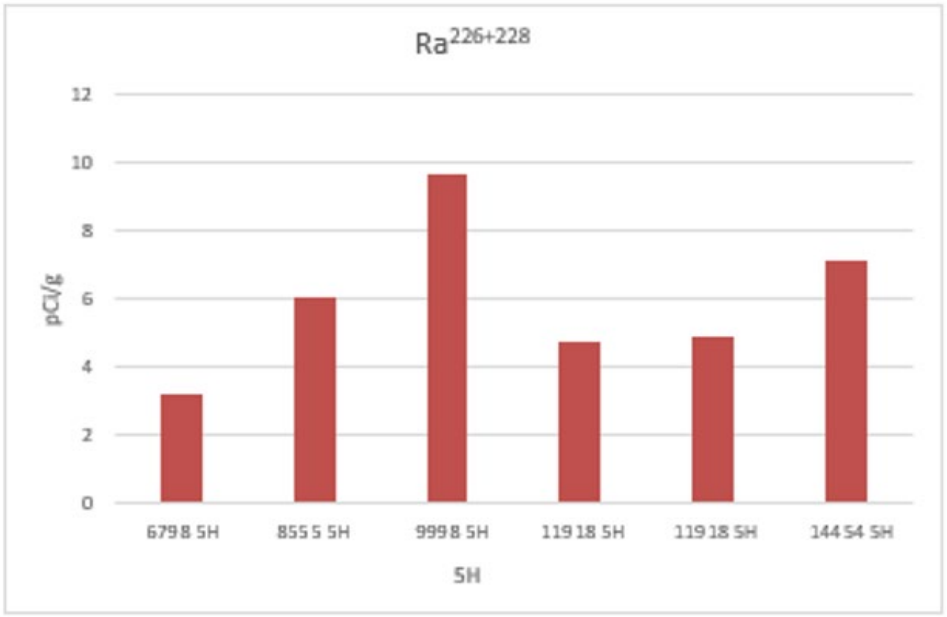

Figure 4.20. Combined Ra 226 + 228 for 5H MIP site.

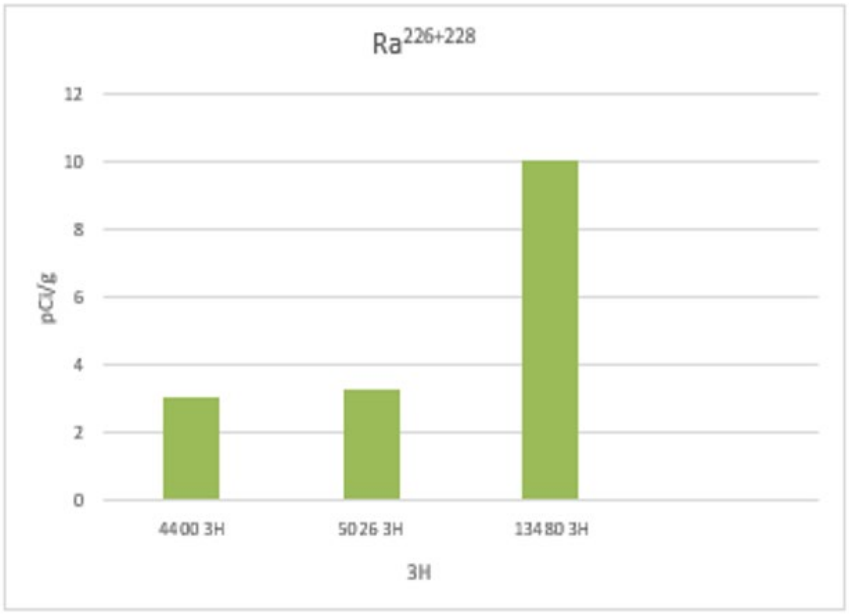

Figure 4.21. Combined Ra 226 + 228 for 3H MIP site.

Major ions – trends in produced water chemistry

While makeup water was characterized by low TDS and dominance of calcium and sulfate ions, produced water from initial flowback is essentially a sodium/calcium chloride water as noted in the earlier discussion regarding results from MIP. Preliminary results from days 0-493 at Boggess 9H and 17H are consistent with earlier results from MIP (Figure 4.18 and Figure 4.19).

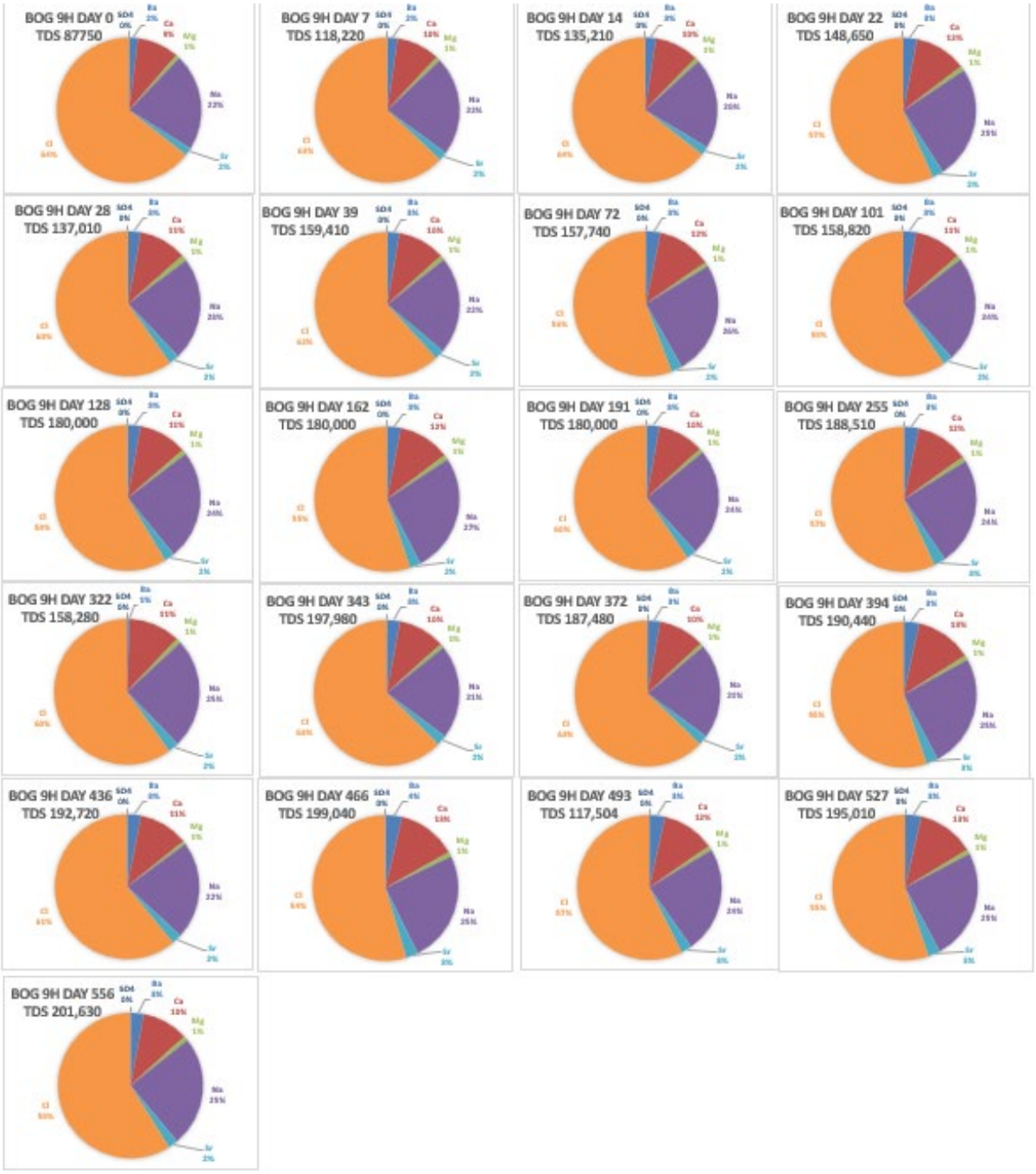

Figure 4.22. Major ion concentrations in produced water from wells Boggess 9H through day 556.

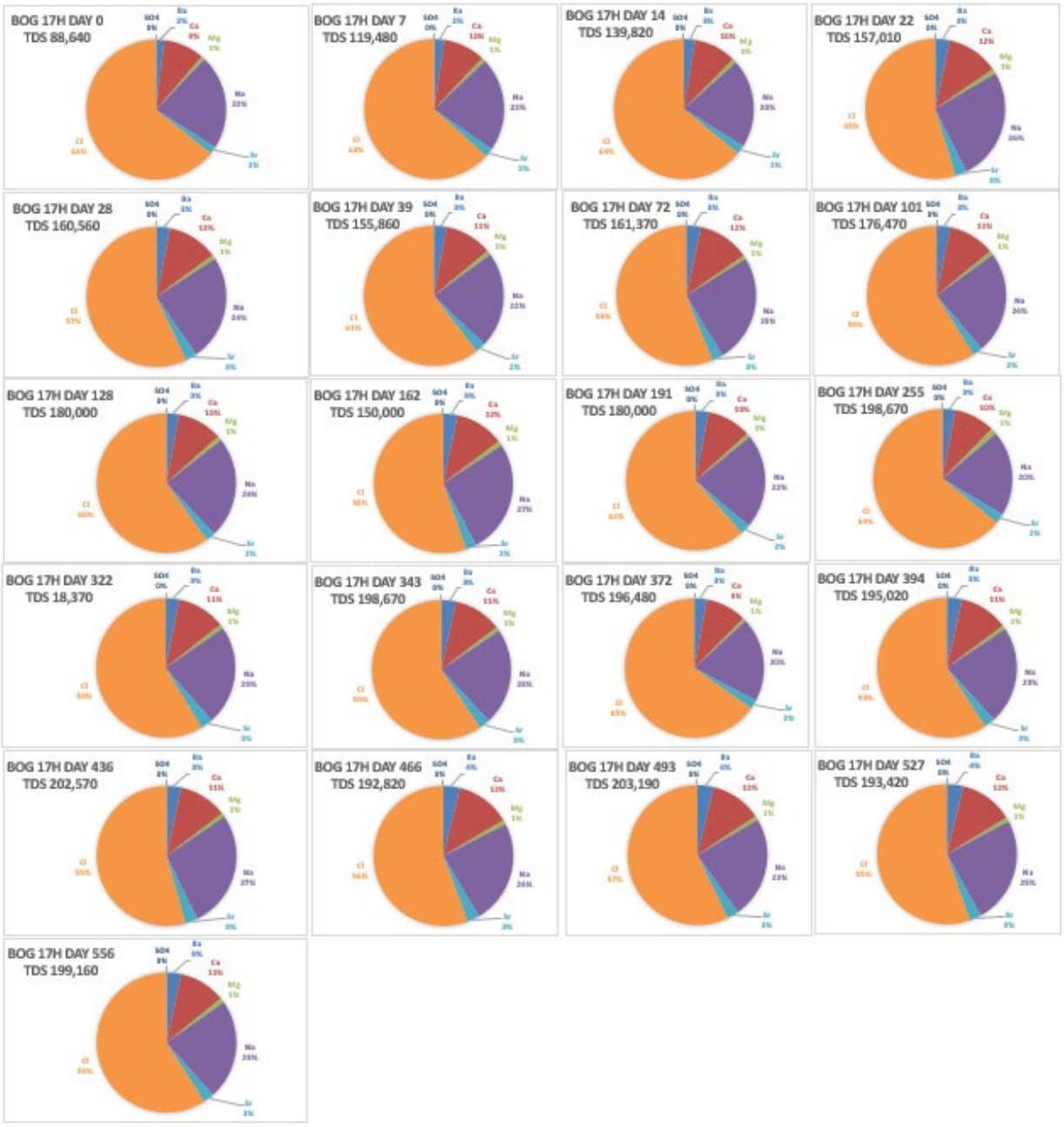

Figure 23. Major ion concentrations in produced water from wells Boggess 17H through day 556.

Preliminary TDS (sdc) at Boggess 9H and 17H show a slight upward trend between days 0 and 493 with the exception of day 322 (Figure 20). Benzene was 19 µg/L (Figure 4.21) and Toluene was 23 µg/L (Figure 4.22) on day 322 at 17H, indicating well stimulation occurred prior to sample collection, resulting in low TDS. As with MIP wells, benzene and tolune at Boggess 9H and 17H remain below 5 µg/L (with the exception of well stimulation near day 322).

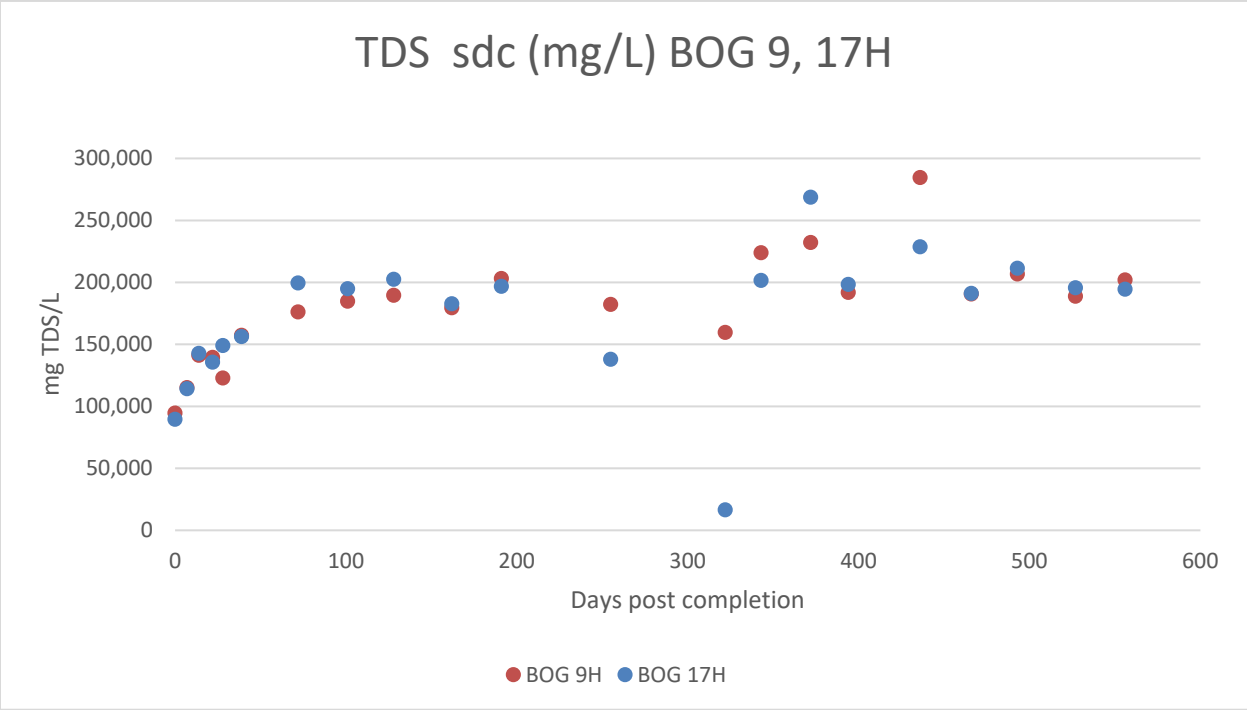

Figure 24. TDS (sdc) at Boggess 9H and 17H; days 0-556

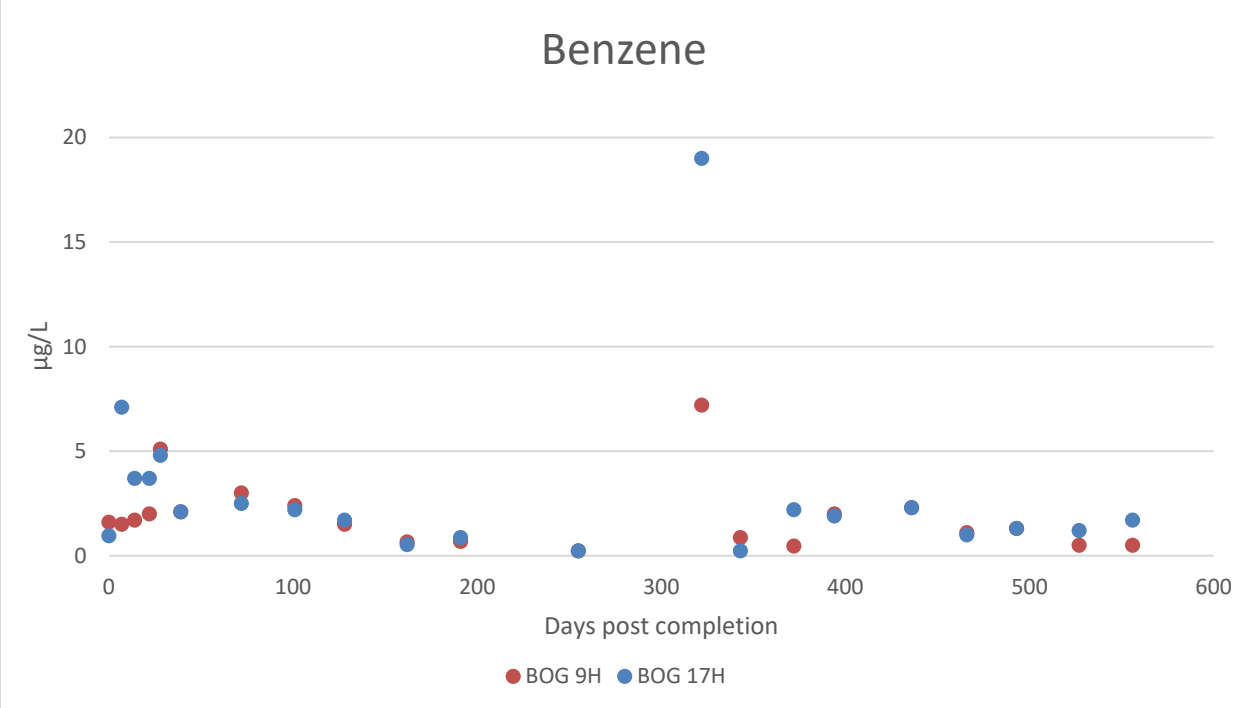

Figure 4.25. Benzene (µg/L) at BOG 9H and 17H through day 556.

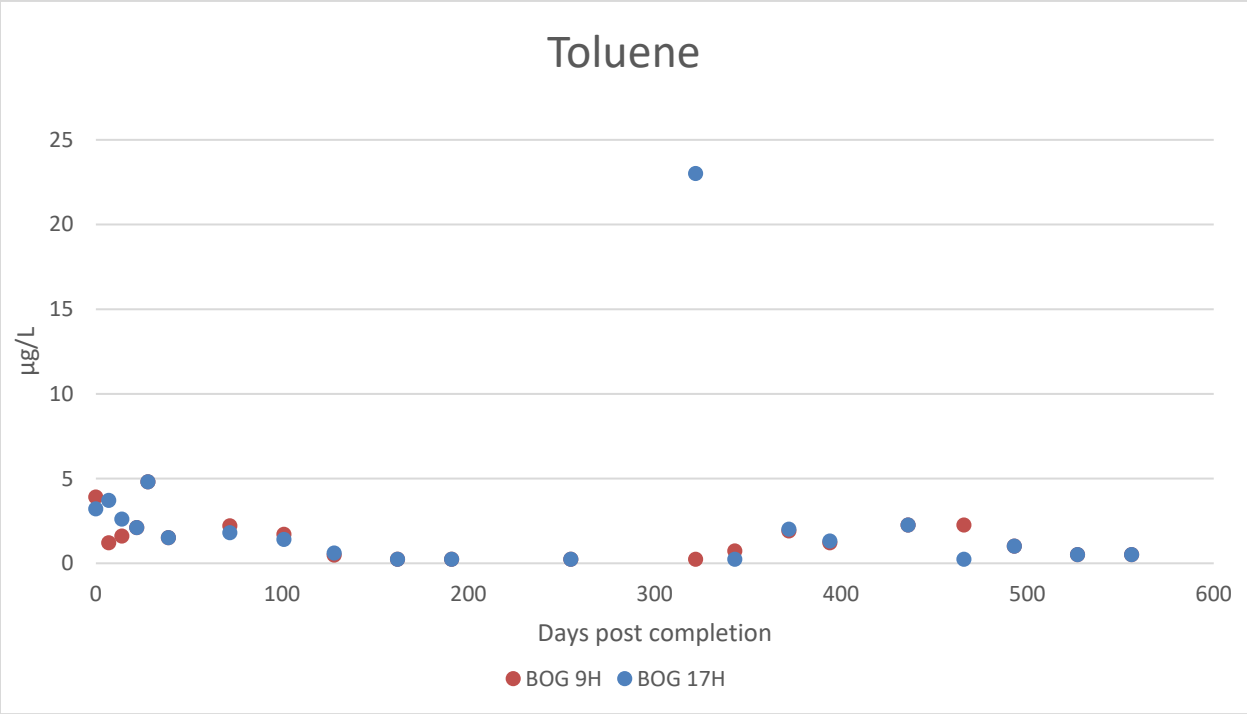

Figure 4.26. Toluene (µg/L) at BOG 9H and 17H through day 556.

Radium concentrations typically range between 10,000 to 23,000 pCi/L at both 9H and 17H at 556 days post-completion (Figure 4.23), with a few exceptions when 9H values were around 1,000 pCi/L.

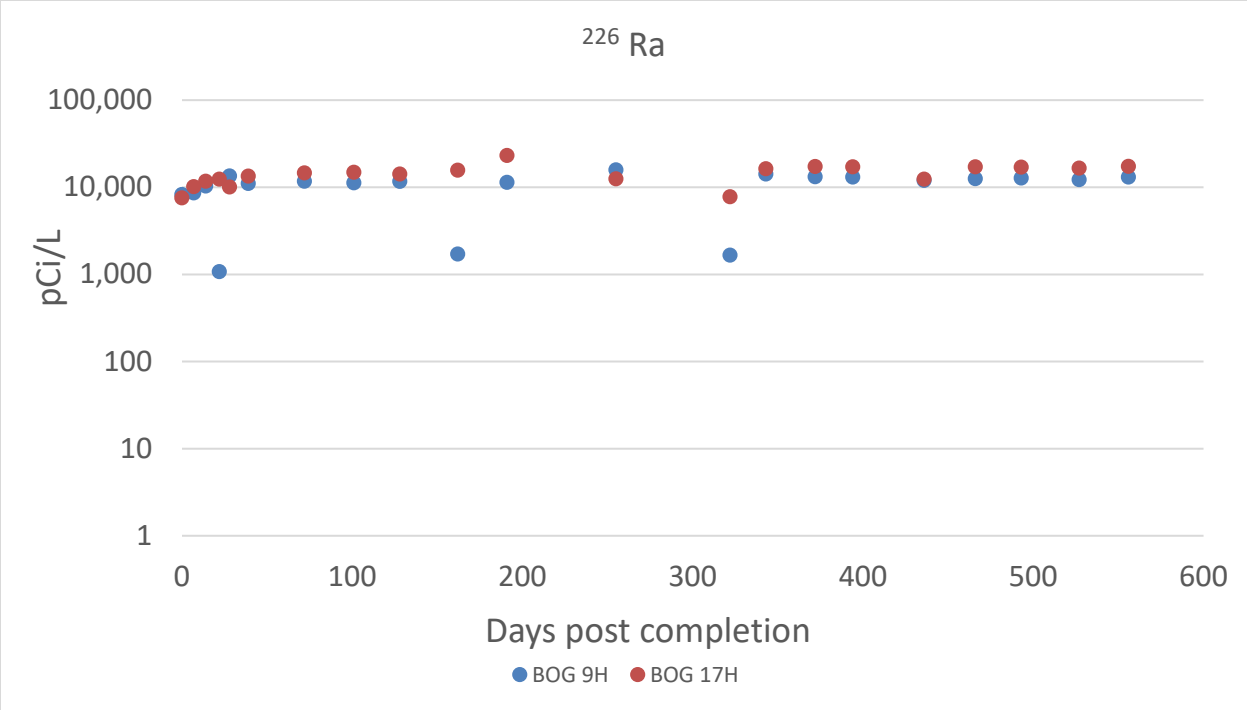

Figure 4.27. The radium isotopes are plotted against days post well completion at Boggess 9H and 17H; days 0-556.

Products

None for this quarter.

Plan for Next Quarter

We will continue monthly sampling at MIP and analyze flowback/produced water (FPW) from MIP 3H, 4H, 5H and 6H if they are online.

We will continue sampling produced water at Boggess Pad control wells 9H and 17H monthly. Following the same protocols used at MIP wells, we will characterize their inorganic, organic and radio chemistries.

Topic 5 – Environmental Monitoring: Air & Vehicular

Approach

All methane and energy audit data have been collected and processed. Processed data have been used with various models to assess temporal variability of methane emissions, methods to indirectly quantify methane emissions, and energy recovery through combined heat and power (CHP) operation during unconventional well drilling. In addition, CHP systems were evaluated for Tier 2 diesel and natural gas engines and in combination with hybrid energy management systems (HEMS) during drilling operations. Our approach has been to complete research on both topical areas by developing publications for journals and conferences, and a scholarly thesis and dissertation.

Results and Discussion

Nothing new to report.

Products

- Johnson, D., and Heltzel, R.*, "On the Long-Term Temporal Variations in Methane Emissions from an Unconventional Natural Gas Well Site," *ACS Omega,* 2021. DOI: 10.1021/acsomega.1c00874.
- Dranuta, D.*, and Johnson, D., "Analysis on Combined Heat and Power and Combined Heat and Power Hybrid Systems for Unconventional Drilling Operations," *Proceedings of the ASME 20202 Internal Combustion Engine Division Fall Technical Conference*, 2021. Accepted.
- Heltzel, R.*, "On the Improvement of the Indirect Quantification of Methane Emissions: A Stationary Single Sensor Approach," Doctoral Dissertation, 2021. Approved and submitted, WVU Research Repository.
- Dranuta Ferrer, D.*, "Analysis on Combined Heat and Power, and Combined Heat and Power Hybrid Systems for Unconventional Drilling Operations," Masters Thesis, 2021. Approved and submitted, WVU Research Repository.

Plan for Next Quarter

- Prepare presentation for 2021 ICEF Conference based on above accepted publication.
- Develop additional NSF/DOE journal publication
- Register for Shale INSIGHT 2021 university research showcase – CHP and possible methane
- Poster(s) for INSIGHT 2021 if selected
- Final summary of Topic 5 research

Topic 6 – Water Treatment

This task is complete and will not be updated in future reports.

Topic 7 – Database Development

Approach

MSEEL data from the MIP and Boggess pads are now online and available to researchers via the ***Get Data*** link (FTP) (Figures 7.1, 7.2 and 7.3). We will work to improve the navigation for obtaining the data. The website has been updated to include new navigation and adding the latest production for both the MIP and Boggess pads (Figure 7.4).

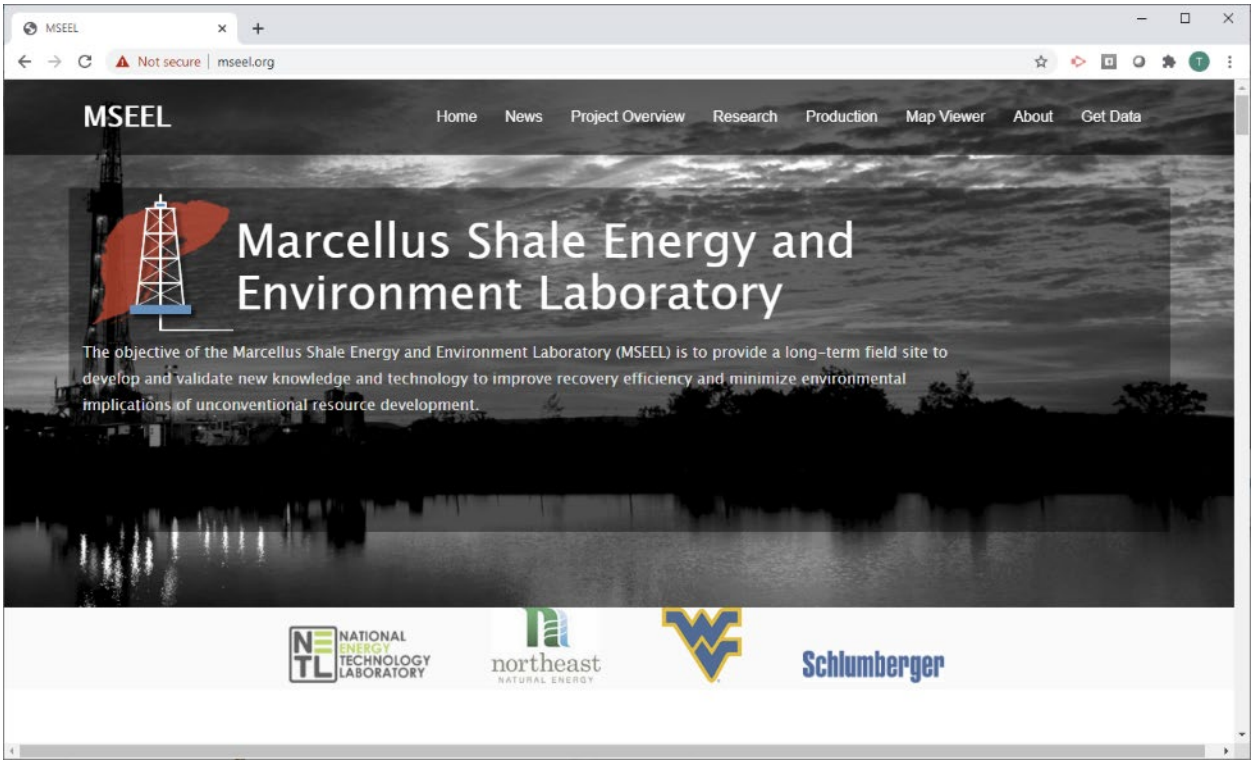

Figure 7.1: MSEEL website at http://mseel.org/.

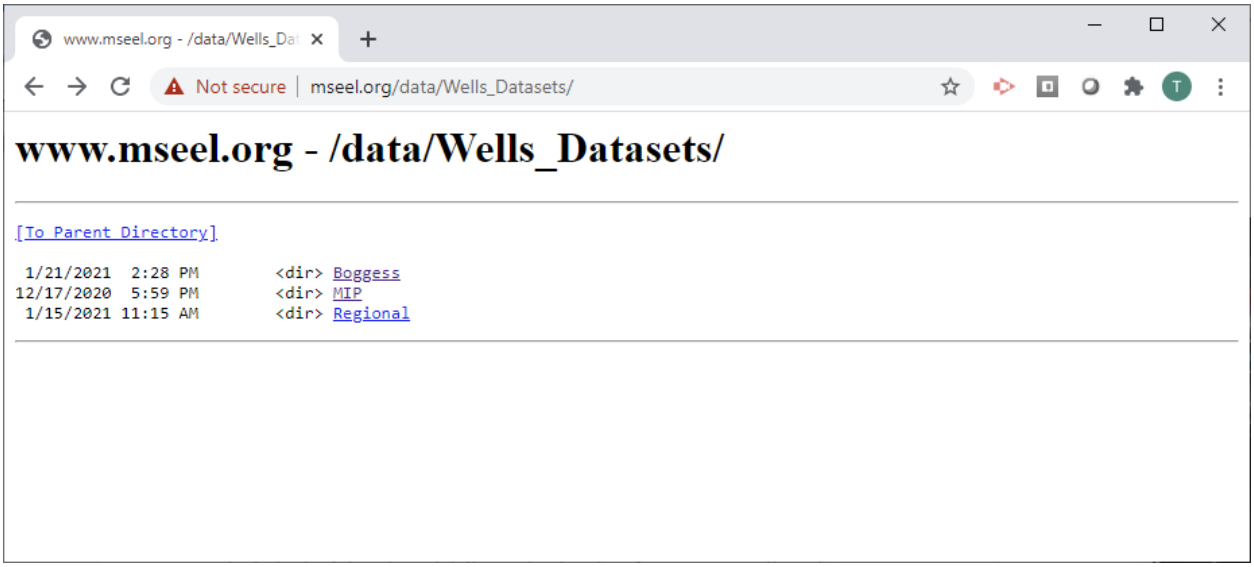

Figure 7.2: Data generated by the MSEEL project is available for download at http://mseel.org/.

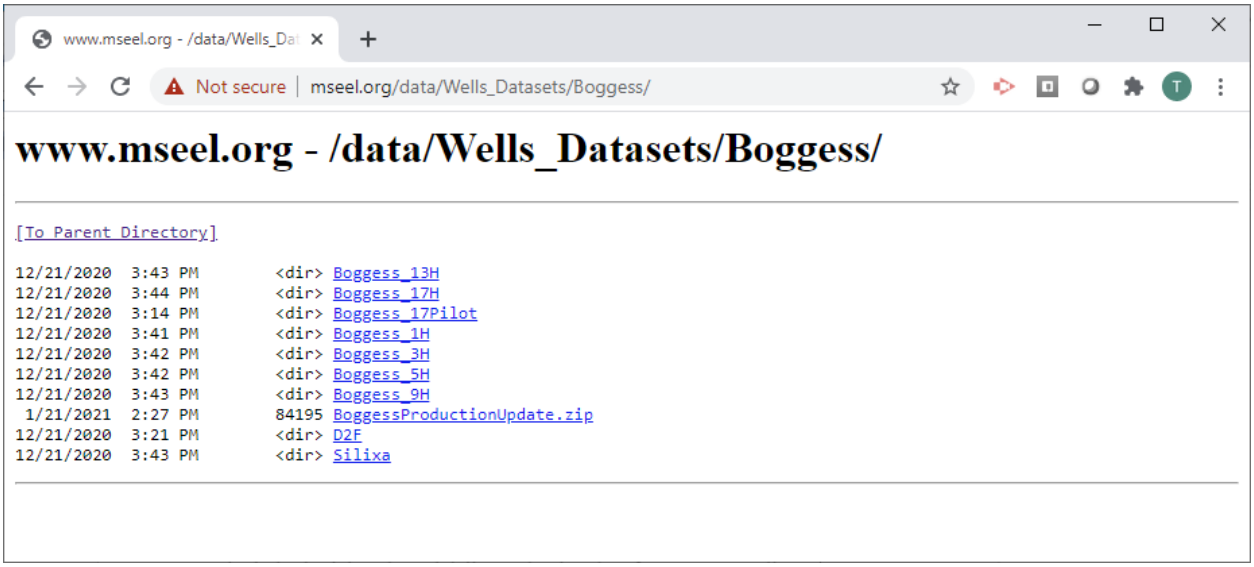

Figure 7.3: Example of data files from the Boggess Pad now available for download at http://mseel.org/.

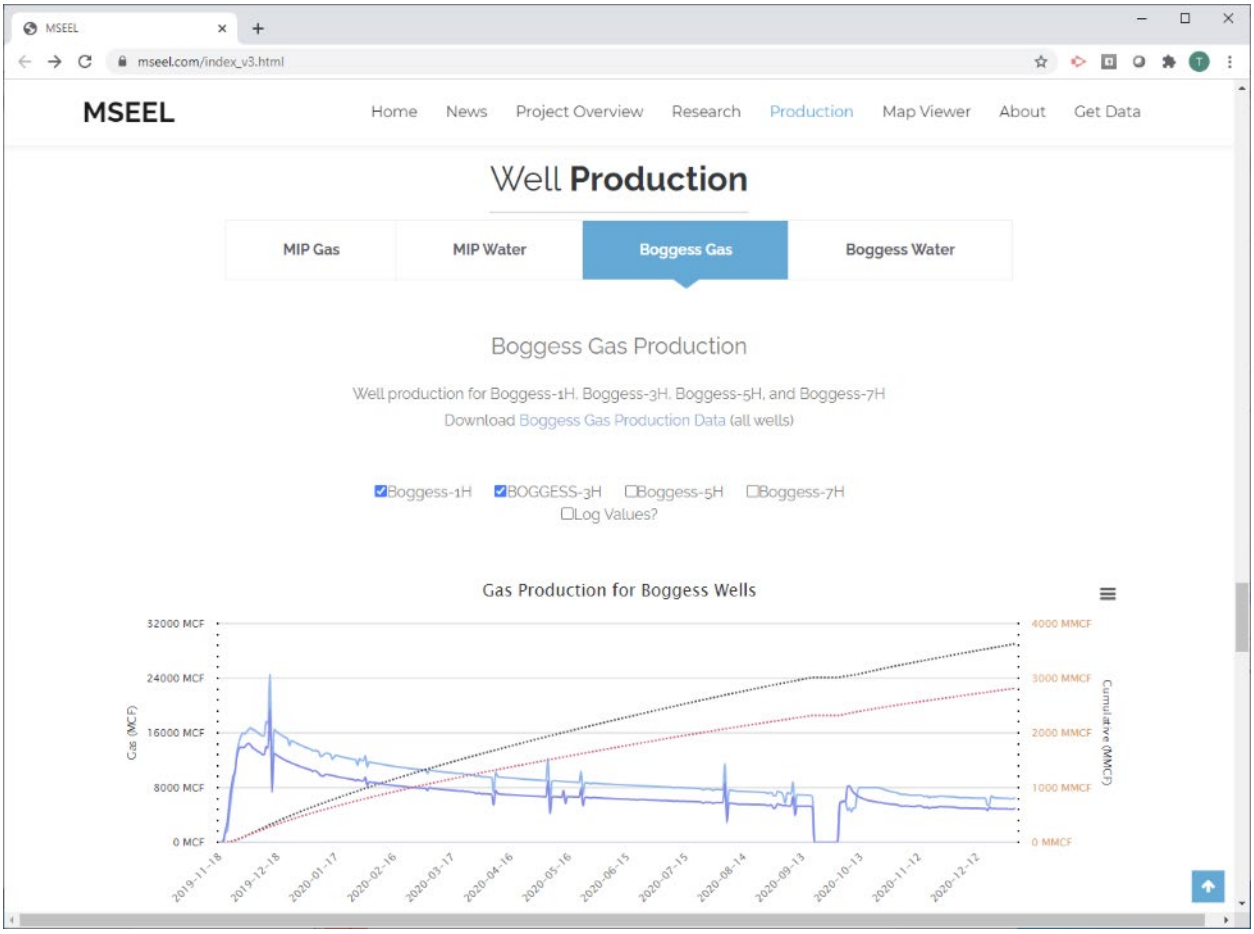

Figure 7.4: Production plots with new navigation to show gas and water production from both the MIP Pad and the Boggess Pad. Gas and water production have been updated through the end of the quarter are available at http://mseel.org/. Addition detailed production data (e.g., pressure etc.) are also available as spreadsheets (such as BoggessProductionUpdate.zip from the Get Data section, Figure 7.3)

Results & Discussion

Quality controlled production and reservoir data are now available at http://mseel.org/.

Products

Web site enhanced and updated.

Plan for Next Quarter

Working to improve web site navigation and increase access to data.

Topic 8 – Economic and Societal

This task is complete and will not be updated in future reports.

Cost Status

Year 1

Start: 10/01/2014 End: 09/30/2019

Baseline Reporting Quarter

	Q1 (12/31/14)	Q2 (3/31/15)	Q3 (6/30/15)	Q4 (9/30/15)
Baseline Cost Plan	(From 424A, Sec. D)			
(from SF-424A)				
Federal Share	$549,000		$3,549,000	
Non-Federal Share	$0.00		$0.00	
Total Planned (Federal and Non-Federal)	$549,000		$3,549,000	
Cumulative Baseline Costs				
Actual Incurred Costs				
Federal Share	$0.00	$14,760.39	$237,451.36	$300,925.66
Non-Federal Share	$0.00	$0.00	$0.00	$0.00
Total Incurred Costs - Quarterly (Federal and Non-Federal)	$0.00	$14,760.39	$237,451.36	$300,925.66
Cumulative Incurred Costs	$0.00	$14,760.39	$252,211.75	$553,137.41
Uncosted				
Federal Share	$549,000	$534,239.61	$3,296,788.25	$2,995,862.59
Non-Federal Share	$0.00	$0.00	$2,814,930.00	$2,814,930.00
Total Uncosted - Quarterly (Federal and Non-Federal)	$549,000	$534,239.61	$6,111,718.25	$5,810,792.59

Start: 10/01/2014 End: 09/30/2019

Baseline Reporting Quarter

	Q5 (12/31/15)	Q6 (3/31/16)	Q7 (6/30/16)	Q8 (9/30/16)
Baseline Cost Plan	(From 424A, Sec. D)			
(from SF-424A)				
Federal Share	$6,247,367		$7,297,926	
Non-Federal Share	2,814,930		$4,342,480	
Total Planned (Federal and Non-Federal)	$9,062,297	$9,062,297.00	$11,640,406	
Cumulative Baseline Costs				
Actual Incurred Costs				
Federal Share	$577,065.91	$4,480,939.42	$845,967.23	$556,511.68
Non-Federal Share	$0.00	$2,189,863.30	$2,154,120.23	$0.00
Total Incurred Costs - Quarterly (Federal and Non-Federal)	$577,065.91	$6,670,802.72	$3,000,087.46	$556,551.68
Cumulative Incurred Costs	$1,130,203.32	$7,801,006.04	$10,637,732.23	$11,194,243.91
Uncosted				
Federal Share	$5,117,163.68	$636,224.26	$1,004,177.30	$447,665.62
Non-Federal Share	$2,814,930.00	$625,066.70	($1,503.53)	($1,503.53)
Total Uncosted - Quarterly (Federal and Non-Federal)	$2,418,796.68	$1,261,290.96	$1,002,673.77	$446,162.09

Start: 10/01/2014
End: 09/30/2019

Baseline Reporting Quarter	Q9 (12/31/16)	Q10 (3/31/17)	Q11 (6/30/17)	Q12 (9/30/17)
Baseline Cost Plan	(From 424A, Sec. D)			
(from SF-424A)				
Federal Share				$9,128,731
Non-Federal Share				$4,520,922
Total Planned (Federal and Non-Federal)				$13,649,653
Cumulative Baseline Costs				
Actual Incurred Costs				
Federal Share	$113,223.71	$196,266.36	$120,801.19	$1,147,988.73
Non-Federal Share	$0.00	$0.00	$0.00	$0.00
Total Incurred Costs - Quarterly (Federal and Non-Federal)	$113,223.71	$196,266.36	$120,801.19	$1,147,988.73
Cumulative Incurred Costs	$11,307,467.62	$11,503,733.98	$11,624,535.17	$12,772,523.90
Uncosted				
Federal Share	$334,441.91	$138,175.55	$17,374.36	$700,190.63
Non-Federal Share	($1,503.53)	($1,503.53)	($1,503.53)	$176,938.47
Total Uncosted - Quarterly (Federal and Non-Federal)	$332,938.38	$136,672.02	$15,870.83	$877,129.10

Start: 10/01/2014 End: 09/30/2019

Baseline Reporting Quarter

	Q13 (12/31/17)	Q14 (3/31/18)	Q15 (6/30/18)	Q16 (9/30/18)
Baseline Cost Plan	(From 424A, Sec. D)			
(from SF-424A)				
Federal Share				$11,794,054
Non-Federal Share				$5,222,242
Total Planned (Federal and Non-Federal)				$17,016,296.00
Cumulative Baseline Costs				
Actual Incurred Costs				
Federal Share	$112,075.89	$349,908.08	$182,207.84	$120,550.20
Non-Federal Share	$0.00	$31,500.23	$10,262.40	$4,338.00
Total Incurred Costs - Quarterly (Federal and Non-Federal)	$112,075.89	$381,408.31	$192,470.24	$124,888.20
Cumulative Incurred Costs	$12,884,599.79	$13,266008.10	$13,458,478.34	$13,583,366.54
Uncosted				
Federal Share	$588,114.74	$238,206.66	$55,998.82	$2,600,771.62
Non-Federal Share	$176,938.47	$145,438.24	$135,175.84	$832,157.84
Total Uncosted - Quarterly (Federal and Non-Federal)	$765,053.21	$383,644.90	$191,174.66	$3,432,929.46

Start: 10/01/2014 End: 09/30/2019

Baseline Reporting Quarter	Q17 (12/31/18)	Q18 (3/31/19)	Q19 (6/30/19)	Q20 (9/30/19)
Baseline Cost Plan	(From 424A, Sec. D)			
(from SF-424A)				
Federal Share			$15,686,642.00	
Non-Federal Share			$9,180,952.00	
Total Planned (Federal and Non-Federal)			$24,867594.00	
Cumulative Baseline Costs				
Actual Incurred Costs				
Federal Share	$80,800.03	$133,776.98	$714,427.48	$1,136,823.21
Non-Federal Share	$4,805.05	$130,449.21	$4,099,491.20	$334,919.08
Total Incurred Costs - Quarterly (Federal and Non-Federal)	$85,605.08	$264,226.19	$4,813,918.68	$1,471,742.29
Cumulative Incurred Costs	$13,668,971.62	$13,933,197.81	$18,747,116.49	$20,218,858.78
Uncosted				
Federal Share	$2,519,971.59	$2,386,194.61	$5,564,355.13	$4,427,531.92
Non-Federal Share	$827,352.79	$696,903.58	$412,612.38	$221,203.30
Total Uncosted - Quarterly (Federal and Non-Federal)	$3,347,324.38	$3,083,098.19	$5,976,967.51	$4,948,735.22

Start: 10/01/2014

End: 09/30/2020

Baseline Reporting Quarter	Q21 (12/31/19)	Q22 (3/31/20)	Q23 (6/30/20)	Q24 (9/30/20)
Baseline Cost Plan	(From 424A, Sec. D)			
(from SF-424A)				
Federal Share				
Non-Federal Share				
Total Planned (Federal and Non-Federal)				
Cumulative Baseline Costs				
Actual Incurred Costs				
Federal Share	$3,098,337.44	$735,358.08	$159,437.40	$276,916.50
Non-Federal Share	$3,163,776.74	$750,301.90	$0.00	$163,643.13
Total Incurred Costs - Quarterly (Federal and Non-Federal)	$6,262,114.18	$1,485,659.98	$159,437.40	$440,559.63
Cumulative Incurred Costs	$26,480,972.96	$27,966,632.94	$28,126,070.34	$28,566,629.97
Uncosted				
Federal Share	$1,629,041.48	$893,683.40	$734,246.00	$1,079,195.50
Non-Federal Share	-$2,942,573.44	-$3,692,875.34	-$3,692,875.34	-$3,856,518.47
Total Uncosted - Quarterly (Federal and Non-Federal)	-$1,313,531.96	-$2,799,191.94	-$2,958,629.34	-$2,777,322.97

Start: 10/01/2014

End: 09/30/2021

Baseline Reporting Quarter

	Q25 (12/31/20)	Q26 (3/31/21)	Q27 (6/30/21)	Q28 (9/30/21)
Baseline Cost Plan	(From 424A, Sec. D)			
(from SF-424A)				
Federal Share				
Non-Federal Share				
Total Planned (Federal and Non-Federal)				
Cumulative Baseline Costs				
Actual Incurred Costs				
Federal Share	$191,315.03	$262,527.46	$296,045.82	
Non-Federal Share	$90,883.68	$28,358.30	$0.00	
Total Incurred Costs - Quarterly (Federal and Non-Federal)	$282,198.71	$290,885.76	$296,045.82	
Cumulative Incurred Costs	$28,848,828.68	$29,139,714.44	$29,435,760.26	
Uncosted				
Federal Share	$887,880.47	$625,353.01	$329,307.19	
Non-Federal Share	-$3,947,402.15	-$3,975,760.45	-$3,975,760.45	
Total Uncosted - Quarterly (Federal and Non-Federal)	-$3,059,521.68	-$3,350,407.44	-$3,646,453.26	

APPENDIX A – Scientific Journal Submissions Supported By MSEEL

Scientific Journals and Associated Media
Evans MV, Sumner A, Daly RA, *Luek JL, Plata D, Wrighton KC, Mouser PJ. Hydraulically fractured natural-gas well microbial communities contain genomic (de)halogenation potential. (2019). *Environmental Science & Technology* Letters, 6, (10), 585-591.
The manuscript from Nixon et al. was published in mSphere. S.L. Nixon, R.A. Daly, M.A. Borton, L.M. Solden, S.A. Welch, D.R. Cole, P.J. Mouser, M.J. Wilkins, K.C. Wrighton. Genome-resolved metagenomics extends the environmental distribution of the Verrucomicrobia phylum to the deep terrestrial subsurface. mSphere. DOI: 10.1128/mSphere.00613-19
Sharma, S., Agrawal, V., & Akondi, R. N. 2020. Role of biogeochemistry in efficient shale oil and gas production. *Fuel,* 259, 116207.
We have worked with LANL to generate a conference paper for the spring meeting of the Association for the Advancement of Artificial Intelligence (March 23-25) at Stanford University. The paper is entitled Physics-informed Machine Learning for Real-time Unconventional Reservoir Management
Sharma, S. Agrawal, V., Akondi R. 2019. Role of Biogeochemistry in efficient shale oil and gas production. Fuel. https://doi.org/10.1016/j.fuel.2019.116207
Phan T., Hakala A., Sharma S. 2019. Application of geochemical signals in unconventional oil and gas reservoir produced waters towards characterizing in situ geochemical fluid-shale reactions. International Journal of Coal Geology (in review)
Akondi, R., Sharma S., Texler, R., Pfifnner S. (2019). Effects of Sampling and Long-Term Storage on Microbial Lipid Biomarker Distribution in Deep Subsurface Marcellus Shale Cores. Geomicrobiology (in review)
Agrawal, V. and Sharma, S. 2019. Are we modelling properties of unconventional shales correctly? Fuel (in review)
Evans, Morgan, Andrew J. Sumner, Rebecca A. Daly, Jenna L. Luek, Desiree L. Plata, Kelly C. Wrighton, and Paula J. Mouser, 2019, Hydraulically Fractured Natural-Gas Well Microbial Communities Contain Genomic Halogenation and Dehalogenation Potential, Environmental Science and Technology Letters, online preprint, 7p., DOI: 10.1021/acs.estlett.9b00473.
Song, Liaosha, Keithan Martin, Timothy R. Carr, Payam Kavousi Ghahfarokhi, 2019, Porosity and storage capacity of Middle Devonian shale: A function of thermal maturity, total organic carbon, and clay content, Fuel 241, p. 1036-1044, https://doi.org/10.1016/j.fuel.2018.12.106 .
Akondi, R., Sharma S., Texler, R., Pfifnner S. (2019). Effects of Sampling and Long Term Storage on Microbial Lipid Biomarker Distribution in Deep Subsurface Marcellus Shale Cores. Frontiers in Microbiology *(in review)*.
Johnson, D., Heltzel, R., and Oliver, D., "Temporal Variations in Methane Emissions from an Unconventional Well Site," *ACS Omega*, 2019. DOI: 10.1021/acsomega.8b03246.
Evans MV, Daly RA, *Luek JL, Wrighton KC, **Mouser PJ.** (Accepted with revisions). Hydraulically fractured natural-gas well microbial communities contain genomic (de)halogenation potential. *Environmental Science & Technology Letters*.
Plata DL, Jackson RB, Vengosh A, **Mouser PJ.** (2019). More than a decade of hydraulic fracturing and horizontal drilling research. *Environmental Sciences: Processes & Impacts* 21 (2), 193-194.

Pilewski, J., S. Sharma, V. Agrawal, J. A. Hakala, and M. Y. Stuckman, 2019, Effect of maturity and mineralogy on fluid-rock reactions in the Marcellus Shale: Environmental Science: Processes & Impacts, doi:10.1039/C8EM00452H.

Phan, T. T., J. A. Hakala, C. L. Lopano, and S. Sharma, 2019, Rare earth elements and radiogenic strontium isotopes in carbonate minerals reveal diagenetic influence in shales and limestones in the Appalachian Basin: Chemical Geology, v. 509, p. 194–212, doi: 10.1016/j.chemgeo.2019.01.018.

Booker AE, Hoyt DW, Meulia T, Eder E, Nicora CD, Purvine SO, Daly RA, Moore JD, Wunch K, Pfiffner SM, Lipton MS, Mouser PJ, Wrighton KC, and Wilkins MJ (2019) Deep Subsurface Pressure Stimulates Metabolic Plasticity in Shale-Colonizing *Halanaerobium*. *Applied and Environmental Microbiology*. doi:10.1128/AEM.00018-19

Kavousi Ghahfarokhi, P., Wilson, T.H., **Carr, T.R.**, Kumar, A., Hammack, R. and Di, H., 2019. Integrating distributed acoustic sensing, borehole 3C geophone array, and surface seismic array data to identify long-period long-duration seismic events during stimulation of a Marcellus Shale gas reservoir. Interpretation, *7*(1), pp. SA1-SA10. https://doi.org/10.1190/INT-2018-0078.1.

Borton MA, Daly RA, O'Banion B, Hoyt DW, Marcus DN, Welch S, Hastings SS, Meulia T, Wolfe RA, Booker AE, Sharma S, Cole DR, Wunch K, Moore JD, Darrah TH, Wilkins MJ, and Wrighton KC (2018) Comparative genomics and physiology of the genus Methanohalophilus, a prevalent methanogen in hydraulically fractured shale. *Environmental Microbiology*. doi: 10.1111/1462-2920.14467

Booker AE, Hoyt DW, Meulia T, Eder E, Nicora CD, Purvine SO, Daly RA, Moore JD, Wunch K, Pfiffner S, Lipton MS, Mouser PJ, Wrighton KC, and Wilkins MJ. Deep subsurface pressure stimulates metabolic flexibility in shale-colonizing *Halanaerobium*. Submitted to *Applied and Environmental Microbiology*. In review.

Additionally since the last report, the team's shale virus paper has been published in *Nature Microbiology*. Citation provided below:

Daly RA, Roux S, Borton MA, Morgan DM, Johnston MD, Booker AE, Hoyt DW, Meulia T, Wolfe RA, Hanson AJ, Mouser PJ, Sullivan MB, Wrighton KC, and Wilkins MJ (2018) Viruses control dominant bacteria colonizing the terrestrial deep biosphere after hydraulic fracturing. *Nature Microbiology*. doi: 10.1038/s41564-018-0312-6

Johnson, D., Heltzel, R.*, Nix, A., and Barrow, R.*, "Development of Engine Activity Cycles for the Prime Movers of Unconventional, Natural Gas Well Development," *Journal of the Air and Waste Management Association*, 2016. DOI: 10.1080/10962247.2016.1245220.

Johnson, D., Heltzel, R.*, Nix, A., Clark, N., and Darzi, M.*, "Greenhouse Gas Emissions and Fuel Efficiency of In-Use High Horsepower Diesel, Dual Fuel, and Natural Gas Engines for Unconventional Well Development," *Applied Energy*, 2017. DOI: 10.1016/j.apenergy.2017.08.234.

3.) **Johnson, D.**, Heltzel, R.*, Nix, A., Clark, N., and Darzi, M.*, "Regulated Gaseous Emissions from In-Use High Horsepower Drilling and Hydraulic Fracturing Engines," *Journal of Pollution Effects and Control*, 2017. DOI: 10.4176/2375-4397.1000187.

Johnson, D., Heltzel, R.*, Nix, A., Darzi, M.*, and Oliver, D.*, "Estimated Emissions from the Prime-Movers of Unconventional Natural Gas Well Development Using Recently Collected In-Use Data in the United States," *Environmental Science and Technology*, 2018. DOI: 10.1021/acs.est.7b06694.

Johnson, D., Heltzel, R.*, Nix, A., Clark, N., and Darzi, M.*, "In-Use Efficiency of Oxidation and Threeway Catalysts Used In High-Horsepower Dual Fuel and Dedicated Natural Gas Engines," *SAE International Journal of Engines*, 2018. DOI: 10.4271/03-11-03-0026.

Luek JL, Hari M, Schmitt-Kopplin P, **Mouser PJ,** Gonsior M. (2018). Organic sulfur fingerprint indicates continued injection fluid signature 10 months after hydraulic fracturing. *Environmental Science: Processes & Impacts*. Available in advance at doi: 10.1039/C8EM00331A.
Evans MV, Panescu J, Hanson AJ, Sheets J, Welch SA, Nastasi N, Daly RA, Cole DR, Darrah TH Wilkins MJ, Wrighton KC, **Mouser PJ.** (*in press*, 2018), Influence of *Marinobacter* and *Arcobacter* taxa on system biogeochemistry during early production of hydraulically fractured shale gas wells in the Appalachian Basin. *Frontiers of Microbiology*.
"Economic Impacts of the Marcellus Shale Energy and Environment Laboratory" has been released by the WVU Regional Research Institute,
Panescu J, Daly R, Wrighton K, Mouser, PJ. (2018). Draft Genome Sequences of Two Chemosynthetic Arcobacter Strains Isolated from Hydraulically Fractured Wells in Marcellus and Utica Shales. Genome Announcements, 6 (20), e00159-18. doi:10.1128/genomeA.00159-18.
University of Vermont seminar, Department of Civil and Environmental Engineering. The Role of Microbial Communities in Hydraulically Fractured Shale Wells and Produced Wastewater, 4/2018.
Gordon Research Conference, Environmental Sciences: Water. The Outsiders: Microbial Survival and Sustenance in Fractured Shale, 6/2018.
Ziemkiewicz, P.F. and He, Y.T. 2015. Evolution of water chemistry during Marcellus shale gas development: A case study in West Virginia. Chemosphere 134:224-231.
*"*Candidatus *Marcellius: a novel genus of Verrucomicrobia discovered in a fractured shale ecosystem."* To be submitted to Microbiome journal. This research is led by a visiting post-doc, Sophie Nixon, in the Wrighton laboratory.
"Genomic Comparisons of Methanohalophilus *and* Halanaerobium *strains reveals adaptations to distinct environments."* This work is led by two graduate students: Mikayla Borton in the Wrighton lab and Anne Booker in the Wilkins lab.
Agrawal V and Sharma S, 2018. Molecular characterization of kerogen and its implications for determining hydrocarbon potential, organic matter sources and thermal maturity in Marcellus Shale. Fuel 228: 429–437.
Agrawal V and Sharma S, 2018. Testing utility of organogeochemical proxies to assess sources of organic matter, paleoredox conditions and thermal maturity in mature Marcellus Shale. Frontiers in Energy Research 6:42.
M.A. Borton, D.W. Hoyt, S. Roux, R.A. Daly, S.A. Welch, C.D. Nicora, S. Purvine, E.K. Eder, A.J. Hanson, J.M. Sheets, D.M. Morgan, S. Sharma, T.R. Carr, D.R. Cole, P.J. Mouser, M.S. Lipton, M.J. Wilkins, K.C. Wrighton. Coupled laboratory and field investigations resolve microbial interactions that underpin persistence in hydraulically fractured shales*. Proceedings of the National Academy of Sciences*. June 2018, 201800155; DOI: 10.1073/pnas.1800155115.
R.A. Daly, S. Roux, M.A. Borton, D.M. Morgan, M.D. Johnston, A.E. Booker, D.W. Hoyt, T. Meulia, R.A. Wolfe, A.J. Hanson, P.J. Mouser, M.B. Sullivan, K.C. Wrighton, M.J. Wilkins. Viruses control dominant bacteria colonizing the terrestrial deep biosphere after hydraulic fracturing. *Nature Microbiology.* (in revision)
R.A. Daly, K.C. Wrighton, M.J. Wilkins. Characterizing the deep terrestrial subsurface microbiome. In R. Beiko, W. Hsiao, J. Parkinson (Eds.), *Microbiome analysis: methods and protocols,* Methods in Molecular Biology. Clifton, NJ: Springer Protocols. (in press)
*"*In vitro *interactions scaled to* in situ *conditions: microorganisms predict field scale biogeochemistry in hydraulically fractured shale."* Review comments have been

"Comparison of Methanohalophilus *strains reveals adaptations to distinct environments."* Invited to submit to Frontiers in Microbiology special topic edition Geobiology in the Terrestrial Subsurface, to be submitted June 2018. An undergraduate researcher, Bridget O'Banion in the Wrighton lab, led this research.
Marcellus Shale model stimulation tests and microseismic response yield insights into mechanical properties and the reservoir DFN. Interpretation. 50p. published December 4, 2017, Interpretation, Society Exploration Geophysicists https://doi.org/10.1190/int-2016-0199.1 Thomas H. Wilson , Tim Carr , B. J. Carney , Malcolm Yates , Keith MacPhail , Adrian Morales , Ian Costello , Jay Hewitt , Emily Jordon , Natalie Uschner , Miranda Thomas , Si Akin , Oluwaseun Magbagbeola , Asbjoern Johansen , Leah Hogarth , Olatunbosun Anifowoshe , and Kashif Naseem,
Akondi R, Trexler R, Pfiffner SM, Mouser PJ, Sharma S 2017. Modified Lipid Extraction Method for Deep Subsurface Shale. Frontiers in Microbiology https://doi.org/10.3389/fmicb.2017.01408
the paper was submitted to the Journal Interpretation. The journal submission is titled Marcellus Shale model stimulation tests and microseismic response yield insights into mechanical properties and the reservoir DFN
Johnson, D., Heltzel, R., Nix, A., and Barrow, R., "Development of Engine Activity Cycles for the Prime Movers of Unconventional, Natural Gas Well Development," Journal of the Air and Waste Management Association, 2016. DOI: 10.1080/10962247.2016.1245220
Preston County Journal: http://www.theet.com/news/local/wvu-project-setting-the-standard-for-researching-oil-and-gas/article_25e0c7d0-279d-59c1-9f13-4cbe055a1415.html
The statesman: http://www.thestatesman.com/news/science/fracking-messiah-or-menace/81925.html
Nova Next article: http://www.pbs.org/wgbh/nova/next/earth/deep-life/
NPR interview: http://www.wksu.org/news/story/43880
Midwest Energy News : http://midwestenergynews.com/2015/11/17/researchers-study-microbes-living-in-shale-and-how-they-can-impact-drilling/
McClatchyDC News: "Could deep earth microbes help us frack for oil?"S. Cockerham http://www.mcclatchydc.com/news/nation-world/national/article29115688.html

APPENDIX B – Conference Papers/Presentations MSEEL

Conference Paper/Presentation
Fathi, E.; Belyadi, F.; Jabbar, B. Shale Poroelastic Effects on Well Performance Analysis of Shale Gas Reservoirs. Fuels 2021, 2, 130–143. https://doi.org/10.3390/fuels2020008
Agrawal, V., S. Sharma, N. Mahlstedt 2019, Determining the type, amount and kinetics of hydrocarbons generated in a Marcellus shale maturity series. Eastern Section AAPG 48th Annual Meeting in Columbus, OH.
Carney BJ, Carr TR, Hewitt J, Vagnetti R, Sharma S, Hakala A. 2019. Progress and Findings from "MSEEL 1" and the Transition to "MSEEL 2": Creating Value from a Cooperative Project. Annual Eastern Section AAPG Meeting, Columbus, Ohio.
Phan TT, Hakala JA, Lopano C L, & Sharma S. 2019. Rare earth elements and radiogenic strontium isotopes in carbonate minerals reveal diagenetic influence in shales and limestones in the Appalachian Basin. GAC-MAC-IAH conference, Quebec City, Quebec, Canada.
Ferguson, B., Sharma, S., Agrawal, V., Hakala, A., 2019. Investigating controls on mineral precipitation in hydraulically fractured wells. Geological Society of America Annual Meeting, Phoenix, (GSA), Annual meeting, Phoenix, Arizona.
Akondi R, Sharma S. 2019. Microbial Signatures of Deep Subsurface Shale Biosphere. Geological Society of America (GSA), Annual meeting, Phoenix, Arizona.
Carr, Timothy R. MSEEL Seismic Attribute Application of Distributed Acoustic Sensing Data, presentation at 53rd US Rock Mechanics / Geomechanics Symposium, 2019 American Rock Mechanics Association (ARMA) Annual Meeting, New York City, NY.
Agrawal, V., S. Sharma, N. Mahlstedt 2019, Determining the type, amount and kinetics of hydrocarbons generated in a Marcellus shale maturity series. Eastern Section AAPG 48th Annual Meeting in Columbus, OH
Evans M, Luek J, Daly R, Wrighton KC, **Mouser PJ**. (2019). Microbial (de)halogenation in hydraulically fractured natural-gas wells in the Appalachian Basin. ACS annual conference, Orlando, FL, Mar 31-Apr 4, 2019.
Luek J, Murphy C, Wrighton KC, **Mouser PJ.** (2019). Detection of antibiotic and metal resistance genes in deep shale microbial community members. ACS annual conference, Orlando, FL, Mar 31-Apr 4, 2019.
Kumar, A., E. V. Zorn, R. Hammack, and W. Harbert, 2017a, Seismic monitoring of hydraulic fracturing activity at the Marcellus shale energy and environment laboratory (MSEEL) Site, West Virginia: Presented at the Unconventional Resources Technology Conference, Paper 2670481.
Tufts University, Dept. of Civil and Environmental Engineering. Microbial Survival and Sustenance in Fractured Shale 10/2018.
University of New Hampshire, Dept. of Earth Science. Microbial Survival and Sustenance in Fractured Shale 09/2018.
GSA conference in Indianapolis, Indiana. 2019
AAPG 2019, San Antonio, Texas.
Agrawal, V., Sharma, S., 2018. New models for determining thermal maturity and hydrocarbon potential in Marcellus Shale. Eastern Section AAPG 47th Annual Meeting in Pittsburgh, WV

Eastern Section SPE and AAPG by Yixuan Zhu and T. R, Carr entitled Estimation of "Fracability" of Marcellus Shale: A Case Study from the MIP3H in Monongalia County, WV, USA. The paper will be presented in Pittsburgh, PA during the meeting (October 9-11)
Kelly Wrighton -19th Annual Microbiology Student Symposium, University of California Berkeley, April 28, 2018
Kelly Wrighton - ASM Microbe, Atlanta, Georgia, June 9, 2018
Mouser PJ**,** Heyob KM, Blotevogel J, Lenhart JJ, Borch T (2018). Pathways and Mechanisms for Natural Attenuation of Nonionic Surfactants in Hydraulic Fracturing Fluids if Released to Agricultural Soil and Groundwater. ACS annual conference, New Orleans, LA, Mar 19-22, 2018.
Hanson AJ, Lipp JS, Hinrich K-U, Mouser PJ (2018). Microbial lipid biomarkers in a Marcellus Shale natural gas well: From remnant molecules to adapted communities. ACS annual conference, New Orleans, LA, Mar 19-22, 2018
University of Maine, Department of Biology and Ecology. Biodegradation of Organic Compounds in the Hydraulically Fractured Shale Ecosystem, 2/2018.
"*Top-down and bottom-up controls on* Halanaerobium *populations in the deep biosphere*." Poster presentation at the Department of Energy's Joint Genome Institute 'Genomics of Energy and Environment Meeting', San Francisco, CA, March 2018. A researcher, Rebecca Daly, in the Wrighton lab, led this work.
Sharma S, Wilson T, Wrighton, K, Borton M & O'Banion. 2017 Can introduction of hydraulic fracturing fluids induce biogenic methanogenesis in the shale reservoirs? Annual American Geophysical Union Conference, Dec 11-15, New Orleans, LA.
Booker AE, Borton MA, Daly R, C. Nicora, Welch S, Dusane D, Johnston M, Sharma S et. al., 2017. Potential Repercussions Associated with Halanaerobium Colonization of Hydraulically Fractured Shales. Annual American Geophysical Union Conference, Dec 11-15, New Orleans, LA.
Mouser P. *Colorado State University, Civil and Environmental Engineering* and *CSU Water Center*, From the Land Down Under: Microbial Community Dynamics and Metabolic processes influencing organic additives in black shales, 11/2017.
Presentation at ISES (International Society for Exposure Science), Raleigh, NC Oct. 16th, 2017 on "Techniques for Estimating Community Exposure from Hydraulic Fracturing Operations
Kavousi, Payam, **Timothy R**. **Carr,** Robert J Mellors, Improved interpretation of Distributed Acoustic Sensing (DAS) fiber optic data in stimulated wells using seismic attributes, [S33B-0865] presented at December 2017 Fall Meeting, AGU, New Orleans, LA, 11-15,https://agu.confex.com/agu/fm17/meetingapp.cgi/Paper/282093
Mellors Robert J, Christopher Scott Sherman, Frederick J Ryerson, Joseph Morris, Graham S Allen, Michael J Messerly, **Timothy Carr**, Payam Kavousi, Modeling borehole microseismic and strain signals measured by a distributed fiber optic sensor, [S33B-0869] presented at 2017 Fall Meeting, AGU, New Orleans, LA, 11-15, https://agu.confex.com/agu/fm17/meetingapp.cgi/Paper/264800
Song, Liaosha and **Timothy R. Carr**, Microstructural Evolution of Organic Matter Pores in Middle Devonian Black Shale from West Virginia and Pennsylvania, USA, SEPM – AAPG Hedberg Research Conference, Mudstone Diagenesis, Santa Fe, New Mexico, October 16-19. http://www.searchanddiscovery.com/pdfz/abstracts/pdf/2017/90283hedberg/abstracts/ndx_song.pdf.html

Carr, Timothy R., The Importance of Field Demonstration Sites: The View from the Unconventional Resource Region of the Appalachian Basin (Invited), [H21K-06] presented at 2017 Fall Meeting, AGU, New Orleans, LA, 11-15 Dec. https://agu.confex.com/agu/fm17/meetingapp.cgi/Paper/242523

Ghahfarokhi, P. K., Carr, T., Song, L., Shukla, P., & Pankaj, P. (2018, January 23). Seismic Attributes Application for the Distributed Acoustic Sensing Data for the Marcellus Shale: New Insights to Cross-Stage Flow Communication. Society of Petroleum Engineers, doi:10.2118/189888-MS.

Presentation of paper at 2017 Annual International SEG meeting: The paper *titled "Relationships of brittleness index, Young's modulus, Poisson's ratio and high TOC for the Marcellus Shale, Morgantown, West Virginia"* by Thomas H. Wilson*, Payam Kavousi, Tim Carr, West Virginia University; B. J. Carney, Northeast Natural Energy LLC; Natalie Uschner, Oluwaseun Magbagbeola and Lili Xu, Schlumberger, was presented at the annual SEG meeting, this past September in Houston, TX.

Thomas H. Wilson and Tim Carr, West Virginia University; B. J. Carney, Jay Hewitt, Ian Costello, Emily Jordon, Northeast Natural Energy LLC; Keith MacPhail, Oluwaseun Magbagbeola, Adrian Morales, Asbjoern Johansen, Leah Hogarth, Olatunbosun Anifowoshe, Kashif Naseem, Natalie Uschner, Mandy Thomas, Si Akin, Schlumberger, 2016, Microseismic and model stimulation of natural fracture networks in the Marcellus Shale, West Virginia: SEG International Exposition and 86th Annual Meeting, 3088-3092, https://doi.org/10.1190/segam2016-13866107.1.

Sharma S 2017. Shale Research at Marcellus Shale Energy and Environment laboratory. 23rd Annual CNSF Exhibition, May 16, Rayburn House, Washington DC.

Elsaig, M., Black, S., Aminian, K., and S. Ameri, S.: "Measurement of Marcellus Shale Properties," SPE-87523, SPE Eastern Regional Conf., Lexington, KY, October 2017.

El Sgher, M., Aminian, K., and S. Ameri: "The Impact of Stress on Propped Fracture Conductivity and Gas Recovery in Marcellus Shale," SPE-189899, SPE Hydraulic Fracturing Technology Conf., Woodlands, TX, January 2018.

Ebusurra, M.: "Using Artificial Neural Networks to Predict Formation Stresses for Marcellus Shale with Data from Drilling Operations." MS Thesis, Petroleum & Natural Gas Engineering, West Virginia University, August 2017.

M. El Sgher, K. Aminian, S. Ameri: "The impact of the hydraulic fracture properties on gas recovery from Marcellus Shale," SPE 185628, SPE Western Regional Conf., Bakersfield, California, April 2017.

Elsaig, M., Aminian, K., Ameri, S. and M. Zamirian: "Accurate Evaluation of Marcellus Shale Petrophysical Properties," SPE-**Error! Reference source not found.**84042, SPE Eastern Regional Conf., Canton, OH, September 2016.

Filchock, J.J., Aminian, K. and S. Ameri: "Impact of Completion Parameters on Marcellus Shale Production," SPE-184073, SPE Eastern Regional Conf., Canton, OH, September 2016.

Tawfik Elshehabi and H. Ilkin Bilgesu: "Well Integrity and Pressure Control in Unconventional Reservoirs: A Comparative Study of Marcellus and Utica Shales," SPE 184056, SPE Eastern Regional Conf., Canton, OH, September 2016

Meso- and Macro-Scale Facies and Chemostratigraphic Analysis of Middle Devonian Marcellus Shale in Northern West Virginia, USA for Eastern Section American Association of Petroleum Geologists Annual Meeting September 26-27. Authors: Thomas Paronish, Timothy Carr, West Virginia University; Dustin Crandall and Jonathan Moore, National Energy Technology Laboratory, U.S. Department of Energy
The presentation was made at the annual SEG convention in Dallas (see http://library.seg.org/doi/pdf/10.1190/segam2016-13866107.1) and the paper was submitted to the Journal Interpretation. The journal submission is titled Marcellus Shale model stimulation tests and microseismic response yield insights into mechanical properties and the reservoir DFN
McCawley M, Dzomba A, Knuckles T, and Nye M. 2017. Use of trace elements for estimating community exposure to Marcellus shale development operations. Poster presented at: Van Liere Poster Competition. WVU Health Sciences Center; 2017; Morgantown, WV
Khajouei Golnoosh, Hoil Park, Jenna Henry, Harry Finklea, Lian-Shin Lin. *Produced water treatment using electrochemical softening system*. Institute of Water Security and Science (IWSS) symposium, February 28, Morgantown, West Virginia.
Wilson T, and Sharma S. 2017. Inferring biogeochemical interactions in deep shale reservoirs at the Marcellus Shale Energy and Environment Laboratory (MSEEL). Joint 52nd northeastern annual section/ 51st north-central annual section meeting March 19-21, Pittsburgh, PA.
Agrawal V, Sharma S, and Warrier A. 2016. Understanding kerogen composition and structure in pristine shale cores collected from Marcellus Shale Energy and Environment Laboratory. Eastern Section American Association of Petroleum Geologists' Meeting, Lexington, Kentucky, September 2016
Akondi R, Trexler RV, Pfiffner SM, Mouser PJ, Sharma S. 2016. Comparing Different Extraction Methods for Analyses of Ester-linked Diglyceride Fatty Acids in Marcellus Shale. Eastern Section American Association of Petroleum Geologists' Meeting, Lexington, Kentucky, September 2016
Booker AE, Borton MA, Daly R, Welch S, Nicora CD, Sharma S, et. al., 2016. Sulfide Generation by Dominant Colonizing Halanaerobium Microorganisms in Hydraulically Fractured Shales. Eastern Section American Association of Petroleum Geologists' Meeting, Lexington, Kentucky, September 2016
Crandall D, Moore J, Paronish T, Hakala A, Sharma S, and Lopano C 2016. Preliminary analyses of core from the Marcellus Shale Energy and Environment Laboratory. Eastern Section American Association of Petroleum Geologists' Meeting, Lexington, Kentucky, September 2016.
Daly RA, Borton MA, Wilson T, Welch S., Cole D. R., Sharma S., et. al., 2016. Microbes in the Marcellus Shale: Distinguishing Between Injected and Indigenous Microorganisms, Eastern Section American Association of Petroleum Geologists' Meeting, Lexington, Kentucky, September 2016
Evert M, Panescu J, Daly R, Welch S, Hespen J, Sharma S, Cole D, Darrah TH, Wilkins M, Wrighton K, Mouser PJ 2016. Temporal Changes in Fluid Biogeochemistry and Microbial Cell Abundance after Hydraulic Fracturing in Marcellus Shale. Eastern Section American Association of Petroleum Geologists' Meeting, Lexington, Kentucky, September 2016

Hanson AJ, Trexler RV, Mouser PJ (2016). Analysis of Microbial Lipid Biomarkers as Evidence of Deep Shale Microbial Life. Eastern Section American Association of Petroleum Geology (AAPG), Lexington, KY, Sept 25-27, 2016.
Lopano, C.L., Stuckman, M.Y., and J.A. Hakala (2016) Geochemical characteristics of drill cuttings from Marcellus Shale energy development. Annual Geological Society of America Meeting, Denver, CO, September 2016.
Pansecu J, Evert M, Hespen J, Daly RA, Wrighton KC, Mouser PJ (2016). Arcobacter isolated from the produced fluids of a Marcellus shale well may play a currently unappreciated role in sulfur cycling. Eastern Section American Association of Petroleum Geology (AAPG), Lexington, KY, Sept 25-27, 2016.
Sharma S, Carr T, Vagnetti R, Carney BJ, Hewitt J. 2016. Role of Marcellus Shale Energy and Environment Laboratory in Environmentally Prudent Development of Shale Gas. Annual Geological Society of America Meeting, Denver, CO, September 2016.
Sharma S, Agrawal V, Akondi R, and Warrier A. 2016. Understanding biogeochemical controls on spatiotemporal variations in total organic carbon in cores from Marcellus Shale Energy and Environment Laboratory. Eastern Section American Association of Petroleum Geologists' Meeting, Lexington, Kentucky, September 2016
Trexler RV, Akondi R, Pfiffner S, Daly RA, Wilkins MJ, Sharma S, Wrighton KC, and Mouser, PJ (2016). Phospholipid Fatty Acid Evidence of Recent Microbial Life in Pristine Marcellus Shale Cores. Eastern Section American Association of Petroleum Geology (AAPG), Lexington, KY, Sept 25-27, 2016.
Wilson T and Sharma S 2016. Assessing biogeochemical interactions in the reservoir at Marcellus Shale Energy and Environment Laboratory Annual Geological Society of America Meeting, Denver, CO, September 2016.
Marcellus Shale Energy and Environment Laboratory (MSEEL): Subsurface Reservoir Characterization and Engineered Completion; Presenter: Tim Carr; West Virginia University (2670437)
Depositional environment and impact on pore structure and gas storage potential of middle Devonian organic rich shale, Northeastern West Virginia, Appalachian Basin; Presenter: Liaosha Song, Department of Geology and Geography, West Virginia University, Morgantown, WV, (2667397)
Seismic monitoring of hydraulic fracturing activity at the Marcellus Shale Energy and Environment Laboratory (MSEEL) site, West Virginia; Presenter: Abhash Kumar, DOE, National Energy Technology Laboratory (2670481)
Geomechanics of the microseismic response in Devonian organic shales at the Marcellus Shale Energy and Environment Laboratory (MSEEL) site, West Virginia; Presenter: Erich Zorn, DOE, National Energy Technology Laboratory (2669946)
Application of Fiber-optic Temperature Data Analysis in Hydraulic Fracturing Evaluation- a Case Study in the Marcellus Shale; Presenter: Shohreh Amini, West Virginia University (2686732)
The Marcellus Shale Energy and Environmental Laboratory (MSEEL): water and solid waste findings-year one; Presenter: Paul Ziemkiewicz WRI, West Virginia University (2669914)
Role of organic acids in controlling mineral scale formation during hydraulic fracturing at the Marcellus Shale Energy and Environmental Laboratory (MSEEL) site; Presenter: Alexandra Hakala, National Energy Technology Laboratory, DOE (2670833)

MSEEL Water and Waste Findings - RPSEA Onshore Workshop
MSEEL Water and Waste Findings - Eastern Sec. AAPG annual meeting
Sharma S., 2016. Unconventional Energy Resources: A view from the Appalachian Basin. US Embassy Berlin, Germany 25 May 2016.
Sharma S., 2016. Biogeochemistry of Marcellus Shale. German National Research Centre for Earth Sciences GFZ, Postdam, Germany. May 22, 2016
Sharma S. 2016,. Biogeochemistry of Marcellus Shale. SouthWestern Energy, Houston, Texas. May 5, 2016.
Sharma S. 2016. Marcellus Shale Energy and Environment Laboratory (MSEEL), West Virginia University Extension Conference, Clarksburg, WV. May 18, 2016.
Sharma S. 2016. Role of Geochemistry in Unconventional Resources Development. Appalachain Geological Society Meeting, Morgantown, April 5, 2016.
Sharma S. 2016. Marcellus Shale Energy and Environment Laboratory (MSEEL), Exxon WVU visit, Morgantown, June 23, 2016.
On July 20, 2016, Paul Ziemkiewicz, Task 5a lead investigator gave a presentation titled: WVU – Northeast Natural Energy Marcellus Hydraulic Fracture Field Laboratory Environmental Research Update at the WVU/PTTC/NETL/RPSEA Onshore Technology WorkshopAppalachian Basin Technology in Canonsburg, PA.
Abstract entitled “Addressing Health Issues Associated with Air Emissions around UNGD Sites” by Michael McCawley, Travis Knuckles, Maya Nye and Alexandria Dzomba accepted for the 2016 Eastern Section – American Association of Petroleum Geologists’ meeting in Lexington, Kentucky on September 27, 2016.
Sharma S. 2016, Environmentally Prudent Development of Unconventional Shale Gas: Role of Integrated Field Laboratories. Invited talk at International Shale Gas and Oil Workshop , India, 28-29 January, 2016
Sharma S. 2016, Role of Geochemistry in Unconventional Resource Development. Invited talk at Appalachian Geological Society Meeting, Morgantown, April 5 2016. Hakala, J.A., Stuckman, M., Gardiner, J.G., Phan, T.T., Kutchko, B., Lopano, C. 2016
Application of voltammetric techniques towards iron and sulfur redox speciation in geologic fluids from coal and shale formations, American Chemical Society Fall Meeting 2016 Philadelphia, PA.
Phan, T.T., Hakala, J.A. 2016. Contribution of colloids to major and trace element contents and isotopic compositions (Li and Sr) of water co-produced with natural gas from Marcellus Shale. American Chemical Society Fall Meeting 2016 Philadelphia, PA.
Environmentally Friendly Drilling Conference on 11/15/2015 by Sunil Moon and Michael McCawley, Diesel Traffic Volume Correlates with Ultrafine Particle Concentrations but not PM2.5.
Agrawal V, Sharma S , Chen R, Warrier A, Soeder D, Akondi R. 2015. Use of biomarker and pyrolysis proxies to assess organic matter sources, thermal maturity, and paleoredox conditions during deposition of Marcellus Shale. Annual Geological Society of America Meeting, Baltimore, MD, November 1-4.
Akondi R, Sharma S, Pfiffner SM, Mouser PJ, Trexler R, Warrier A. 2015. Comparison of phospholipid and diglyceride fatty acid biomarker profiles in Marcellus Shale cores of different maturities. Annual Geological Society of America Meeting, Baltimore, MD, November 1-4.

Mouser, PJ, Daly, RA, Wolfe, R. and Wrighton, KC (2015). Microbes living in unconventional shale during energy extraction have diverse hydrocarbon degradation pathways. Oral presentation presented at 2015 Geological Society of America Annual Conf. Baltimore, MD, Nov 1-4.

Sharma S and Wilson T. 2015. Isotopic evidence of microbe-water-rock interaction in Shale gas produced waters. Annual Geological Society of America Meeting, Baltimore, MD, November 1-4.

Sharma S, Chen R, Agrawal V. 2015 Biogeochemical evidences of oscillating redox conditions during deposition of organic-rich intervals in the middle Devonian Marcellus Shale. Annual Geological Society of America Meeting, Baltimore, MD, November 1-4.

Trexler RV, Pfiffner SM, Akondi R, Sharma S, Mouser PJ.(2015) Optimizing Methods for Extracting Lipids from Organic-Rich Subsurface Shale to Estimate Microbial Biomass and Diversity. Poster session presented at: 2015 Geological Society of America Annual Meeting. 2015 Nov 1-4; Baltimore, MD.

Wrighton, KC; Daly, R; Hoyt, D; Trexler, R; MacRae, J; Wilkins, M; Mouser, PJ (2015), Oral presentation at the American Geophysical Union Annual Meeting. Something new from something old? Fracking stimulated microbial processes. Presentation# B13K-08. San Francisco, CA, Dec 14-18, 2015.

Mouser, P, The Impact of Fracking on the Microbiology of Deep Hydrocarbon Shale, American Society for Microbiology (ASM) Annual Conference, New Orleans, LA, May 30-June 2, 2015.

Wrighton et al, Drivers of microbial methanogenesis in deep shales after hydraulic fracturing. American Society of Microbiology. New Orleans, LA. May 30-June 2, 2015.

Daly et al, Viral Predation and Host Immunity Structure Microbial Communities in a Terrestrial Deep Subsurface, Hydraulically Fractured Shale System. American Society of Microbiology. New Orleans, LA.

APPENDIX C – Special MSEEL Sessions

Paper prepared for presentation at the Unconventional Resources Technology Conference (URTeC) held in Denver, Colorado, USA, 22-24 July 2019, 10 pages, DOI 10.15530/urtec-2019- 415.
Odegaarden, Natalie and Timothy Carr, Vein Evolution due to Thermal Maturation of Kerogen in the Marcellus Shale, Appalachian Basin, Paper presented at the Annual Meeting of the Geological Society of America 22-25 September 2019 Phoenix, AZ.
URTeC (URTeC: 2902641) for presentation in Houston (July) by Payam Kavousi Ghahfarokhi, Timothy Carr, Shuvajit Bhattacharya, Justin Elliott, Alireza Shahkarami and Keithan Martin entitled A Fiber-optic Assisted Multilayer Perceptron Reservoir Production Modeling: A Machine Learning Approach in Prediction of Gas Production from the Marcellus Shale. 2019
8/15/2017 - Coordinate and hold MSEEL session at URTEC 2017 (Scheduled 8/30/2017; Completed 8/30/2017)
4/30/2017 - Conduct preliminary analysis of production log data and present to DOE. (Completed and being worked into a new reservoir simulation – Review meeting held at WVU
26 Jul 2017: URTeC, Austin, TX, Manuscript attached
27 Sep 2017: Marcellus Shale Coalition, Shale Insight,
SPE-184073, SPE Eastern Regional Conf., Canton, OH, September 2016.
2016 SEG meeting in Dallas
2014 American Geophysical Union (AGU) Fall Meeting in December 2014 to discuss next steps in the project. At AGU, we hosted a special session on Biogeochemistry of Deep Shale,

National Energy Technology Laboratory

626 Cochrans Mill Road
P.O. Box 10940
Pittsburgh, PA 15236-0940

3610 Collins Ferry Road
P.O. Box 880
Morgantown, WV 26507-0880

13131 Dairy Ashford Road, Suite 225
Sugar Land, TX 77478

1450 Queen Avenue SW
Albany, OR 97321-2198

Arctic Energy Office
420 L Street, Suite 305
Anchorage, AK 99501

Visit the NETL website at:
www.netl.doe.gov

Customer Service Line:
1-800-553-7681